Analysis of the Climatology and Transport Pathways of Iraq Dust Storms between 1985-2013

A thesis submitted to the University of Manchester for the degree of Doctor of Philosophy (PhD) in the Faculty of Science and Engineering

(2019)

Zeyad Wahab Ahmed

School of Earth and Environmental Sciences

CONTENTS

Final Word Count: 40717 Inc. References

List of Figures

List of Tables

List of Acronyms

AAI Absorbing Aerosol Index

AERONET AErosol RObotic NETwork

AI Aerosols Index

AOD Aerosol Optical Depth

AVHRR Advanced Very High-Resolution Radiometer

ECMWF European Centre for Medium-Range Weather Forecasts

EGMM European Geostationary Meteorological Meteosat

ERTS Earth Resources Technological Satellite

EVI Enhanced Vegetation Index

FLEXPART FLEXible PARTicle dispersion model

GDAS Global Data Assimilation System

HYSPLIT HYbrid Single-Particle Lagrangian Integrated Trajectory

IDCS Image Dissector Camera System

IMO Iraqi Meteorological Organisation

IPCC Intergovernmental Panel on Climate Changes

IR Infrared

LADUNEX LAgrangian DUst iNversion Experiment

MODIS Moderate Resolution Imaging Spectroradiometer

BT Brightness Temperature

BTD Brightness Temperature Difference

CALIPSO Cloud-Aerosol Lidar and Infrared Pathfinder Satellite Observations

$CaSO_4$ Calcium Sulfate

MSG Meteosat Second Generation

NASA National Aeronautics and Space Administration

NCDC National Climate Data Centre

NDVI Normalised Difference Vegetation Index

NMMB/BSC-Dust model Non-hydrostatic Multiscale Model/Barcelona Supercomputing Centre

NNA Nearest Neighbour Analysis

NO_2 Nitrogen dioxide

NOAA National Oceanic and Atmospheric Administration

NWP Numerical Weather Prediction

PM Particulate Matter

RGB Red-Green-Blue

RVR Runway Visual Range

SEVIRI Spinning Enhanced Visible and Infrared Imager

SO_2 Sulphur dioxide

CH_4 Methane

CO Carbon monoxide

CO_2 Carbon dioxide

DAOD Dust Aerosol Optical Depth

DREAM Dust REgional Atmospheric Model

SYNOP Surface SYNOPtic

THIR Temperature Humidity Infrared Radiometer

TIR Thermal Infrared

TOMS Total Ozone Mapping Spectrometer

VIR Visible and near-Infrared

WHO World Health Organisation

WMO World Meteorological Organisation

Abstract

The interest of investigating the phenomenon of dust storms comes from their direct impact on human and ecosystem health and climate global change. Despite that the majority of previous investigations performed in many parts of the Middle East, Africa and China, however the main source regions of dust storms in Iraq and the processes that govern their evolution have not been well studied, making their effects an important fact of uncertainty in future dust storms predictions in the region.

The key importance of this study is determining the meteorological, source regions and transport pathways. The analysis in this work was based on a 3 hourly meteorological dataset (dust storms, wind speed and wind direction observations) collected over a 29 year period (1985-2013) which was obtained from the Iraqi Meteorological Organisation (IMO), for which systematic observations were available for 11 ground surface stations across Iraq. As well as that this thesis investigated in the Iraqi dust storms events from SEVIRI (Spinning Enhanced Visible and Infrared Imager) satellite data point of view, the ECMWF (European Centre for Medium-Range Weather Forecasts) 10m wind-field reanalysis data and air mass history of backward and forward trajectories from the HYSPLIT (HYbrid Single-Particle Lagrangian Integrated Trajectory) model.

Dust storms were found to be highly associated with north-westerly winds and are often associated high wind speeds (15-20 ms^{-1}). Dust storms were observed to be more frequent during March-September, particularly in the daytime (06:00-15:00) and that they are short lived (<6 hours) with the period of greatest frequency being between (0-3 hours). Source region of large dust storms (12 major dust storms) was identified based on a dust characterisation using the absolute radiance difference of (12.0-10.8 μm) and (10.8-8.7 μm), in addition to (10.8 μm) from the SEVIRI. The early stages of the 12 large dust storms were investigated, the development of the storms was tracked and the main source region explored. A frequency distribution of the occurrence of dust in all these storms revealed that the source region was consistent across all storms and was centred on the Euphrates River basin (34.20.00°-36.50.00° N to 38.00.12°-41.00.20° E) on the Syrian-Iraqi border. This region has been subject to recent conflict and hence reduced agricultural development but also has received reduced water supply due to upriver water management in Turkey. This work shows that these changes have given rise to an increase in major dust storms and identified the region as the major cause of large dust storms across Iraq.

All of the 12 major dust storms were generated during periods when the region was impacted by low pressure systems that had travelled eastward from the Mediterranean Sea and were highly associated with the Shamal north-westerly winds causing massive dust concentration along the most populated region in the valley of the Tigris and Euphrates Rivers of the Alluvial Plain. The advection of large storms carried on and ended up in south and south east of Iraq, Kuwait, The Arabian Gulf and Iran.

The outcomes presented in this thesis offer new insight for dust storms studies in Iraq regarding where are major regions of dust storms, on why the Euphrates River basin has become an important source of dust outbreaks and on what are transport pathways of large dust storms events. Therefore, an increasing demands in future dust storms predictions and forecasting in the region can be raised and consequently, this could probably lead to further investigations on the significant of dust impacts on human in the region and the utility of using satellite and surface data in dust applications.

Declaration

Candidate Name:

Zeyad Wahab Ahmed

Faculty:

Science and Engineering

Thesis Title:

Analysis of the Climatology and Transport Pathways of Iraq Dust Storms between 1985-2013

I declare that no portion of this work referred to in this thesis has been submitted in support of an application for another degree or qualification of this or any other university or other institute of learning.

Copyright Statement

ACKNOWLEDGEMENTS

First, thanks to **Allah** for all blessings upon my family and myself.

I thank my dear family, to my mother **'Balqees Taha'** who I believe if she was alive and not wandering in the heaven right now with the beautiful angels, she would be very proud and pleased for me! Thanks to my great father **'Wahab Ahmed'** for his support and belief.

Primarily, I would like to thank my supervisors, a huge and special thanks to **Hugh Coe** for his encouragement, time and for being like a brother to me. Thanks for being patient with all the nonsense I was making, starting with me from scratch with each bit of the work. I will always be grateful to you. Thanks to my co-supervisor **Grant Allen** for his time and his great support which have been evident since the first time **Hugh** asked him to be a supervisor on the study.

Many people have helped me throughout this journey. I am very pleased that they have started off as colleagues and have ended up as friends. A special thanks to **Eoghan Darbyshire** and **Joe Pitt** for their enormous and valuable help with MATLAB and IGOR programs. I am very lucky to be surrounded with people like them, supporting me despite their own studies and commitments. Thanks to **Rami Alfarra**, **Akram Al-Sabbagh, Mahdi Ahmed, Moafaq Sachit, Tareq Ali (Nasiriyah Met Office), Khalid Harbi, Jaber Al-Badri** and all my **colleagues** in office 4.52.

I would like to thank **The Higher Committee for Education Development in Iraq (HCED)** for sponsoring the PhD program and for giving me a chance to study in a great country like **The UK** and a great University like **The University of Manchester**. To **Dr. Hassan (HCED)** who suggested this subject, thank you! I hope that **Allah** blesses you with mercy in heaven.

Thanks to the **Iraqi Meteorological Organisation** for providing me with surface observations. Special thanks go to my colleague in Iraq **'Ali Majeed'** for collecting the data physically from Baghdad in a process that took around 15 consecutive months. Thanks also to **The Department of Geography in Thi-Qar University in Iraq** for giving me permission to study abroad.

Finally, I would like to thank **Lionel Messi** and **Football Club Barcelona** for the gladness I have been endued with ever since I supported them. Thanks to the excellence of **Messi** which led to an incredible achievement of winning 5 out of 7 Spanish league titles during the PhD study period (2013-2019) and for scoring (27) goals against Real Madrid (so far) up to the final thesis submission date on 15th August 2019.

'Blank page'

Chapter One: Introduction

1.1 The Phenomena of Dust Storms

1.1.1 Background

Dust storms have become a matter of researchers' interest in the environmental and atmospheric sciences since 1940s of the last century. The interest of investigating the phenomenon of dust storms comes from their potential impact, for instance on human health, climate, nutrient cycling and agriculture. Some areas around the world suffer from lack of vegetation, low precipitation and high wind velocities particularly in the dry season in deserts and arid and semi-arid regions where dust storms are common.

The airborne suspension of dry, unstabilised sediments can take place in a wide variety of environments across the world and hence many local common names exist for dust-bearing winds from region to region, (Goudie and Middleton, 2006). Dust has become a main component of the atmosphere, annually an average of approximately 1000-3000 (Tg) of dust is emitted from arid and semi-arid regions into the atmosphere, (Cakmur et al., 2006). This leads to substantial effects on global climate changes due to the role of dust in altering atmospheric circulation and global hydrologic cycles, (Zhang and Christopher, 2003). However, dust particles are also produced from glacial sources (e.g. (Mahowald et al., 1999; Petit et al., 1981) through rocks grinding under massive ice sheets, (e.g. Fisher, 1979; Smalley, 1966; Thompson and Mosley-Thompson, 1981).

The grinding process forms glaciogenic silt-sized particles which are transferred via rivers and lakes during melting period of the ice sheets, (Mahowald et al., 2006). The particles entertain into the air by wind during the seasonal deposition of channels of rivers and lakes, (Hinman and Lindstrom, 1996). Although the majority of studies concentrate on dust that is generated from deserts, arid and semi-arid regions because current climatic conditions promote the formation of desert dust, (e.g. Prospero et al., 2002), there is strong evidence of dust storm activity in some parts of the world (China in particular) during the last glacial period which led to some changes in climate, (e.g. Cowie et al., 2013; Cragin et al., 1977; Hammer et al., 1985). It remains important therefore to investigate dust particles from glaciogenic sources in palaeo-records (for more information see (Bullard, 2013; Crusius et al., 2011; Prospero et al., 2012).

Terminology is often inconsistent or conflicting across the vast array of dust storm literature. Confounding this scenario is the substantial contribution to the literature from non-English language publications. There is confusion in the literature regarding the difference between dust storms and sand storms. Sand storms are characterised mainly from the perspective of the particles' size as being >63 μm in comparison with dust particles size <63 μm, (Semenov, 2012). Dust storms typically arise due to strong winds, which loft large quantities of these dust particles (<63 μm) from the land surface into the air and act to reduce visibility to <1 km and cause significant impacts on human health, (Shepherd et al., 2016). Dust particles in the range size of 0.1-1 μm are capable of being transported over hundreds of miles from the original source of dust, (Chung et al., 2003; Semenov, 2012; Sodemann et al., 2015), figure 1.1.

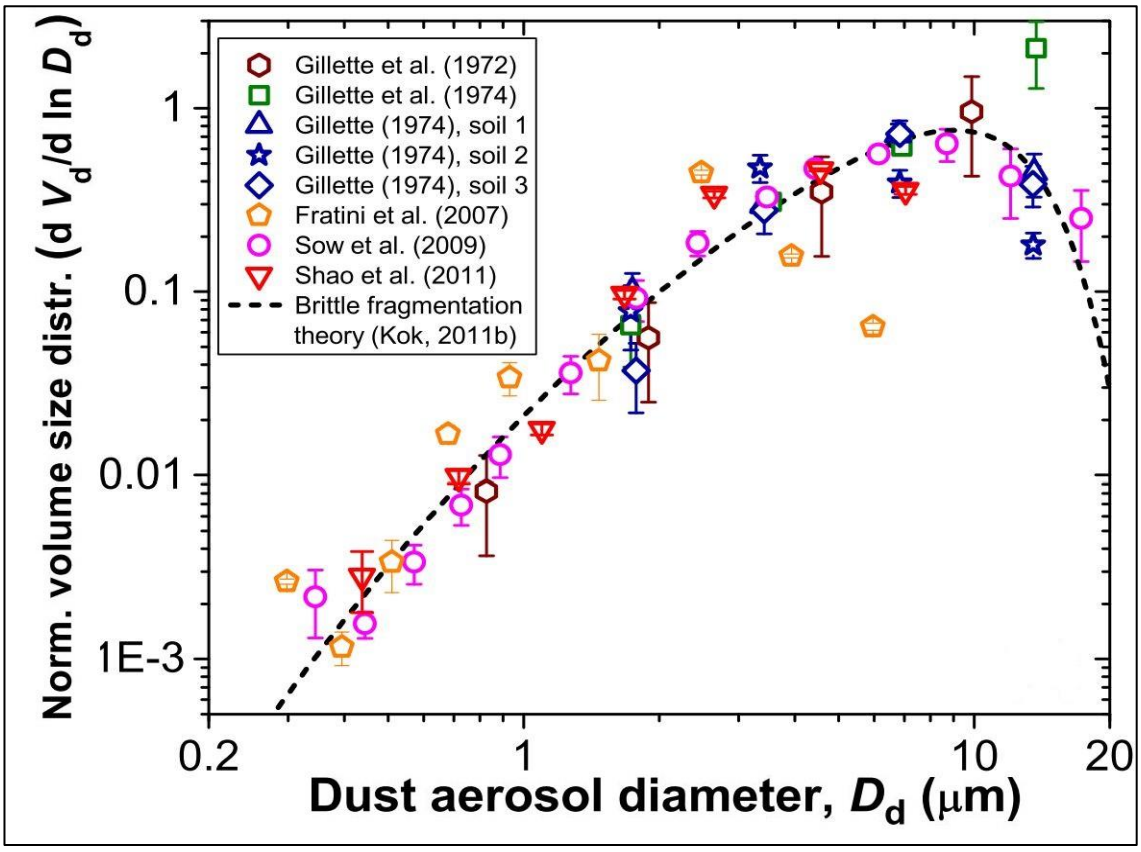

Figure 1.1: Compilation of measurements of dust aerosol size distributions at the time of emission, from (Mahowald et al., 2014).

1.1.2 The Life Cycle of Dust Storms

A number of facts contribute to the generation of dust storms in the regions where they regularly occur and affect their lifetime in the atmosphere. Dry, disassembled and unprotected soils are liable to be re-suspended and to do so requires a minimum threshold of wind velocity of ≥ 7 ms^{-1} at low levels near the ground surface, (https://www.nodc.noaa.gov/woce/woce_v3/wocedata_1/woce-

uot/document/wmocode.htm, accessed on 12/03/2016). Typically there might be some other preferable meteorological conditions, such as low pressure systems and cold fronts suspend the dust, (Crook, 2009). Whilst soil condition and wind speed are processes that directly linked to dust generation, there are some other conditions (e.g. convective clouds or surface turbulence) that cannot easily be mapped to dust generation, but they do influence it, such as in Haboobs (this will be discussed in chapter 2).

First, the horizontal aerodynamic entrainment of dust particles was mainly analysed as an attribution to the friction force of wind when flowing near the ground surface rather than pressure forces, (Wang, 2016). The resuspension of dust occurs when sufficient wind shear is available to lift fine dust aerosols (<63 μm) from dry and unprotected soils, (Varoujan K et al., 2013). The mechanism of dust resuspension is significantly affected by the minimum threshold of wind velocity and soil type (this will be discussed in sects 2.4.2 and 2.2). The highest wind speeds result in largest friction force of wind on the dust particles during the aerodynamic lifting, (Balme et al., 2003). Clay or sand particles may act as strong aggregates and fine aerosols may not release during low wind conditions, while in strong winds, the resistance of soil aggregates may diminish and dust aerosols can be released, (Shao, 2008).

The mechanism of dust uplift was also described by (Squires, 2007) as “the force of wind passing over loosely held particles increases, particles of sand first start to vibrate, then to saltate (‘leap’), as they repeatedly strike the ground, they loosen and break off smaller particles of dust, which then begin to travel in suspension. At wind speeds above that, which causes the smallest to suspend, there will be a population of dust grains moving by a range of mechanisms: suspension, saltation and creep”. However, the actual physical process of dust uplift was well described in details by (Shao, 2001). They demonstrated three forces that are directly involved in dust production; these are the aerodynamic force (*fa*) (dependent on wind speed and particle size), the gravitational force (*fg*) (which depends on dust particle size) and the inter-particle cohesive force (*fi*) (which can be enhanced by the amount of moisture in the dust particles). The three forces act upon dust particles that are located on the surface and their relative magnitude determines the range of dust particle sizes that are entrained into the atmosphere. Consequently, dust may form during one or more of three stages (Shao, 2008), figure 1.2:

a) Aerodynamic lift: where dust can be lifted from the ground surface by aerodynamic forces and the magnitude of dust particles tend to be (<63 μm).
b) Saltation bombardment: particles in this stage strike the ground surface, breaking into smaller fragments and so adding to the finer particle mode; however the size of the particles remains larger than that arising from aerodynamic lift above.
c) An aggregate of clay and sand strike the ground surface by saltation or creeping leading to breaking the aggregation into smaller particles modes.

(Knippertz and Stuut, 2014) illustrated the importance of the 3 mechanisms above. Soil particle density, size and shape play a vital role in dust particle uplift because they determine its terminal fall velocity which is controlled by the vertical motion and velocity of air. They identified 3 categories of dust particles movement based on their size distribution. Dust particles of approximately D_p >1,000 μm move along the surface with a creeping motion, while dust aerosols in the range of 70-1,000 μm are moved in saltation motion and particles of <70 μm may be lifted by the aerodynamic force directly.

During saltation bombardment dust particles can be released directly from the surface or formed from the disaggregation of the soil particles, (Knippertz and Stuut, 2014). It has been proved that the saltation mechanism can produce fine dust aerosols (<70 μm), thus leading to dust emission that remains suspended during long-range transport, (Shao et al., 2011; Sow et al., 2009). This is because the terminal fall velocity (as mentioned above) is lower than the vertical wind velocity which results in long life-time of dust particles in the atmosphere.

Second, once dust storms have been generated, dust might be transported for a few kilometres, not far from source region, before settling or it may travel over continental distances. This depends on the relationship between dust particles size and wind energy, (see Tegen and Fung, 1994). Dust aerosols (<10 μm) may be transported over some thousands of kilometres and they can exist in the atmosphere up to 15 days, while the coarser dust mode (>10 μm) may be transported to around 100-1000 km and has a potentially short lifetime in the atmosphere (few hours - <1 day), (Chung et al., 2003; Tegen and Fung, 1994).

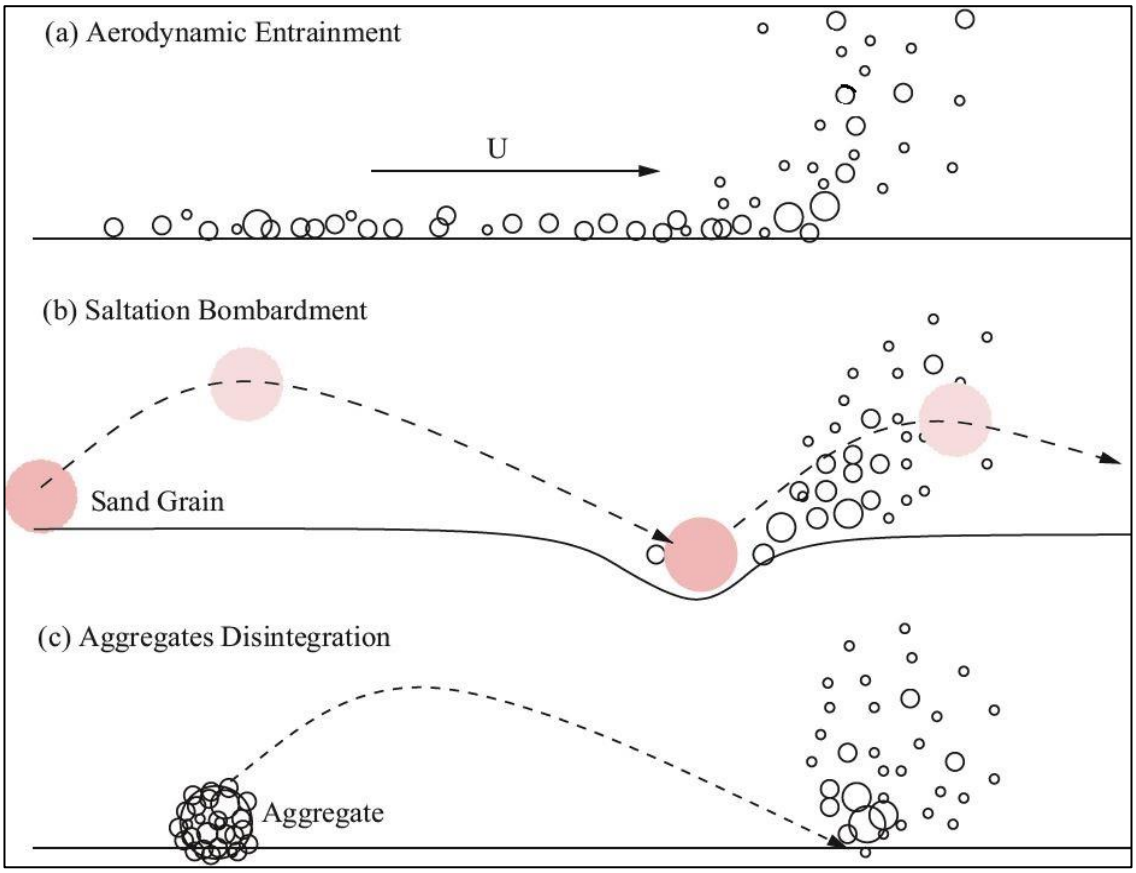

Figure 1.2: Dust formation processes: a) aerodynamic lift, b) through saltation process and c) through disaggregation of dust, from (Shao, 2008).

In some cases of dust transport, (see figure 1.3) storms can appear like an intense wall of dust airborne and they can rise to high altitudes when travelling, (Goudie and Middleton, 2006). The typical altitude ranges of dust storms are between 1-2 km, but can also reach 2.5-12 km in extreme episodes, (Goldman, 2003).

Third, dust storms are eventually deposited back to the ground by gravitational settling or by wash out. Dust aerosols size plays an important role in its deposition where larger particles (>10 μm) deposit first, often not far from the source region due to gravitational sedimentation, comparing to finer particles (<10 μm) that are more typically transported further and deposit to the surface far away from the source region, (Tegen, 2003). Vertical load of dust in the atmosphere and the characteristics of the land surface features are other facts rather than dust size that influence the deposition of dust making it a huge challenge to overcome when predicting the progression and spatial extent of a dust storm, (Duce et al., 1991). However, the deposition can be 'wet' where droplets of rain capture dust in the air and deposit it back to the ground, (Shao, 2008) or it can be 'dry' where dust particles deposit back to the ground by downward turbulent diffusion and gravitational settling, (Harrison et al., 2001).

Figure 1.3: Dust wall during transportation of dust storm. This episode occurred on 26th April 2005 in Al-Anbar city in Iraq near the Iraqi, Syrian and Jordanian borders. The USA Marine Corp Weather Forecasters estimated the wall height of the storm to 1200-1500 metre, from (http://www.thelivingmoon.com/45jack_files/03files/Weather_Warfare_Sand_Storms_Over_Iraq.html, accessed on 11/05/2017).

On the one hand, wet deposition is more efficient at removing dust mass from the atmosphere in wet weather conditions, (e.g. in Spring 2001, 1.96 ton/km^2 of dust in the North Pacific Ocean East of Asia around 30°N-40°N was deposited due to wet weather conditions, in contrast 1.10 ton/km^2 of dry deposition of dust in the same region and time). On the other hand, dry deposition can be greater near the source region of dust, (e.g. 11.72 ton/km^2 of dry deposited dust in China in Spring 2001, while only 1.35 ton/km^2 of wet deposited dust in the same region and time), (Zhao et al., 2003).

1.2 The Influences of Dust Storms

1.2.1 On Humans

There are several studies that have reported dust effects on human health and how dust particles cause serious diseases, such as respiratory ailments, cardiovascular diseases and meningitis, (e.g. Brunekreef and Forsberg, 2005; Griffin and Kellogg, 2004; Patz et al., 2012) and yet a systematic study of the negative contribution of dust storms on human health in Iraq is still lacking, despite the fact that a large population is potentially exposed to airborne dust and aerosol as well as the emphasis of the World Health Organization (WHO, 2013) who summarised that dust particles considered one of the most dangerous pollutants for human health. They reported that chronic exposure to fine particulates is associated with premature death due to respiratory and cardiovascular diseases, acute lower respiratory infections and lung cancer.

The WHO report in 2013 explained the process of dust inhalation when fine dust aerosols are taken into the human body. For instance in respiratory and asthma which represent chronic airway disorders, the inhalation of dust particles causes inflammation and contraction of small muscles around airways that restricts the flow of air and leads to irritation of the airways or acts as a trigger of allergic reactions. Cardiovascular problems arise since some fine dust aerosols are capable of accessing blood-vessels via the airways and causing a restriction in blood supply to tissues which is known as (Ischemia).

Figure (1.4) shows a schematic of the transport pathway of dust particles through nasal and oral cavities and its possible stages via the airways to the lungs during the inhalation process. The smaller dust particles have the greater of reaching the human lungs. Inhaled dust particles with size of $PM_{2.5}$ or smaller have a considerable opportunity to access through the airways deep to the structure of the alveolus inside the lungs, consequently they may cause serious inflammation when inhaled in high doses (Krug and Wick, 2011).

Dust particles can further exacerbate human health when combined with pollutants as they are capable of adsorbing gases and chemicals (e.g. $CaSO_4$ (Plumlee et al., 2013), CO (carbon monoxide), NO_2 (nitrogen dioxide) and SO_2 (sulphur dioxide) (see Fang et al., 2003; Yang, 2006) or microorganism and pollutants such as bacteria, (Griffin, 2007; Plumlee et al., 2003) during their lifetime in the atmosphere. The combination of dust with cultivatable airborne microorganisms can lead to worse health problems on humans. The danger is that when fine dust materials are inhaled they can react chemically with the airways fluids in the human body, (Kellogg et al., 2004) causing allergy and asthma diseases as reported by the National Institute of Allergy and Infectious Diseases, (Griffin et al., 2001). Furthermore, a high content of bacteria has been found in dust particles collected from dust storms episodes that have occurred in a number of cities in Iraq between December 2008 and March 2009. Bacteria species identified included elevated concentrations of Bacillus and E. Coli species that cause serious sicknesses were detected in 42.9% and 9.5% of samples, respectively, (Al-Dabbas et al., 2012). The dangers of bacteria in aerosol dust can be extended to affect human through agriculture as a result of input from crop yields, plants and trees.

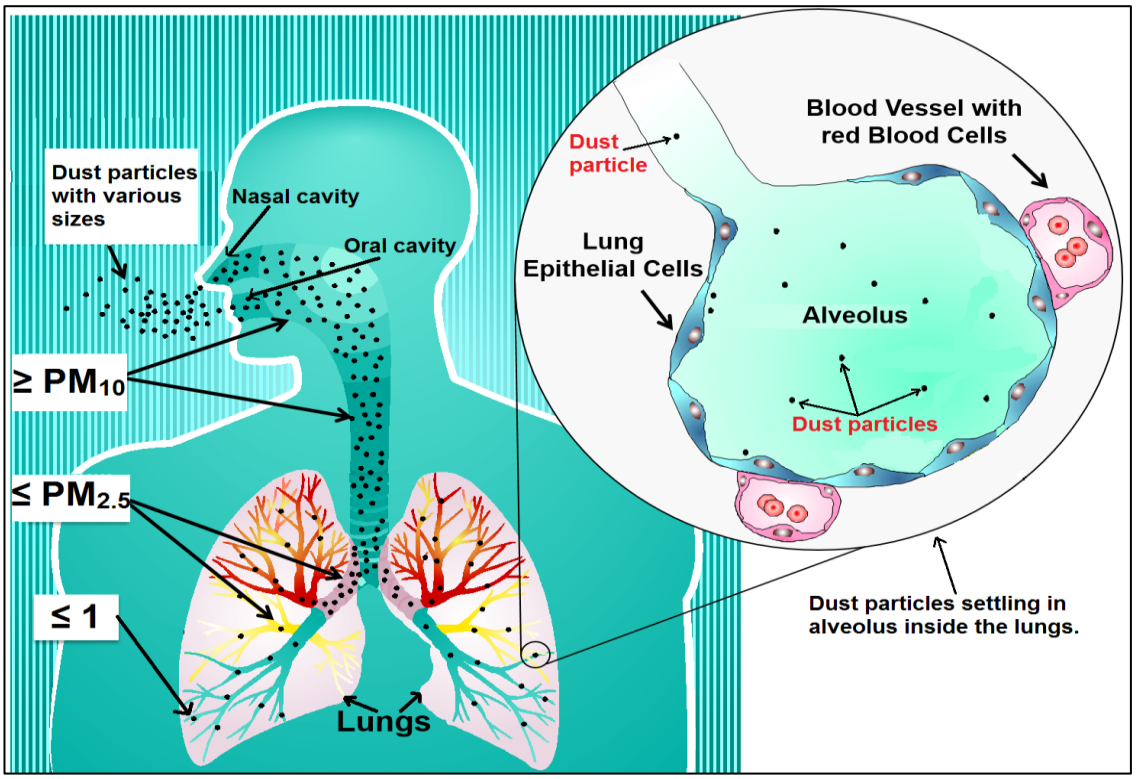

Figure 1.4: A medical diagram of the penetration of dust particles in the airways tracts, modified after (Krug and Wick, 2011).

During a light dust storm event in Beijing, dust concentrations of $PM_{2.5}$ (Particulate Matter) increased up to 630 $\mu g/m^{-3}$, (https://www.independent.co.uk/news/world/asia/china-dust-storm-air-quality-decline-gobi-desert-mongolia-beijing-visibility-pollution-children-a7717241.html, accessed on 21/06/2017) while in a severe dust storm event that occurred in Sydney, the concentration of PM_{10} reached 11,000 $\mu g/m^{-3}$ and 1,600 $\mu g/m^{-3}$ of $PM_{2.5}$, (Merrifield et al., 2013). This mass loading is extremely high and it is well above the standard of air quality of the World Health Organisation (WHO) that recommends concentration of dust should not exceed 10-20 $\mu g/m^{-3}$, (World Health Organization, 2006). High PM load from dust can lead to serious human health impacts particularly in the urban areas where the populations are high and exposed to its danger.

A positive relationship has been found between different aerodynamic sizes of dust particles and mortality on all ages of populations. In Kuwait, for example, a study identified mortality due to respiratory and cardiovascular diseases in relation to dust storms events during the period January 1996 to December 2000 and found that during 39 days with intense PM_{10} concentration (>1000 $\mu g/m^{-3}$) and 569 days of less intense PM_{10} concentration (>200 $\mu g/m^{-3}$), 987 deaths were identified to be attributable to respiratory problems and 7977 cases were due to cardiovascular failure, (Al-Taiar and Thalib, 2014).

There is a difference in the literature between acute and chronic exposure of dust. A thorough review by World Health Organisation (WHO, 2013) found that chronic exposure and mortality can be positively related to PM_{10} resulting from short-lived dust storms events, whereas acute exposure related to severe and long transport of dust. For instance, during 11 short-time dust storms events (<1 day) happened between 1992-1994 in Brisbane city in Australia, 166 people of age range 4-74 years old visited asthma emergency sections at hospitals, (Rutherford et al., 1999) while 52 people died on 26-27 May 2008 due to one severe dust storm affected eastern Mongolia, (Jugder et al., 2011).

The influence of dust storms on agricultural practices has been well studied globally (e.g. Gonzalez-Martin et al., 2014). A study by (Stefanski and Sivakumar, 2009) listed that loss of crops, livestock, plants leaves and soil erosion as being the main key facts of how dust storms economically affecting on agriculture, for instance the total damage of dust storms on agriculture in Beijing in the year 2000 was around £90 million, (Ai and Polenske, 2008).

Dust storms can effectively disrupt transport by reducing visibility causing an increase in road accidents and delaying aircrafts. Such disruption can be seen in Beijing, for example where the air transport sector reported about £3 million loss due to dust storm events that led to the cancellation of 129 flights during the year 2000, (Ai, 2003; Ai and Polenske, 2008).

1.2.2 On Environment (Climate Change)

Dust storms have a considerable impact on climate and weather systems. The Intergovernmental Panel on Climate Changes (IPCC) discussed the role of airborne dust on surface heat fluxes, convective activity, heating rates and radiation budgets, (Field, 2012). The latter has been given a particular attention due to its direct effect on climate change. It shows that dust aerosols can highly regulate the amount of solar radiation through absorbing and scattering processes, (Tegen and Lacis, 1996). For instance, the amount of solar radiation near the ground surface showed to be decreased by about 40% and 10% during two single dust storm events that occurred in Beijing in April, 2013 in comparison with non-dust storms days, (Zhou et al., 1994). Also, evidence that the concentrations of greenhouse gases, such as CO_2 (carbon dioxide) and CH_4 (methane) can be increased during dust storms events. A study on a number of dust storms events happened in different regions in Asia showed that the concentration of CO_2 and CH_4

before the storm occurs was approximately 376 ppm and 1.73 ppm, respectively. While concentrations increased to about 393 ppm and 1.85 ppm on the day of the dust storms events for the given gases, respectively (Guo et al., 2012). Dust blocks upwelling terrestrial radiation of the ground surface from escaping to the space, subsequently increasing the downward longwave flux at the same time, (Shenk and Curran, 1974).

1.2.3 Other Dust Storms Influences

Dust storms also have other impacts, for instance disease transmission on human, plants, animals suffocation, soil stability, (Goudie and Middleton, 2006; Goudie and Middleton, 1992) and several economic losses (the latter will be discussed in more details in chapter 5). For example, dust is capable to transfer nutrients from land to oceans ecosystems, this can occur during dust advection in the atmosphere where nutrients adhere to dust particles and travelling in combination with dust increasing source of iron in the deposition regions, (see Claquin et al., 1999; Mahowald et al., 2014). Furthermore, dust deposition on oceans, lakes, ice, soils and snow changes the albedo and can therefore affect melting rates. Such depositions are increasingly used to reconstruct past climates, (Knippertz and Stuut, 2014).

1.3 Thesis Overview

Dust storms studies involve a number of applications, such as climate change, economic losses and impacts on human health that indicates to the importance of dust storms to be investigated. But, the influences of dust storms on human health receive growing attention. Iraq, being part of the Middle East region, has been the subject of a number of wider studies, however it has received a scant attention in the research literature and no previous study has investigated dust storms in Iraq in detail and no systematic study of dust storm has been carried out to date in the same approach of this thesis.

The Arabian Peninsula deserts, together with the majority of the Middle East deserts have been well-studied (see sect 2.4); however there is little known about dust storms in Iraq, despite the fact that a large population is potentially exposed to airborne dust and aerosol. Consequently, the main relevance of this thesis is to increase our understanding about dust storms phenomena in the region of Iraq so it can help to reach some findings and establish to lead for more investigations in the future. This thesis has employed a set of surface meteorological data (see sect 3.1) that have been obtained from the Iraqi Meteorological Organisation (IMO); no single study has used this data in a similar

analysis in the past and this reflects the necessity of such study to understand some perceptions of dust storms in the region. Furthermore, it is the first time in Iraq that routine surface observation data that was measured on the ground at Iraqi meteorological stations was analysed in this thesis in a climatological way on a station by station basis.

In addition to that this thesis will also investigate in the Iraqi dust storms events from satellite data point of view. The latter investigation aims to identify source regions and the transport pathways of Iraqi dust storms events, (see sect 4.2).

'Blank page'

Chapter Two: Study Area and Literature Review

This chapter demonstrates some information about Iraq as a study region from the perspectives of the geographical location, topography, soils and climate. Also, it provides a review of dust storm properties and processes based on global, regional and local studies in order to identify gap in knowledge and current uncertainties. This chapter will mainly focus on studies that are geographically located near to Iraq and might have an influence on the region in terms of dust generation and transport. The chapter will present the phenomena of dust storms from the following aspects; main source regions, meteorological conditions, frequency distribution, duration, transport and trajectories in addition to the recent trends of dust storms in Iraq. The key theme of this chapter is to identify uncertainties and lack in knowledge that will inform the direction of this thesis.

2.1 The Geographical Location of Iraq

Iraq is located in the south west of Asia between latitudes 37.5° N-29.6° N and longitudes 48.45° E - 38.45° E and it has a total area of 437072 km^2. Iraq borders Turkey from the north, Iran from the east, Saudi Arabia and Kuwait from the south and Saudi Arabia, Jordan and Syria from the west, (see figure 2.1).

It has been shown that some of the countries adjacent to Iraq are classified as major sources of dust in the Middle East and they have an explicit impact on exporting dust to other regions, (Goudie and Middleton, 2006). The north of Saudi Arabia, east of Jordan and East, North East and South East of Syria are all desert regions, and when dust generate in those regions it can be transported to Iraq via depressions that are generated over the East of the Mediterranean Sea as mentioned earlier. The depressions move from the East of the Mediterranean eastwards across Lebanon, Palestine, Jordan, Israel, Syria, northern Saudi Arabia, then over Iraq and Iran thus transferring dust to and between these regions. Two typical examples of this dust transport reached Iran on 18-19th May 2010, (Ashrafi et al., 2014) and 22-23 February 2010, (Abdi Vishkaee et al., 2012). The backward trajectories for those two events indicated that the source regions of dust were transported from the east of the Mediterranean across east Jordan and North East of Saudi Arabia and North East and East Syria across Iraq and settled in Iran.

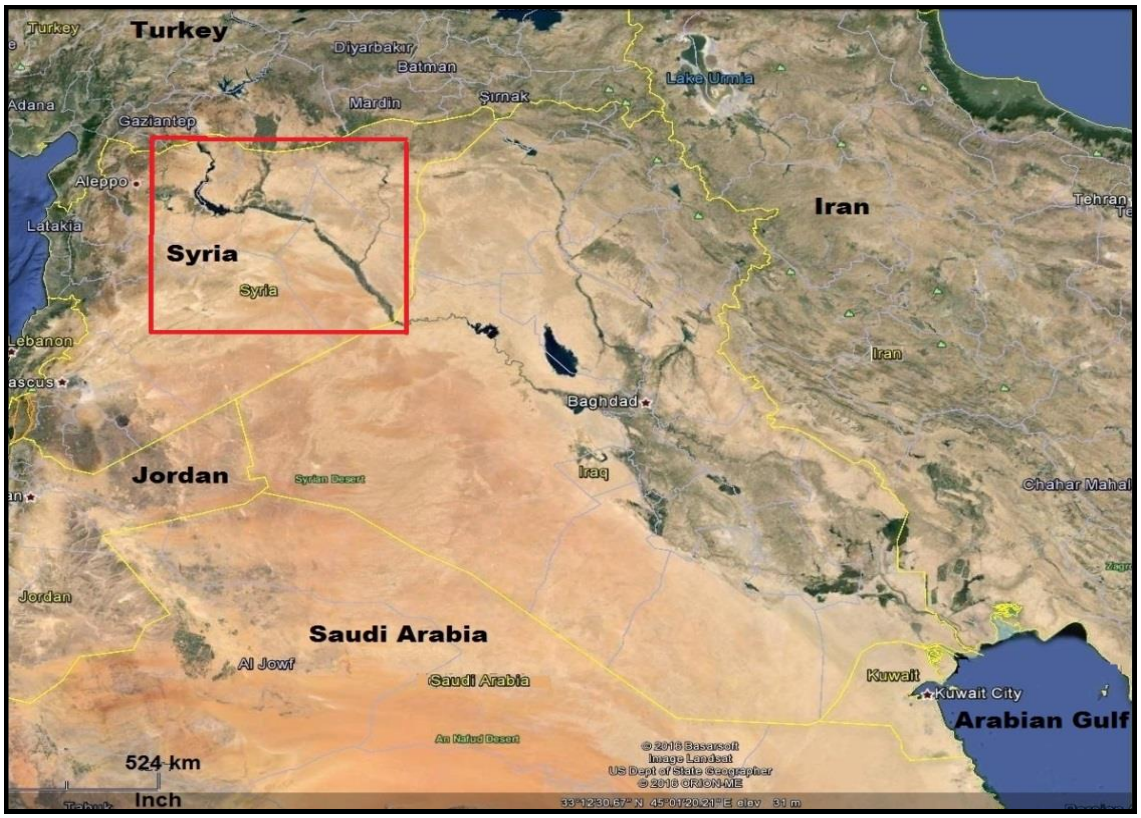

Figure 2.1: The map of Iraq and surrounding countries. The red square indicates to the Euphrates River basin on the Syrian-Iraqi borders (this basin will be discussed in chapter 4) source: (GoogleEarth, 2013).

2.2 The Topography and Soils of Iraq

Figure (2.2) shows that there are four primary principal of topographies in Iraq; (https://www.britannica.com/place/Iraq#toc22923, accessed on 21/11/2017). First the western Plateau (area of around 198000 km^2 and 300-800 metre amsl), which extends along the South West and west regions of Iraq. The main soil structure of the Plateau is hamada coarse rocks. Second, the Alluvial Plain (132000 km^2) (https://en.wikipedia.org/wiki/Mesopotamian_Marshes#Geography, accessed on 21/11/2017) that contains mostly silty to silty clay soils and it represents the most fertile and inhabited region of Iraq.

The Alluvial Plain extends along the valley of the Tigris and Euphrates Rivers from northern Baghdad to the Arabian Gulf. It also considers the lowest topography in Iraq (approximately ≤170 metre elevation) which represents the southern part of the Mesopotamia Plain that extends from the borders of North West of Iraq, North and North East of Syria and southern Turkey. The Marshlands (about 20000 km^2 area) locates at the lower of the Alluvial Plain southern Iraq.

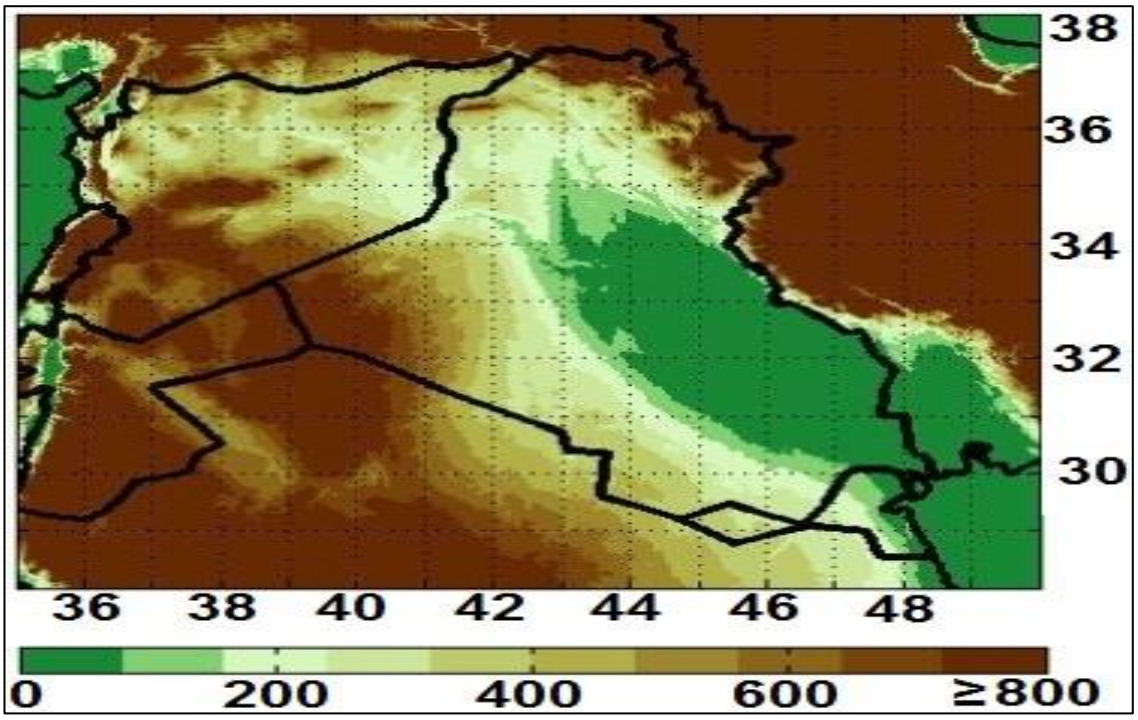

Figure 2.2: Map of terrains in Iraq (metre). The western Plateau (300-800), the valley of the Tigris and Euphrates Rivers in the Alluvial Plain (≤170), the deserts (>170-230) and the mountainous region (800-3600), from (Amante and Eakins, 2009).

Third, the deserts (area of approximately 168000 area km^2 and around >170-230 metre amsl) that extends along the western side of the Alluvial Plain and the eastern side of the western Plateau and it mainly consists of coarse sand particles. Lastly, the mountainous region (about 800-3600 metre amsl) in the north and north East of Iraq that extends into Turkey and North West and West of Iran.

The soil types in Iraq are classified as 62.2% aridisols and 16.2% entisol, respectively (Muhaimeed et al., 2014). Both soil types have a significant accumulation of silty, silt loam and silty clay materials and they occupy the majority of the South East (lower Mesopotamia Plain) and the Central regions of Iraq. The agricultural practices in those regions play a role in breaking the soil further into finer material leading to easier re-suspension of dust. While in the South and South West regions, soils comprise more sand and gravel materials, in addition to the activities of sand dunes in the south west terrace that extents to the Saudi Arabia and Kuwait borders, (Buringh, 1960).

2.3 Climate of Iraq

The climate of Iraq is characterised as being dry and continental, this is because Iraq is distant from upwind seas and oceans, lacks precipitation for most of the year (annual average 85.4-706.6 mm) and has high average temperature (12.2°C in January to 43°C in July), (Al-Malikey, 2007). According to Köppen Geiger's climate classification

regions, the north of Iraq has features consistent with a Mediterranean climate, while the central and western parts of Iraq are a Steppe climate and the rest of the country (east, south, south west and south east) are typically classified as desert climate regions, (Al-Dassea, 2010). This results in a variety of air masses crossing Iraq.

In winter (December-February), the quasi-permanent Asian high extends over Iraq and reduces temperature averages relative to summer, while in spring (March-May), low-pressure systems associated with mid-latitude cyclones play a considerable role in weather variability, such as increasing wind speed and temperature averages, (Hanson, 2007). In summer (June-August), Pakistan's thermal low and the monsoon over Asia extend north-westward over Iraq; result in the locally-named "Shamal" wind (see sect 2.4.2 for more details about the Shamal). This regime is characterised by increases in wind speed to 5.1-12.8 ms^{-1}, (Wilderson, 1991). Lastly in autumn (September-November), the wind speed is less than in summer, and rain showers increase in frequency as the Asian high starts to build, (Crook, 2009).

In terms of temperature, precipitation and wind, the typical mid-latitude characteristics of transition seasons (spring and autumn) are not manifest in Iraq. The prevailing climate regime of those two seasons are very comparable to summer months, (Gordon, 1948).

2.4 Literature Review

The recognition of the importance of dust storms is not recent and to date a considerable amount of literature has been published in it. This interest has greatly increased during the last 40 years due to the rapid land deterioration and desertification, (Mabbutt, 1986). There is a growing body of literature that recognises the importance of dust storms and their impacts on human and environment particularly in the Sahara, deserts of Southern Africa, deserts of South West and Central Asia, China, Mongolia, deserts of the Middle East and Arabian Peninsula, deserts of North and South America and Australia. However, up to now, little attention has been paid to dust storms in Iraq and more systematic and quantitative analyses are needed. The next sections will demonstrate dust storms phenomena from local, regional and global scales by discussing its source identification and spatial distribution, the meteorological associated with dust storms events, frequency, duration and transport aspects. In addition to the recent trends of dust storms events in Iraq and some adjacent countries.

2.4.1 Source Identification and Spatial Distribution of Dust Storms

The contribution of arid and semi-arid regions and deserts as major sources of dust re-suspending to the atmosphere is well documented, (e.g. Goudie, 1983; Goudie and Middleton, 2006; Idso, 1976; Middleton, 1986b; Parsons and Abrahams, 1994; Pewe, 1981; Youlin et al., 2002). Despite that, there is little evidence in the literature about the contribution of lands with poor farming and agriculture managements can also be source of dust emissions, (Feng et al., 2002; Tegen et al., 2004). However, a much more quantitative study would be more beneficial to identify how human can contribute to dust re-suspending in the atmosphere. Therefore, identifying the source region of dust storms is clearly important for understanding pathways of dust storms during their transport whether for short or long distances.

The major global dust sources have been well-identified by Prospero et al (2002) who used TOMS (The Total Ozone Mapping Spectrometer) sensor on the Nimbus 7 satellite data to map the spatial distribution of dust sources. The dust belt according to this study extends from west coast of North Africa, over the Middle East, Central and South Asia, to China (figure 2.3). The study highlighted that the spatial distribution of the dust belt is compatible with the distribution of the regions that receive an annual rainfall between 200-250 mm or less and that major active dust sources are remotely far from human settlements, therefore research literature shows a very scant evidence that major dust sources can be mapped in regions close to large human population centres.

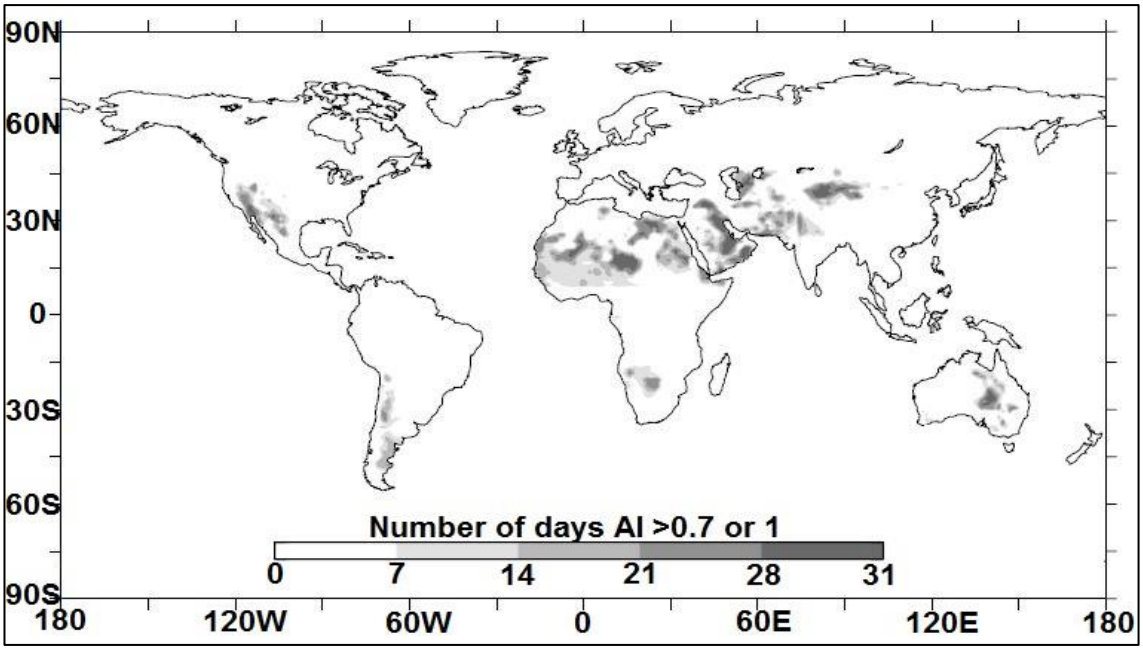

Figure 2.3: The spatial distribution of dust sources around the globe by TOMS AI (Aerosols Index). The threshold used indicates dust in shades of grey at value of 1, or value of >0.7 indicates no dust, from (Prospero et al., 2002).

In terms of the distribution of the main dust aerosols hot spots, the aerosol index (AI) highlights the Bodélé Depression of south central Sahara, West Sahara in Mali and Mauritania and Arabian Peninsula (Southern Oman-Saudi Arabia border) as the largest sources of dust emissions globally with ≥30, ≥24 and ≥21 (AI) values, respectively, (Goudie and Middleton, 2006). Iraq has not been identified as one of the world's major dust sources; however Baghdad (220 t km^{-2} yr^{-1}), Basrah, (Um Qasr 193 t km^{-2} yr^{-1} and Khur Al-Zubir 76 t km^{-2} yr^{-1}) together with other nearby countries (e.g. Kuwait 270 t km^{-2} yr^{-1} and Riyadh 392 t km^{-2} yr^{-1}) have been classified as regions with high depositional rates of dust, (Al-Dousari et al., 2013). A number of different methods in the literature have been proposed to draw a map of dust sources in different regions.

First of all, there are a wide number of studies that employed ground surface climatological and weather observations at local and regional stations, which are recorded using WMO (World Meteorological Organisation) SYNOP (Surface Synoptic) observations codes. This is considered to be one of the most common source of information that has widely and extensively been used, (https://public.wmo.int/en/our-mandate/focus-areas/environment/sand-and-dust-storm, accessed on 08/05/2017). For instance, (Cowie et al., 2014) used long-term (1984-2012) of diurnal, seasonal and geographical surface observations from 70 different observing stations across Sahara and Sahel regions in Africa. Their findings showed high frequency of dust emissions observed in Sudan, Algeria, Niger and Chad stations, the latter two stations are close to the Bodélé Depression of south central Sahara which is classed as one of the main dust sources in the region, (Goudie and Middleton, 2006). The meteorology associated with such dust events is called a Haboob, which is generated due to low-level convective storms (more details about this will be discussed in the next section). The importance of Haboobs comes from their high frequency and possible transport to the Middle East.

Another example of such work (Surface Synoptic data) mapped the Middle East as one of the regions within which most frequent high dust loads occur, (Hamidi et al., 2013; Idso, 1976; Middleton, 1986a; Pease et al., 1998; Rezazadeh et al., 2013; Wilderson, 1991). Hamidi et al (2013) identified 3 regions in the Middle East as potential dust source regions. The highest among those regions was mapped as region 3 (see figure 2.4) which extended from the desert of the Rub Al-Khali that occupies much of the Arabian Peninsula, southern Syria, west of Iraq and eastern Jordan, in addition to the Central of Iran.

Two early studies were conducted by (Coles, 1938) and (Al-Najim, 1975) who employed monthly averages of surface observations of dust storm in Iraq. Coles reported that high dust loading was recorded in 5 different regions (Rutbah, Mosul, Hinaidi, Shaibah and Diwaniyah) during the years 1933-1935, while Al-Najim sought to examine the period (1941-1970) and concluded that the desert of South West Iraq is the main source of dust in the region which is not consistent with the region mapped in Coles' study. Coles' and Al-Najim's studies were considered preliminary work; their studies based on monthly averages surface observations for a quite small number of meteorological stations (maximum 5 stations as in Coles' study) and therefore might not interpret the meteorological of dust storms in much detail. Further research using, for example a present weather data over a wide range of meteorological stations for a long period can assist to explain dust storms behaviour in the region in more details.

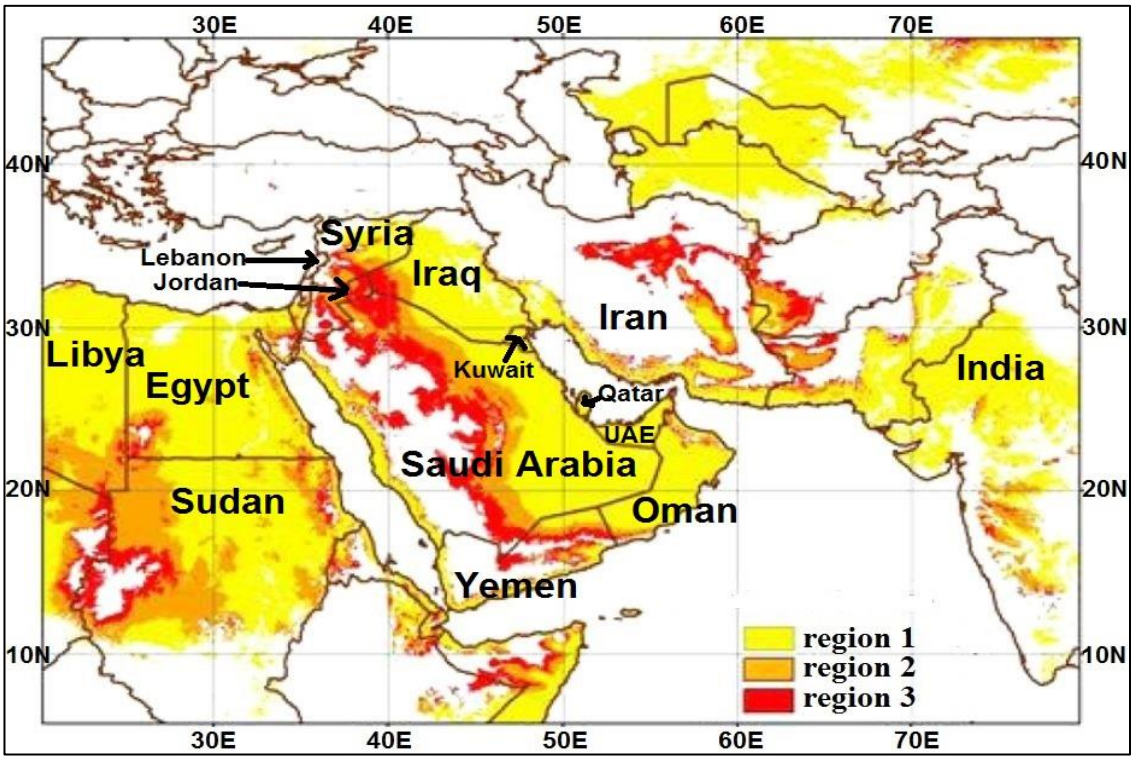

Figure 2.4: The most potential dust source regions in the Middle East based on SYNOP observations. Highest dust intensity in region 3 (areas shaded in red), while region 1 (areas shaded in yellow) covers Oman, south east and east of Saudi Arabia, Kuwait and southern, central and north west of Iraq. The lowest intensity mapped over the Central of Saudi Arabia and North West of Sudan in region 2 (areas shaded in orange), from (Hamidi et al., 2013).

Whilst a number of studies have been carried out using climatological surface observations to identify dust source regions, satellite data and imagery represents a powerful tool in identifying source regions providing vital observations from large to small scales, (Benedetti et al., 2014). Satellite instruments can offer products through a number of visible and near-infrared (VIR) and thermal infrared (TIR) channels, where

the TIR provides more precise information during the night time in comparison with the VIR channels that offer good results during the daylight hours only, (Li et al., 2007).

There are a number of meteorological satellites that provide dust observations starting from 1970s, for example the Temperature Humidity Infrared Radiometer (THIR) and Image Dissector Camera System (IDCS), (Shenk and Curran, 1974) Earth Resources Technological Satellite (ERTS-1), (Griggs, 1975) the Advanced Very High-Resolution Radiometer (AVHRR), (Ackerman and Chung, 1992) the Meteosat Second Generation (MSG), (Schmetz et al., 2002) the Moderate Resolution Imaging Spectroradiometer (MODIS) and TOMS, (Ginoux et al., 2012; Prospero et al., 2002). Although the TOMS instrument is not currently in use, it provided sufficient and vital information about near real time dust observations and dust main sources between 1978-2006, (McPeters et al., 1998).

Some previous studies have utilised the Aerosol Index (AI) product produced from TOMS data. For instance (Alpert and Ganor, 2001) compared TOMS (AI) with synoptic observations of dust in the Middle East for the period 14-17 March, 1998. Their findings showed high AI values (2.6-≥3.4) in Israel, Jordan, Lebanon, Syria, north of Saudi Arabia and western Iraq and Prospero et al (2002) who found TOMS a useful tool when composing global dust maps (as mentioned earlier). However, the main drawback associated with the use of TOMS is that aerosols in the range height of 1-2 km cannot by fully detected when there are clouds in the TOMS field of view, (Herman et al., 1997).

One of the powerful tools is MODIS that provides one observation per day via Terra and Aqua satellites which provide 10:30 and 13:30 local equatorial overpass times, respectively, (Miller, 2003) figure 2.5. The spectral range of MODIS is (0.41-15 μm) and it can derive aerosol products over land through 3 visible wavelengths, (see Remer et al., 2005). In conjunction with AOD (Aerosol Optical Depth) and ground surface dust observations, MODIS can be more effective in providing information about dust source region. Ginoux et al (2012), for instance used (0.1°) high resolution maps of MODIS Deep Blue products to identify anthropogenic and natural dust sources at global scale and found that the most active parts of the world for dust generation is the area that extends from west coast of North Africa across the Middle East to Central Asia, (Jafari and Malekian, 2015; Moridnejad et al., 2015) and this is very consistent with the TOMS dust belt that identified by Prospero et al (2002).

Furthermore, (Abdi Vishkaee et al., 2012) investigated the role of the winter Shamal wind on a one single event that affected North West Iran on 22-23 February 2010 by using MODIS/Aqua. The study ran backward trajectories for that single dust storms event and it showed that the source region of dust that affected North West Iran was the borders of East and North East of Syria and North West of Iraq (this source region will be discussed in detail in sect 2.4.6).

Although MODIS and TOMS have been useful to draw global and regional pictures of dust sources, recently the European Geostationary Meteorological Meteosat (EGMM) satellites were designed to offer new insights regarding dust aerosols source

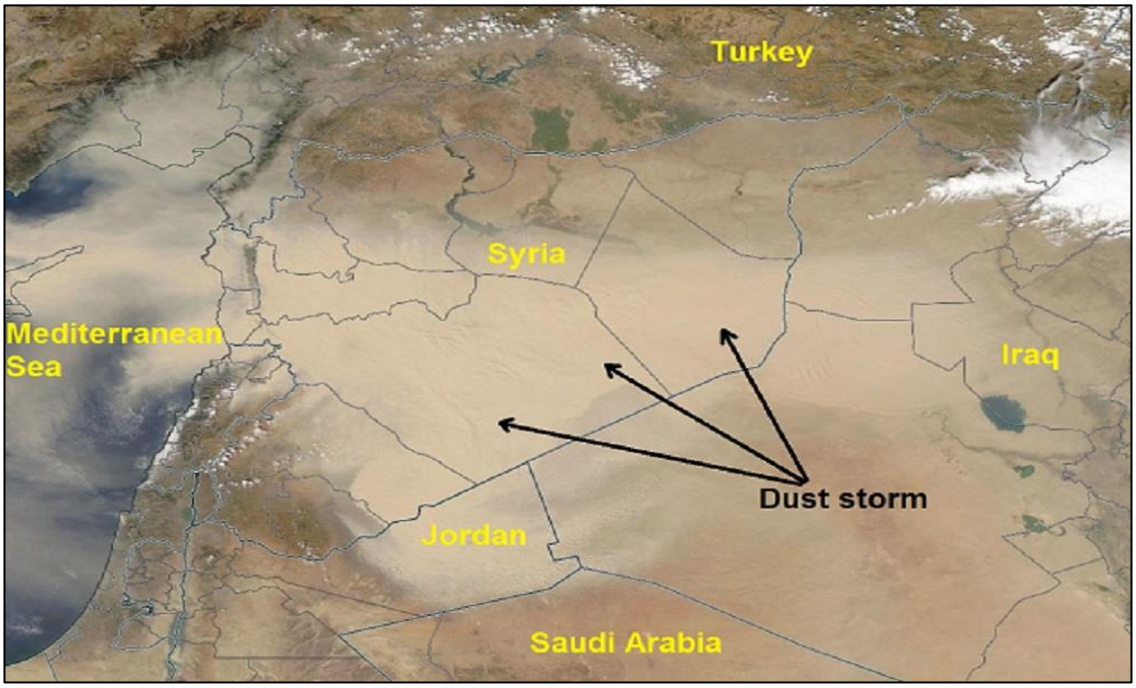

Figure 2.5: Dust storm event captured on 7th September 2015 by MOSID/Aqua. This true colour image taken at 13:30 UTC local equatorial overpass time, source: https://worldview.earthdata.nasa.gov/?p=geographic&l=MODIS_Aqua_CorrectedReflectance_TrueColor,Reference_Features&t=2015-09-07&z=3&v=26.126352770309786,24.742570626809773,59.876352770309786,41.52968000180977, accessed on 17/05/2017.

identification and some other meteorological applications too, (e.g. clouds and wind fields). On board, the new generation of (EGMM) called Meteosat Second Generation (MSG) where SEVIRI (Spinning Enhanced Visible and Infrared Imager) instrument represents a primary tool for dust aerosols applications, (Aminou, 2002).

The SEVIRI provides a number of meteorological and dust observations with a high resolution repeat cycle of 15 minutes which makes the MSG satellites a unique and powerful tool in providing numerous observations, particularly those meteorological

elements that constantly and rapidly change, such as via convection, (Schmetz et al., 2002). This feature is not obtainable on the polar orbiting satellites (e.g. MODIS) that offer one observation per day only, (Kaufman et al., 2005). The SEVIRI also scans the full disk of the Earth involving 12 different channels, of which 4 of them are at visible and near infrared wavelengths that scan the Earth with 1 km sampling resolution. In addition 5 infrared channels scan the Earth with 3 km sampling resolution (Schmid, 2000) (see section 4.1.2 regarding all channels). Retrieval of dust from SEVIRI, as with most of the satellite instruments, can be confounded under certain circumstances, such as the shape and size of dust particles, (Brindley et al., 2012), the altitude of dust layer and its density in the atmosphere, (Darmenov and Sokolik, 2005; Pierangelo et al., 2004) and cloud presence, (Chaboureau et al., 2007).

The utility of SEVIRI for dust retrieval is based around the RGB (Red-Green-Blue) products in the natural true colours and thermal infrared channels. The images composited from RGB SEVIRI show dust aerosols as pink to magenta with high accuracy which is quite distinguishable and unique, (Hudson et al., 2008) figure (2.6). Furthermore, the RGB products of SEVIRI can be derived from the inputs of a number of channels or from subtracting the values of two different images, driving a Brightness Temperature Difference (BTD) (this will be discussed in section 4.1.2).

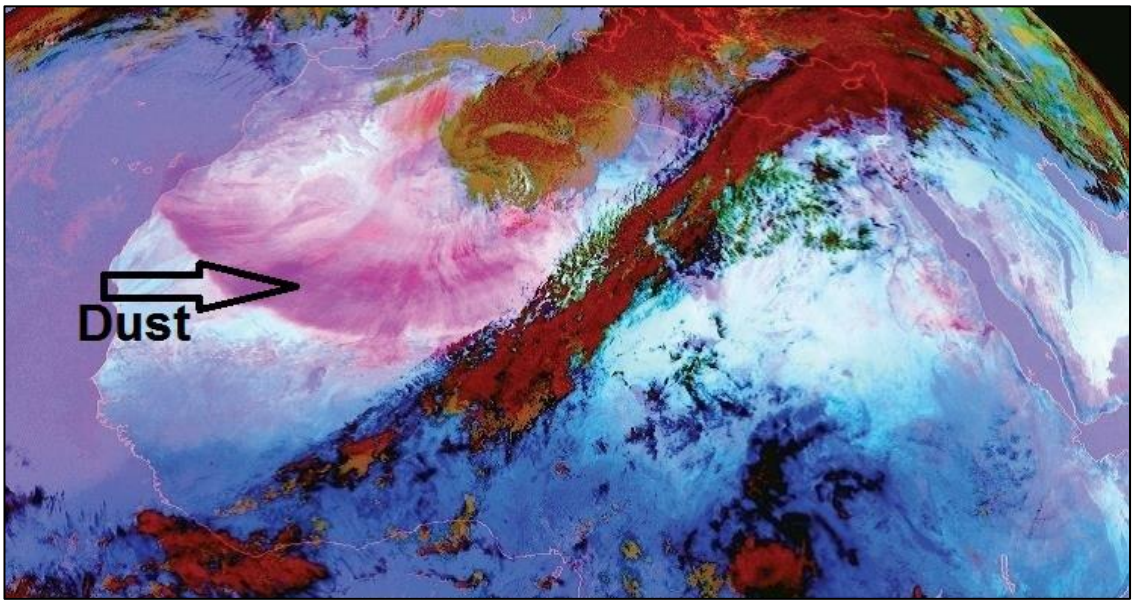

Figure 2.6: Dust natural RGB observation from SEVIRI. It shows dust in pink in the North West of Africa on 3rd March 2004 at 12:00 UTC, source: (Martínez et al., 2009).

This is particularly effective when using the 8.7 μm, 10.8 μm and 12.0 μm IR (Infrared) channels of SEVIRI, (for more information see

https://www.meted.ucar.edu/satmet/multispectral_topics/rgb/navmenu.php?tab=1&page=3-2-4&type=text, on 20/11/2017).

The vast majority of studies that have utilised SEVIRI have mostly focused on the Sahara, (e.g. Ashpole and Washington, 2012; Banks and Brindley, 2013; Brindley et al., 2012; Li et al., 2007; Martínez et al., 2009; Schepanski et al., 2007; Schepanski et al., 2012; Schepanski et al., 2009; Slingo et al., 2006) while very little work has been published on the deserts of southern Africa, (e.g. Vickery et al., 2013) and the Middle East deserts, (Banks and Brindley, 2013) although those regions has been globally classified as main dust sources, (e.g. Choobari et al., 2014; Goudie and Middleton, 2006; Middleton, 1986a).

Far too little work has been done in the literature regarding SEVIRI RGB/BTD dust products in Iraq. Up to now, a study by Banks and Brindley (2013) who collected an archive data of Dust Aerosol Optical Depth (DAOD) and half hourly dust observations (daylight only) of high temporal resolution from SEVIRI for the months January and June of the year 2009 to determine the diurnal patterns of dust loadings for the regions of North Africa and the Middle East. They employed the mean (BTD) via 2 IR channels (10.8-8.7 μm) to isolate dust particles and their findings showed that the highest dust emissivity were recorded over northern coasts of Algeria, Libya and Egypt, Central Saudi Arabia and South West of Iraq which is consistent with the Al-Najim (1975) and Hamidi et al (2013) studies.

The key theme from the review above is to highlight procedures of the identification of dust sources in the literature and how satellite products can be vital tools, in addition to the surface observations of local and regional climate stations that utilise in the aspect of the climatological conditions at the time of dust generation. This can be important to draw the pathways of dust storms during their transport (this will be discussed in sect 2.4.5).

2.4.2 Meteorological Conditions Associated with Dust Storms Generation

As discussed earlier, dust storms may occur as a result of a wide range of vigorous meteorological conditions, such as low pressure systems, cyclones, fronts and convective plumes. In most situations the key conditions leading to generation of dust storms lead to generation of strong wind shear near the ground surface that blows across

the dust source region, which may be caused by intense low pressure or strong surface turbulence, (Shao, 2008). The detailed processes can be different from one region to another and depend on which parts of the world dust storms are being generated, for example dust storms are known as haboobs in Africa.

Haboob is an Arabic origin name meaning strong wind and describes an intense and dominant mechanism of dust generation that mainly occurs in the Sahara, (Heinold et al., 2013). The meteorology driving haboobs results from the downdraughts of cold air occurring during convective storms which reach the ground and spread in different directions producing a turbulent gust front and lifting up dust particles from the surface into the air forming imposing and churning walls, (Marsham et al., 2013; Roberts and Knippertz, 2012). This mechanism of haboob generation mostly occurs in the summer climate of Sahara when heating can be very intense and complex since large scale convective circulation allows monsoonal and moist air to be circulated in medium and upper-level dynamics over the dry-disassembled soils across Sahara creating strong and deep convective storms with their associated cold air downdrafts, (Allen et al., 2013; Roberts and Knippertz, 2012). The more proposed mechanism of Haboob was detailed by (Knippertz et al., 2007) as "synoptic situation of north-westerly vertical wind shear, deep cumulonimbus clouds forming over elevated terrain blowing towards the Sahara side of the Atlas chain where the evaporation of precipitation falling through the dry and hot lowland regions leads to the formation of a cold pool that accelerates downslope toward the Sahara driven by the density and thus pressure differences to the environment", figure 2.7.

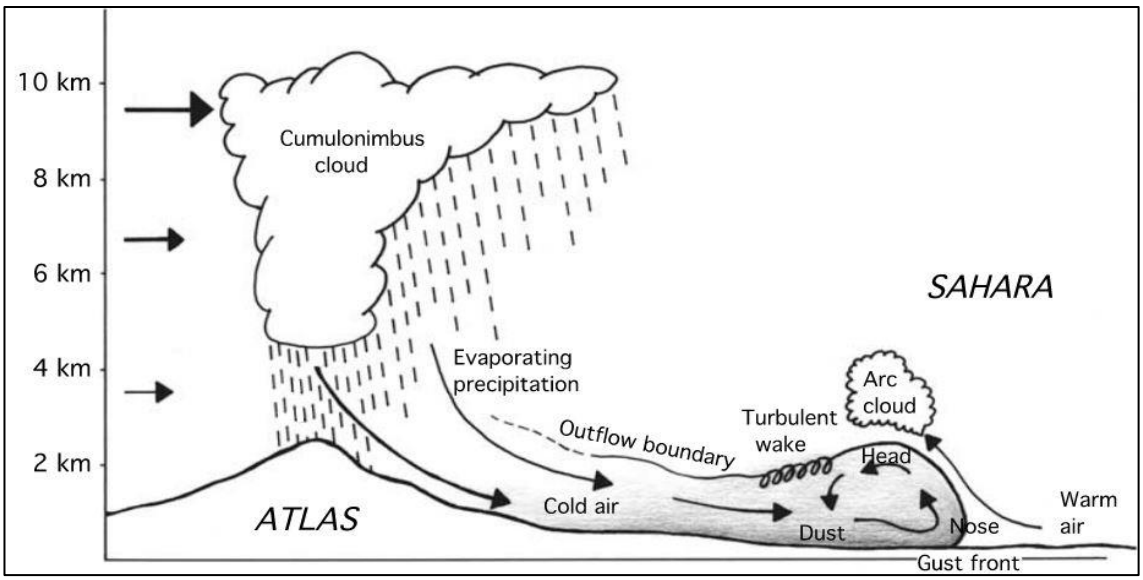

Figure 2.7: Schematic depiction of Haboob most frequent mechanism, from Knippertz et al., 2007.

In the Middle East, Middleton (1986b) mentioned that convective cells, fronts and low pressure systems are the main meteorological phenomena causing dust storms events. This discussed in more detail in Hamidi et al. (2013) who found that the main meteorological conditions leading to dust storms is the difference in pressure gradient winds. They classified dust storms in the Middle East into two groups; the first one is a class of frontal dust storms that are associated with low-pressure systems and the second group is where high pressure systems are located over northern Africa, south of the Mediterranean Sea and Central Europe. The latter synoptic situation occurred during (Ashrafi et al., 2014) which used backward trajectories from HYSPLIT (HYbrid Single-Particle Lagrangian Integrated Trajectory) to track the source region of wind that transferred a dust storm on 18th May 2010. The study found that wind transferred from the East of the Mediterranean across northern Iraq to South West of Iran.

The World Meteorological Organisation identified a minimum wind speed threshold of $\geq$7 ms^{-1} that corresponds to dust storm generation; however this threshold only represents wind speeds that report at manned weather stations, (https://www.nodc.noaa.gov/woce/woce_v3/wocedata_1/woce-uot/document/wmocode.htm, accessed on 12/03/2016). For instance, Middleton (1986b) (who referred to (Grant, 1983)) mentioned that wind speeds in the Shamal wind during dust storm events over southern Iraq and Kuwait were between 10-12 ms^{-1}. Further studies were established on the threshold of Shamal wind speed in the Middle East region, for example wind speeds of 13 ms^{-1} in Qatar, (Bartlett, 2004) 7.5 ms^{-1} (De Villiers, 2010) and 15-20 ms^{-1} over the Persian Gulf, (Rao et al., 2003) have been reported. However, wind speeds are effective at suspending dust when the surface soils are dry.

The Shamal term is used in the literature to refer to a local wind that blows from the north and north-west directions in Iraq, Kuwait and Arabian Peninsula. Wilkerson (1991) interpreted the synoptic situation leading to Shamal winds as a collision zone that is created due to a subtropical ridge that extends over northern Arabian Peninsula and Iraq and a Monsoon Trough that extends from the Mediterranean Sea across into Southern Arabian Peninsula and southern Iran. Therefore, studying wind fields patterns responsible for suspending and advecting dust wind is one important of assessing the drivers of dust storms events.

Soil susceptibility to wind speed is quite variable and depends largely on the content of soil moisture and the type of soil as well. Firstly, moisture sticks dust particles to each other and hence the resistance of particles to re-suspension from wind energy is increased, leading to a reduction in dust emissions, (Tsoar and Pye, 1987). It has been proven that dust particles can be supressed under wet soil conditions, for example an analysis of two different dust storms events that occurred in Horqin Sandy Land in China showed that the maximum of dust concentration in the air measured as 312.3 µg/m3 during a wet dust storm event (May 19th 2010) whereas a loading of 953.1 µg/m3 was observed during a dry dust storm event (May 2nd 2010), (Li and Zhang, 2014). However, the effect of soil moisture may diminish on dust emissions when the residence time of surface water in the soil is short and so the moisture content in the soil will not reach a stage of saturation which is identified as 0.410 v/v, (Park et al., 2010). The effect of moisture is also reduced when the soil moisture is retained at a depth in the soil of more than 5 cm below the ground surface, (Li and Zhang, 2012). Secondly, the type of the soil can determine its response to wind velocity. It has been stated that agricultural soils need 15.6 ms^{-1} threshold of wind speed to form dust, while typical deserts and river channel soils require 8 and 6.7 ms^{-1} wind speeds, respectively (Goudie and Middleton, 2006).

From the literature research above, there was some evidence that dust storms in Iraq and most of the Middle East regions are associated to Shamal winds, pressure gradients and fronts. However, one exception to this main driver of dust generation was proposed by Coles (1939) who observed that in Mosul city in the north of Iraq some localised dust storms were generated due to thunderstorm downdrafts that occurred most frequently (a monthly average of 4-5 days) between April-May in the years of 1929-1934, but the evidence for this relationship is quite local and inconclusive. Subsequently, the literature shows that wind speed and direction and air pressure regions are meteorological processes that directly linked to dust generation and they can be mapped to it, while there are some other meteorological conditions (e.g. convictive cells and thunderstorms) which consider more complex regarding dust formation, however they still do influence it.

2.4.3 Frequency Distribution of Dust Storms

It is important to understand the frequency of dust storm events across different regions. The frequency of dust storms changes across a range of timescales from day to day to

inert-annual due to, for instance changes in the extent of the source region dust supply (this will be discussed in more detail in sect 2.4.6) leading to changes in their effects on climate change and human health, (Goudie and Middleton, 1992).

2.4.3.1 Seasonal Frequency Distribution

The importance of investigating the seasonality of dust storms is to identify when most of the dust is generated and the type of the meteorological drivers that cause the events. The seasonality of dust storms is highly affected by regional climatological factors, the main ones of which are wind conditions, the time of day, intensity of depressions and rainfall.

The monthly mean seasonal dust frequency distribution for haboobs in the Sahel and Sahara occurs particularly between 15-20° N during March in Sudan and July in Bordj Mokhtar (south west of Algeria) with a frequency of approximately 20% and 18%, respectively (Cowie et al., 2014). This was consistent with (Laurent et al., 2008) who found that the monthly averages of dust emissions between the years (1996-2001) were at their highest peak in July and June (around 80 Tg - 65 Tg) in the region of western Sahara with a monthly average occurrence of 8% and 7.5%, respectively.

Locally, Coles (1939) reported that the northern and western regions of Iraq are dominated by high pressure systems during June-August, which limited the occurrence of dust storms in those regions and resulted in the lowest frequency of dust storms with a monthly average of only 1 day in August in Rutbah (western station) and Mosul (northern station), respectively. While the highest frequency recorded between March-July in the region of southern Iraq (e.g. 10 days in Shaibah station in July) was due to depressions moving eastward from the Mediterranean. However, Coles' work showed no evidence about whether dust storms were generated over the region of North West of Iraq or not.

The case seems to be slightly different in Al-Najim's (1975) study that showed the regions of Central of Iraq (Baghdad 21.5 days) and southern Iraq (Basrah 14.7 days) were the stations with the highest dust storm frequency, however it is important to mention that the data of Al-Najim's analysis (monthly average data of meteorology and dust storms for the period 1941-1970) represents a different period in comparison with the one used in Cole's study.

Moreover, a 21 year (1973-1993) of 3 hourly meteorological data (Kutiel and Furman, 2003) was used to assess the seasonal frequency distribution of dust storms across the Middle East. The study identified that the highest dust storm frequency (30% of the time occurrence) happened in summer in the north-eastern of Iraq (where the mountains of Zagros are located), north-eastern Syria and the southern Arabian Peninsula. While only 15% of the time occurrence of dust storms were recorded in western Iraq and western Syria, Jordan, Lebanon, northern Israel, northern of Arabian Peninsula and southern Egypt in spring. This was not the case in a study by Rezazadeh et al (2013) who analysed surface data of dust storms events from multiple meteorological stations across the region of the Middle East between 1998-2003. They found that approximately 50% of the time dust storms were observed in the lower Mesopotamia Plain in Iraq and parts of Saudi Arabia occurred in winter due to in association with north-easterly and north-westerly winds. There is not enough evidence in the literature to support high dust storm frequency in winter in the region of southern Iraq.

2.4.3.2 Diurnal Frequency Distribution

A considerable amount of literature has focussed on the diurnal cycle of dust storms. These tend to show that dust storms are at their greatest between late morning to late afternoon. During that period of the day, the daily evolution of the boundary layer plays a vital role in dust uplift, as well as airflow patterns. The boundary layer is the lowest layer of the troposphere and is influenced by the surface. It can extend to between 10 m and 5 km in height depending on the characteristics of the earth's surface, such as topography, heat transfer, friction and turbulence (Cakmur et al., 2004), surface moisture and the solar heating rate. During the daytime hours, the lower part of the boundary layer acquires temperature due to heat transfer from the earth's surface which leads to generating an upward flow of warm air (Lazaridis, 2011), figure (2.8). The warm air rises in a vertical motion and mixing with colder air in the upper layers of the boundary layer creating turbulences, (Cuesta et al., 2009). The turbulence acts on the earth's surface via drag and this acts both as an energy loss mechanism from the atmosphere and also to resuspend particles of dust. In arid and semi-arid regions soils are dry leading to significant surface heating and large vertical temperature gradients. This leads to the development of highly energetic deep convective boundary layers that promote dust generation. Since the soil is dry, disassembled and unprotected particles

from the top layer of the soils can be readily made airborne as they are liable to be re-suspended in the air, (Shao, 2008).

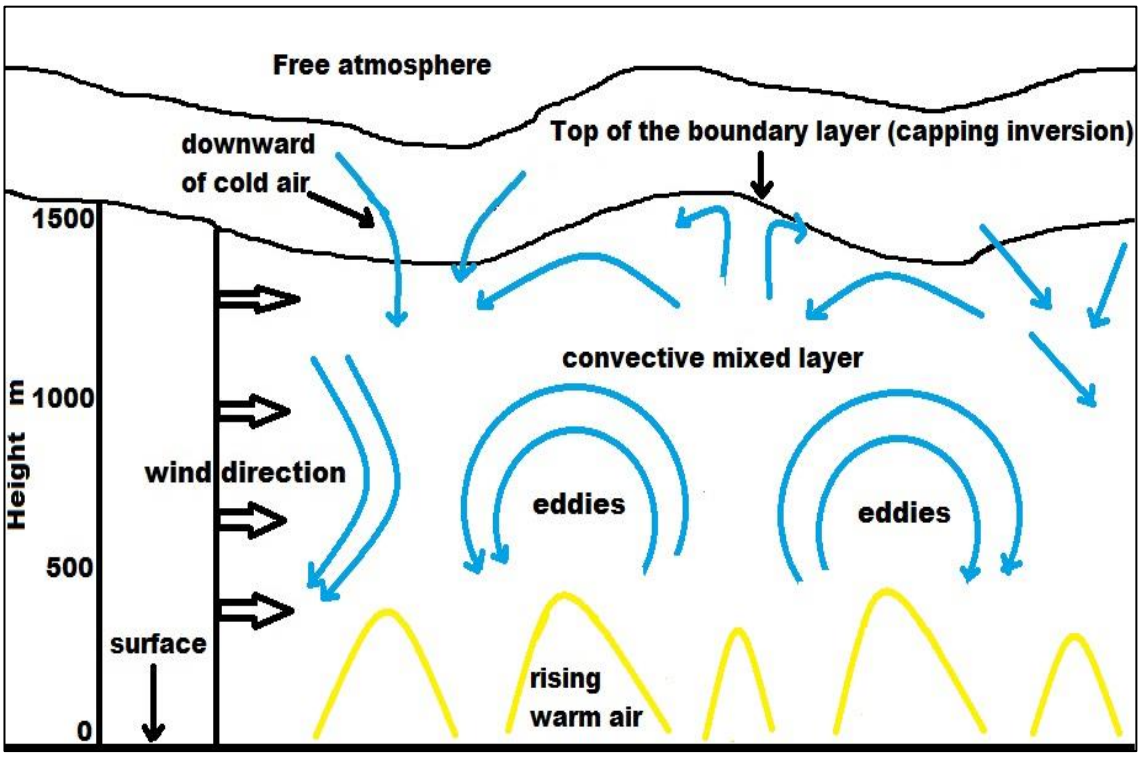

Figure 2.8: Schematic of air entrainment and circulation through a convective boundary layer, modified after (Kaimal and Finnigan, 1994; Lazaridis, 2011).

This general picture is true of haboobs. For instance, (Cowie et al., 2014) reported that approximately 23% and 15% of dust uplift occurred at 12:00-15:00 and 12:00 hours in Sudan and Egypt, respectively. While the most frequent dust storms events in Gobi desert observed during the period 1937-1999 at frequency of 24%, 21% and 19% at 15:00-18:00, 12:00-15:00 and 18:00-21:00 hours, respectively (Natsagdorj et al., 2003).

A few studies have investigated the diurnal variation of dust storms in the Middle East. For example, in Kuwait, around 78 dust storm events happened between 10:00-19:00 and this comprised > 50% of the events between 1962-1982, (Safar, 1980). The only single work in the literature that analysed dust storm diurnal distribution in Iraq was by Coles (1939) who observed that most of dust storms happened in the morning between 08:00-09:00 (Iraqi local time GMT+3) and they vanish between 15:00-16:00 in the months June-August of the years 1929-1934. They also reported that in some regions in Iraq, dust storms may commence at very early time in the morning (e.g. 03:00-05:00 at Mosul city in October), however more research using a varied set of data and time for a number of stations in the region is needed to understand the diurnal distribution of dust storms in Iraq.

The fact that most dust storms are generated during daylight hours is an important key aspect to draw an attention towards the relationship between their occurrence and the climate since they affect radiation balance and their impact on human health since exposure will be greatest.

2.4.4 Duration of Dust Storms

Dust storm events can last from a few hours to a few days, however they generally tend to be short lived, (Goudie and Middleton, 2006). The duration of dust storms is reliant on variables such as wind properties (e.g. energy, velocity and direction), atmospheric circulation, land surface features and the size of dust aerosols generated, (Parsons and Abrahams, 1994).

The duration of dust storms is now well established from a variety of studies in many regions around the world, for instance (Natsagdorj et al., 2003) showed that dust storms events in Mongolia usually last between 1-9 hours, and very rarely to last more than 24 hours. However, the vast majority of those events lasted between 3-6 hours (e.g. about 35% of the time occurrence of dust storms lasted between 3-6 hours in St.358-Zamiin-Uud station between 1937-1999). Another analysis by (Orlovsky et al., 2005) found that 72% of dust storms events between the years 1981-1995 lasted between ≤4 hours, while 20% continued for 4-8 hours and only 0.1% of dust storms events that lasted for ≥20 hours in Turkmenistan. So far, there has been no quantitative analysis in the literature about dust storms duration in Iraq and this will be the focus as part of this thesis.

2.4.5 Transport of Dust Storms

Dust storms are capable of travelling over a range of distances in the atmosphere, therefore identifying pathways of dust storms is related to identifying the source regions and dust particles size distribution and both are vital for determining their transport. On one hand, coarse particles (>20 μm) may be suspended for only a few hours travelling distances of around 100-1000 km, (Knippertz and Stuut, 2014) but that does not mean that they cannot transport over 1000 km. For instance, dust particles at range of 0.5-20 μm transported from Sahara to Evora, Portugal on 26 May 2006 after a dust storm episode, (Wagner et al., 2009). On the other hand, fine particles (<20 μm) may be transported over distances of thousands of kilometres. During such large transport, dust airborne may remain for a day or few days, (Chung et al., 2003). For instance, the French Alps have been affected by a dust storm event that travelled from China for over

a distance of ≥20000 km, (Grousset et al., 2003) - such transportation can take place over several days to few weeks.

In Africa, Haboobs are well-known with their transport of dust over mesoscale distances (200-2000 km), (Gillies et al., 1996) which may extend to (2000-10000 km) during specific intense meteorological conditions, (Miller et al., 2008). There has been some strong evidence that uplift and transport of Haboobs from African regions to the Middle East occurs particularly in the summer. This was observed during the field season of the Fennec campaign in 2011 based on a hypothesis via (Marsham et al., 2008) which confirmed that a towering haboob wall with a vertical elevation of approximately 3 km transferred from northern Sahel across the Sahara to the western edge of the Middle East region in Egypt and Sudan, (Flamant et al., 2007; Knippertz et al., 2007), (for more information about Haboobs see, (Allen et al., 2013; Cowie et al., 2014; Knippertz et al., 2007; Sodemann et al., 2015).

The transport of dust storms can be monitored by a number of complementary approaches. These include, for instance aerosol optical depth data from satellite-borne (e.g. CALIPSO Cloud-Aerosol Lidar and Infrared Pathfinder Satellite Observations) that provide an important information about vertical distribution of dust particles, (Amiridis et al., 2013), dust transport models, for example NMMB/BSC-Dust model (Non-hydrostatic Multiscale Model/Barcelona Supercomputing Centre) (figure 2.9) and meteorological satellites that consist of a number of data products, such as RGB dust products from MODIS or SEVIRI, (for more information see: Shepherd et al., 2016).
Satellite data products combined with present weather data of the surface observations from local and regional meteorological stations, e.g. NCDC (National Climate Data Centre) or The European Centre for Medium-Range Weather Forecasts (ECMWF) can offer important climatological information which can help to understand dust storms spatial scales. For example, a recent study by (Basart et al., 2016) that combined a number of observational datasets (in-situ AERONET ‘Aerosol Robotic Network’ stations, reanalysis meteorological data from ECMWF, surface weather observations from NCDC), NMMB/BSC-Dust model together with satellite aerosols data from MODIS via Aqua and SEVIRI to model dust transport over the complex topographical region of West of Asia between 17-20th March 2012.

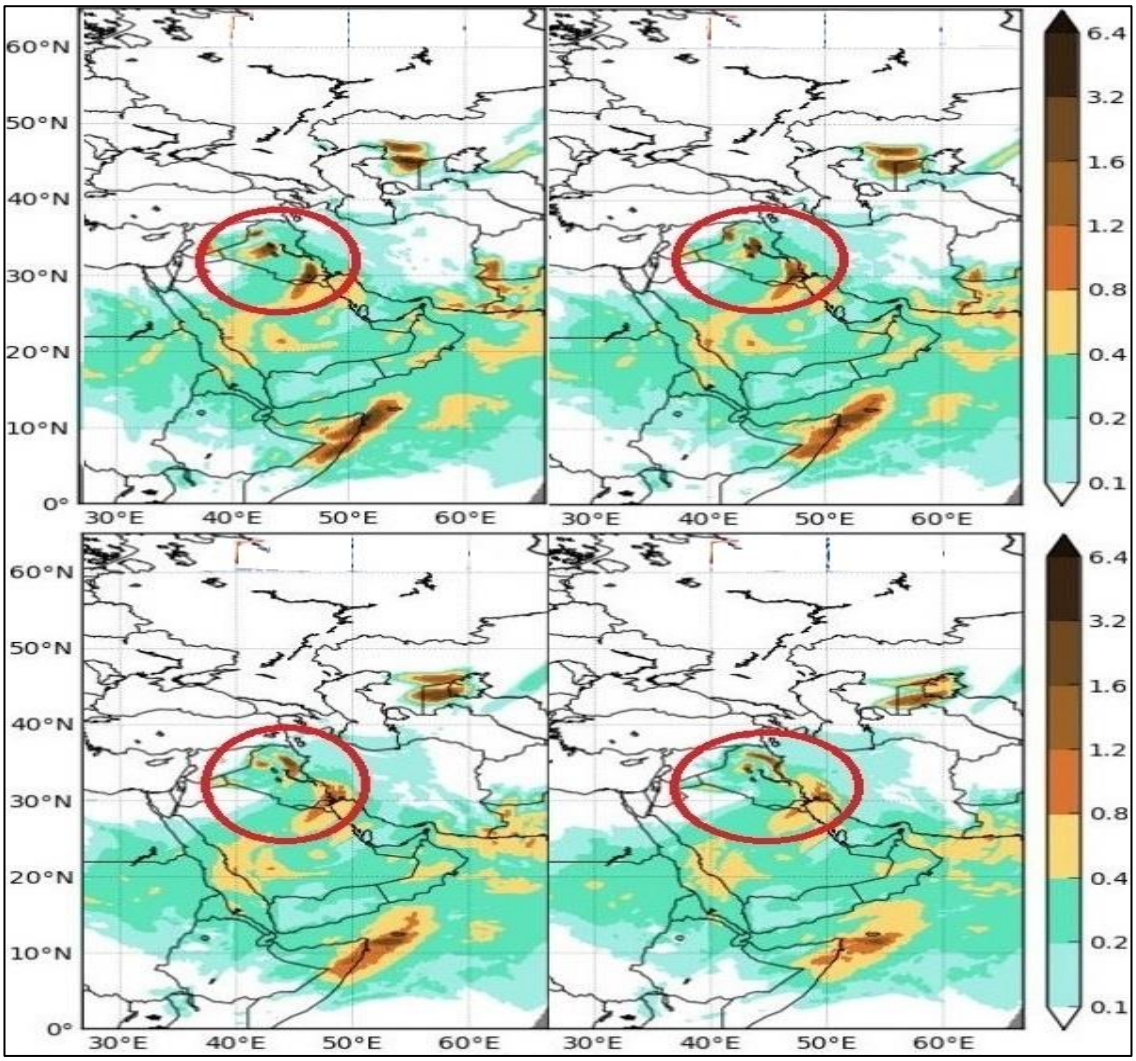

Figure 2.9: Iraq dust storm episode as captured by NMMB/BSC-Dust model. Red circle represents dust load (g/m^2) over Iraq at a resolution (1° x 1°) starting from 00:00 UTC (top left) on 31 August 2015, 03:00 UTC (top right), 06:00 UTC (bottom left) and 09:00 UTC (bottom right), source: https://dust.aemet.es/forecast/nmmb-bsc-dust-forecast-dust-load.

They showed that the model was able to represent dust propagation over the mountainous regions of south-western of Saudi Arabia, Yemen and Oman. The basic principle behind transport models is to compute simple or complex air parcel from the source region of dust storms to where they vanish. However, they are critical to use as they provide a numerical output to test against surface observations, model performance and determine transportation processes, (see Liu et al., 2011).

A number of trajectory models are commonly used for assessing air mass transport including, for instance FLEXPART (FLEXible PARTicle dispersion model) and HYSPLIT, (Draxler and Hess, 1997). Sodemann et al (2015) used FLEXPART during the Fennec/Lagrangian Dust Source Inversion Experiment (LADUNEX) in combination with a wide range of detailed aircraft measurements to estimate dust transport in western Sahara. The study showed that there was an intense convective system led to

emission and transport of dust from central Mali to northern Mauritania on 19th June 2011 at 20 ms^{-1} resulting in dust mobilization of 169.3 gm^2.

The other Lagrangian model is HYSPLIT which defined as an advection model that computes simple to complex transportation, dispersion and deposition for multiple applications in the atmosphere (e.g. air mass and air pollutants), (Stein et al., 2015). HYSPLIT, which was developed by the Air Resources Laboratory of NOAA (National Oceanic and Atmospheric Administration), is capable of identifying air parcel backward trajectories and forecasting future air parcel pathways via forward trajectories, (Fleming et al., 2012) (e.g. figure 2.10). The calculations of HYSPLIT require output from a Numerical Weather Prediction model (NWP); this includes meteorological variables, such as wind fields. In the case of backward trajectories, the NWP output and worldwide meteorological observations are assimilated to provide a reanalysis datasets. A number of model outputs can provide HYSPLIT with the required meteorological variables, but commonly GDAS (Global Data Assimilation System) meteorological fields are used (for more information see https://www.ncdc.noaa.gov/data-access/model-data/model-datasets/global-data-assimilation-system-gdas, accessed on 18/10/2017).

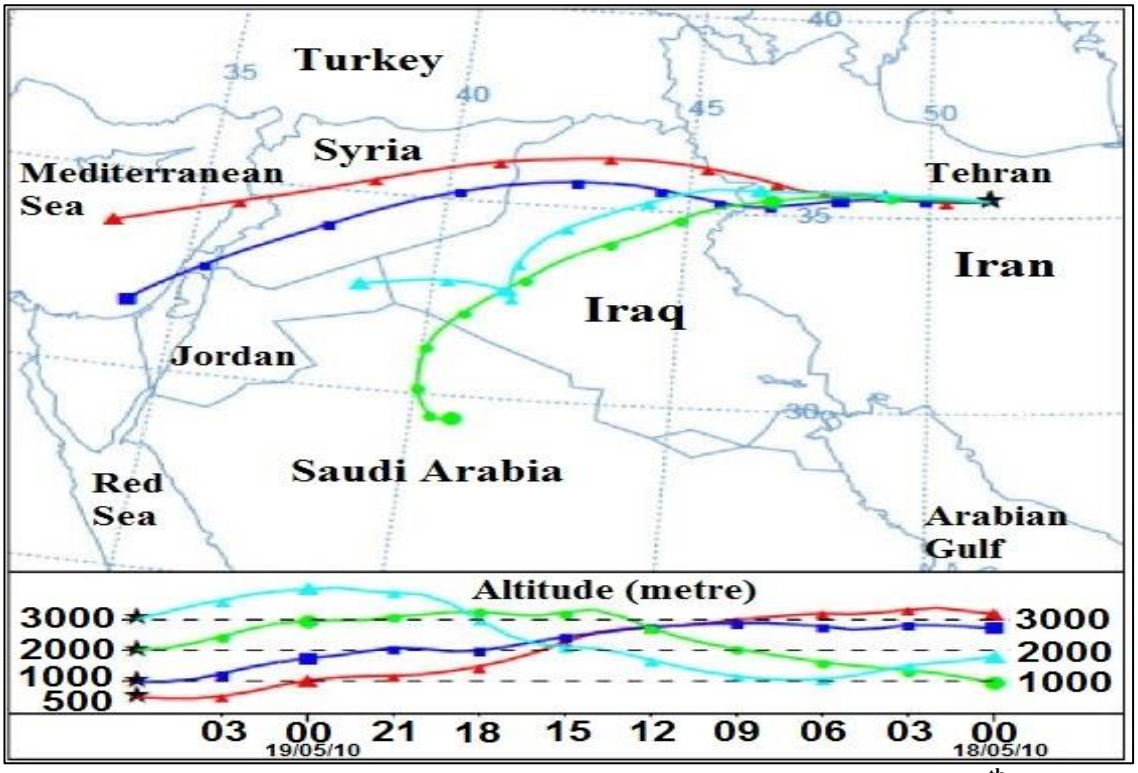

Figure 2.10: HYSPLIT backward trajectory. This released at 06:00 UTC on 19th May 2010 for 30 hours (ending at 00:00 UTC on 18th May 2010) and it shows that the source region of the air parcel when a dust storms affected Tehran (35.42° N – 51.25° E) was the East of the Mediterranean region, East Jordan and North East of Saudi Arabia, from (Ashrafi et al., 2014).

Although trajectory models remain a powerful tool for identifying transport pathways, they are not capable in capturing vertical motion, particularly in convective regions where turbulence is active in the atmosphere, (see Fleming et al., 2012). Given these limitations and the lack of priori observations, trajectory models are not typically used operationally to predict the pathways of dust storms, instead wind fields and other meteorological output from NWP are used within process models in order to estimate the transport and dispersion of dust.

The existing body of research on monitoring dust storm transport in the regions of Iraq and the Middle East shows that HYSPLIT model, for example was used first by (Draxler et al., 2001) to estimate the concentration of PM_{10} in dust storms over Iraq, Kuwait and Saudi Arabia, while (Abdi Vishkaee et al., 2012) interpreted ECMWF data and 72 hours backward trajectories from HYSPLIT to obtain further in-depth detail on the dynamical processes controlling a dust storm event that occurred on 22-23 February 2010 over Syria, Iraq and North West Iran. The latter study identified that the source region of dust was the East of the Mediterranean Sea, East Syria and North West of Iraq. Furthermore, (Notaro et al., 2013) conducted an analysis of surface hourly data from NCDC for the period 2005-2012 over 13 stations in Saudi Arabia as well as satellite images from MODIS and computed 84 hour backward trajectories via HYSPLIT. According to the analysis of backward trajectories of this study, northern and eastern regions of Saudi Arabia are influenced by remote dust transferred from the deserts of south west of Iraq and Syria.

Despite the importance of dust, there remains a paucity of evidence in the literature about dust storms in the Iraq region and more detail studies that can employ surface and satellite observations together with dust transport models are needed in Iraq.

2.4.6 Recent Trends of Dust Storms in Iraq and Syria

The extent to which dust storm frequency has changed over time may be due to, for example rapid soils deterioration, desertification or geopolitical reasons. There have been some significant changes in dust storms across Iraq and Syria over the last two decades, particularly in the Euphrates River basin (upper of Mesopotamia Plain, see figure 2.1) on the borders of North West of Iraq and East and North East of Syria (approximately 34.20.00°-36.50.00° N to 38.00.12°-41.00.20° E).

It is apparent that due to hydro-politics and geopolitical considerations, (Carkoglu and Eder, 2001; Shamout and Lahn, 2015) Turkey (as the upstream user) has been controlling the headwater of the Tigris and Euphrates Rivers basin and this has had an impact on the downstream users in Syria and Iraq. It has been observed, (Voss et al., 2013) that particularly during the period 2003-2009, the lower Euphrates River basin lost about 144 km^3 of water. This resulted in a paucity of water supplies in the downstream countries, for example the amount of water dropped from approximately 145 metre (elevation) on 7th September 2006 to 120 metre on 15th September 2009 in the Qadisiyah reservoir in Iraq due to the continuous demands on supply and the low inflows from the upstream dams in Turkey, (figure 2.11). Moreover, according to the Ministry of Water Resources of Iraq, Turkey has decreased the monthly averages of the Euphrates and Tigris water discharge (cubic meter per second) from 967 between 1948-1972 to 553 between 1985-2007 in the Euphrates River (at Haditha dam) and from 927 between 1960-1999 to 520 between the years 2000 and 2012 in the Tigris River (at Sarai Baghdad station) (Al-Ansari, 2013; Al-Shahrabaly, 2008). These statistics were consistent with other neutral sources and references, such as (Jongerden, 2010) who reported a severe water-supply shortage during the year 2009 where water supply in the Euphrates and Tigris Rivers in Iraq had dropped from 40 billion cubic metre in 2006 to 11 billion cubic metre in 2009 (consistent with the NASA satellite image (shown in fig. 2.11) of water reduction during the same period above). The key point behind the emphasis on the shortage in water-supply via Turkey is to introduce water reduction as one vital environmental driver which can lead to decreased farming activity in the Euphrates River basin, consequently reducing vegetation cover (as showing in figure 2.12) or causing land deterioration and decreasing population in the basin region.

The hydro-politics of reducing water supplies has resulted in decreasing the vegetation cover in the Euphrates River basin; this can be seen through the Normalised Difference Vegetation Index (NDVI), figure 2.12. It shows that the vegetation cover decreased fairly steadily between September 2003 and September 2009 which is the exact same period when 144 cubic kilometres of water was lost in the Euphrates River basin and has reasonably remained at consistently lower fractional cover to the present day. Furthermore, it shows that during the deterioration of the vegetation cover, the local climatology of the Euphrates River basin was consistent and there were no extreme changes during the period above and instead, for example monthly averages of temperature (1.85-32 C), (GLDAS_NOAH10_M v2.0/ Model at 1 degree) and rainfall

(0-17 cm), (TRMM_3A12 v7 at 0.5 degree) were consistent and they possibly enhance the negative role of the hydro-politics in the basin.

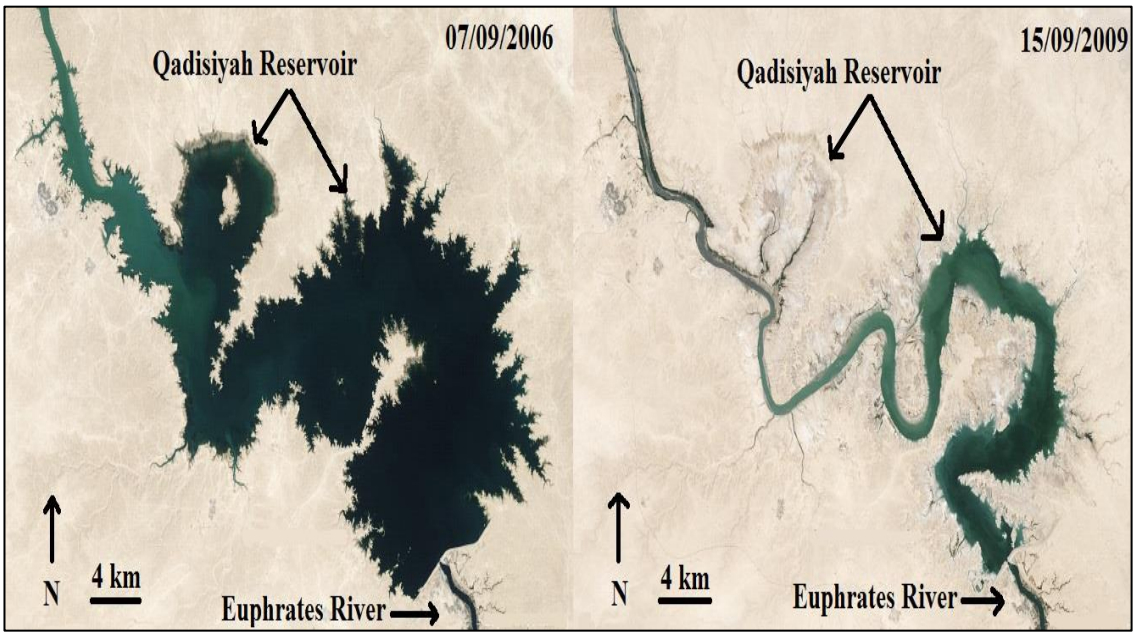

Figure 2.11: True colour images by Landsat 5 TM satellite, NASA (National Aeronautics and Space Administration). The images show shrinking in the water level in the Qadisiyah reservoir in Iraq, source: (https://earthobservatory.nasa.gov/IOTD/view.php?id=80613, accessed on 24/11/2017).

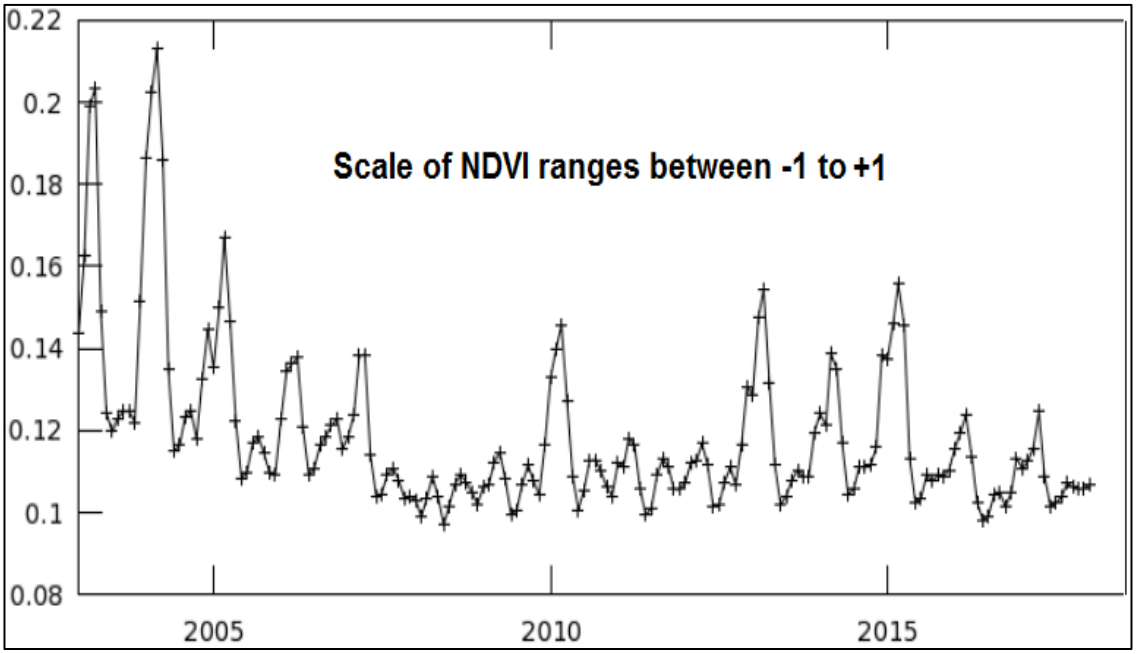

Figure 2.12: The monthly averages of the vegetation cover from NDVI from (MODIS-Aqua MYD13C2-0.05 degree). This was for the period September 2003-December 2018 in the Euphrates River basin 34.20.00°-36.50.00° N to 38.00.12°-41.00.20° E (see figure 2.1 for easier identification). Source: (https://giovanni.gsfc.nasa.gov/giovanni/#service=TmAvMp&starttime=2015-08-31T00:00:00Z&endtime=2015-08-31T23:59:59Z&bbox=35.9033,28.5645,48.6475,38.0127&data=MOD08_M3_6_Deep_Blue_Aerosol_Optical_Depth_550_Land_Mean_Mean%2CMYD08_D3_6_Deep_Blue_Aerosol_Optical_Depth_550_Land_Mean&variableFacets=dataFieldMeasurement%3AAerosol%20Optical%20Depth%3B accessed on 21/12/2017**).**

Moreover, a deeper and more representative analysis was performed to quantify the significance of the changing in the vegetation cover during the period when water supply had massively decreased in the Euphrates River basin due to the hydro-politics. Figure (2.13) shows the average Enhanced Vegetation Index (EVI) (derived in the same procedure as in NDVI which described in sect 2.4.6 and figure 2.12, for more information see e.g. (Boegh et al., 2002; Sims et al., 2008)) in the Euphrates River basin and its surrounding regions for the period 01/02/2000 to 31/03/2019. The enhanced vegetation index averaged over the entire period shows whether the changes in available water between 2003-2009 have had a lasting impact on the vegetation of the region. The figure largely shows the basin region under a high rate of desertification (particularly around areas with yellow arrows in northern and north east of Syria) and in contrast, it distinctly demonstrates high vegetation cover (blue areas) essentially in Turkey and its territories northern of the Euphrates River basin.

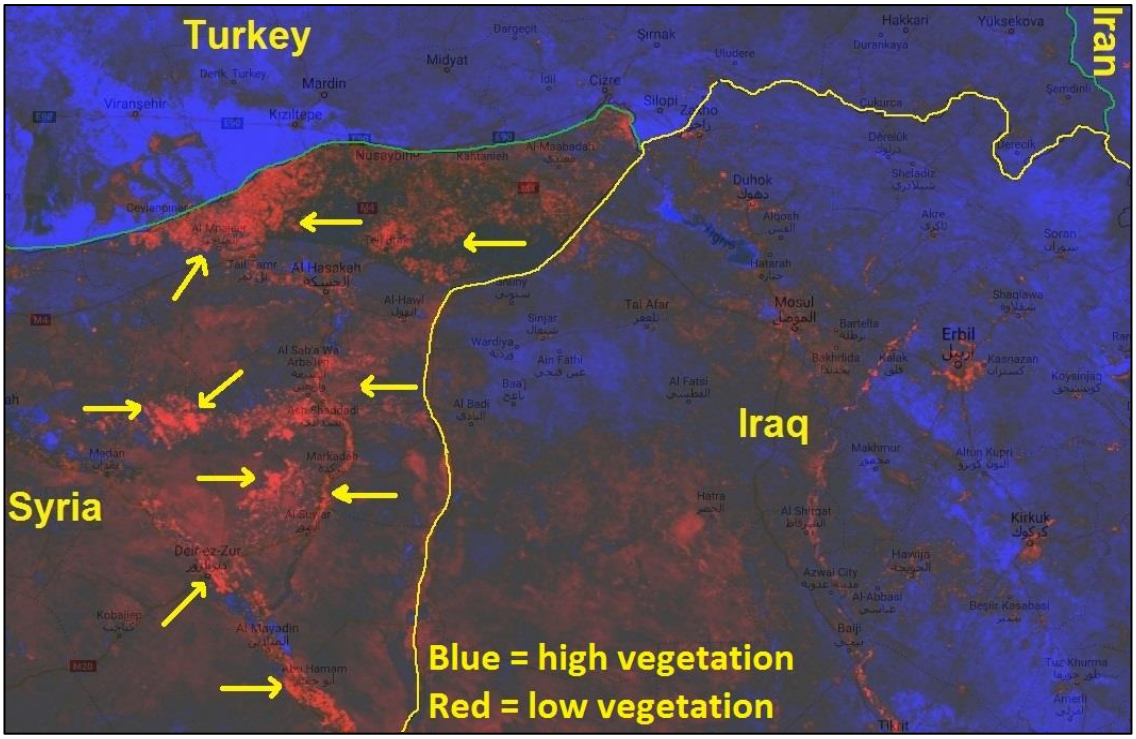

Figure 2.13: The monthly averages of the Enhanced Vegetation Index (EVI) from (MODIS-Terra CMG 0.05 degree MOD13C2 v006). This was for the period 01/02/2000 to 31/03/2019 in the Euphrates River basin and its surrounding regions. Source: (https://giovanni.gsfc.nasa.gov/giovanni/#service=TmAvMp&starttime=&endtime=&data=MOD13C2_006_CMG_0_05_Deg_Monthly_EVI&dataKeyword=evi, accessed on 05/01/2019).

Although, few studies were conducted to show satellite products of dust storms event in the Middle East, (e.g. Banks and Brindley, 2013; Basart et al., 2016; Ginoux et al., 2012; Jafari and Malekian, 2015; Kutuzov et al., 2013; Moridnejad et al., 2015; Parolari et al., 2016; Wang, 2015), however no systematic study of changes in dust storms

frequency has been carried out to date, particularly regarding the Euphrates River basin in Syria and Iraq. For instance, a study by (Kutuzov et al., 2013) employed a combination of RGB products from SEVIRI, DEEP BLUE from MODIS, isotopic analysis and HYSPLIT backwards trajectories reported dust generation, transport and deposition between 2009-2012. The study showed that 13 incidents of dust events were generated over the Middle East and deposited dust on Mount Elbrus, four among these were specifically transported from the Euphrates River basin.

A key importance of the previous discussion is to identify if there is a connection between the limited water supplies from Turkey in the Euphrates River basin and changes in dust generation in the region. Consequently, more detail and strong evidence regarding the Euphrates River basin dust generation is certainly needed.

2.5 Thesis Objectives

There are two primary questions that this thesis attempts to answer in order to achieve the thesis objectives. The first question is "what are dust storms climatologies in Iraq between (1985-2013)?". This aim will be achieved by analysing the relationships between surface wind speed and direction of dust storms frequency to statistically interpret dominant meteorological controls and local climatology in Iraq across a range of timescales from intra-day to annual in order to understand whether dust storms events are short or long lived duration. This will be achieved by using a set of 3-hourly meteorological data that have been obtained from the Iraqi Meteorological Organisation for the period 1985-2013.

The second question will be "where are the source regions of major dust storms located in the region?". This aim will be addressed by employing the same Iraqi surface observing data above, in addition to retrieval of dust data from the SEVIRI instrument for the same period above. Identifying source regions of dust storms can assist to understand their spatial distribution in the region, therefore leading to investigating of transport pathways.

The third main aim in this thesis is addressed as; "what are the transport pathways of Iraqi major dust storms?". By using the outcomes of the previous question, long range transport pathways of large dust storms events will be investigated via backward and forward air mass trajectories from the HYSPLIT model as well as wind-fields data from ECMWF to identify climatologies features of the long range transport type of storms

which would enhance knowledge of spatial extent characteristics. To sum up, case studied from the outcome of all the objectives above will be demonstrated to present an example of an actual event of dust storms from the observing and satellite data.

2.6 Thesis Structure

This thesis adopts a geographical approach by addressing elements of climatology. The thesis will be structured as follows: chapter 1 presents an introduction of dust storms, e.g. definition, life cycle in the atmosphere and influences on humans and the environment. Chapter 2 illustrates Iraq as a study region from the perspectives of the geographical location, topography, soils and climate properties, in addition to a literature review of the previous studies that investigated in dust storms from global, regional to local scales to identify the state of knowledge and highlighting current uncertainties. Chapter 3 discusses the interpretation of surface observations in terms of dust storms climatology; followed by chapter 4 that sheds light on the identification of the source region of the majority of large dust storms events in Iraq and assess the main transport pathways. Chapter 5 explores in the economic impacts of dust storms on human as well as discussing of producing a potential dust storms early warning system in the region. A summary of the main findings will be demonstrated in chapter 6. Additional materials of the thesis will be presented in a (CD) in supporting to chapter 4, in addition to presenting large dust storms events because of the high resolution and effect of tracking dust plumes from the source regions which can be visually localised and readily observed by inspecting consecutive images during dust advection.

'Blank page'

Chapter Three: Climatology of Dust Storms in Iraq between 1985-2013

The specific objective of this chapter is to determine the frequency distribution of dust storms events in Iraq and its relationship to the meteorology of the region to provide a linked statistical climatology. In order to achieve this objective, 3-hourly meteorological datasets that have been obtained from the Iraqi Meteorological Organisation for the period 1985-2013 was used. The objective of this chapter points to national mitigation measures involving local agriculture and land management practices being required to reduce the impact dust on human health close to densely populated regions of the country.

3.1 Data and Methodology

A meteorological dataset of 29 year (1985-2013), was obtained from the Iraqi Meteorological Organisation, for which systematic observations were available for 11 stations across Iraq, (see figure 3.1). The observations were employed in this thesis to examine relationships between surface winds parameters and dust storms leading to identify the frequency distribution of dust storms to statistically interpret dominant meteorological controls and local climatology in Iraq. The surface observations were also used in this thesis to investigate the spatial characteristics of Iraqi dust storms with a focus on the identification of dust storms source regions and transport pathways. The latter purpose will be addressed by employing satellite data too (this will be discussed in section 4.2). The dataset consists of 14 thermodynamic variables that have been observed and recorded at 3-hourly intervals (all times stated in this chapter represent the local time in Iraq, GMT+3 hours). The parameters that have been used in this study are: wind direction, wind speed and dust storm observations (and their classification that described further below) that observed at 11 IMO observing stations, these are: Aziziyah, Baiji, Baghdad, Basrah, Diwania, Hai, Hilla, Khalis, Najaf, Nasiriyah and Simawa, (see table 3.1).

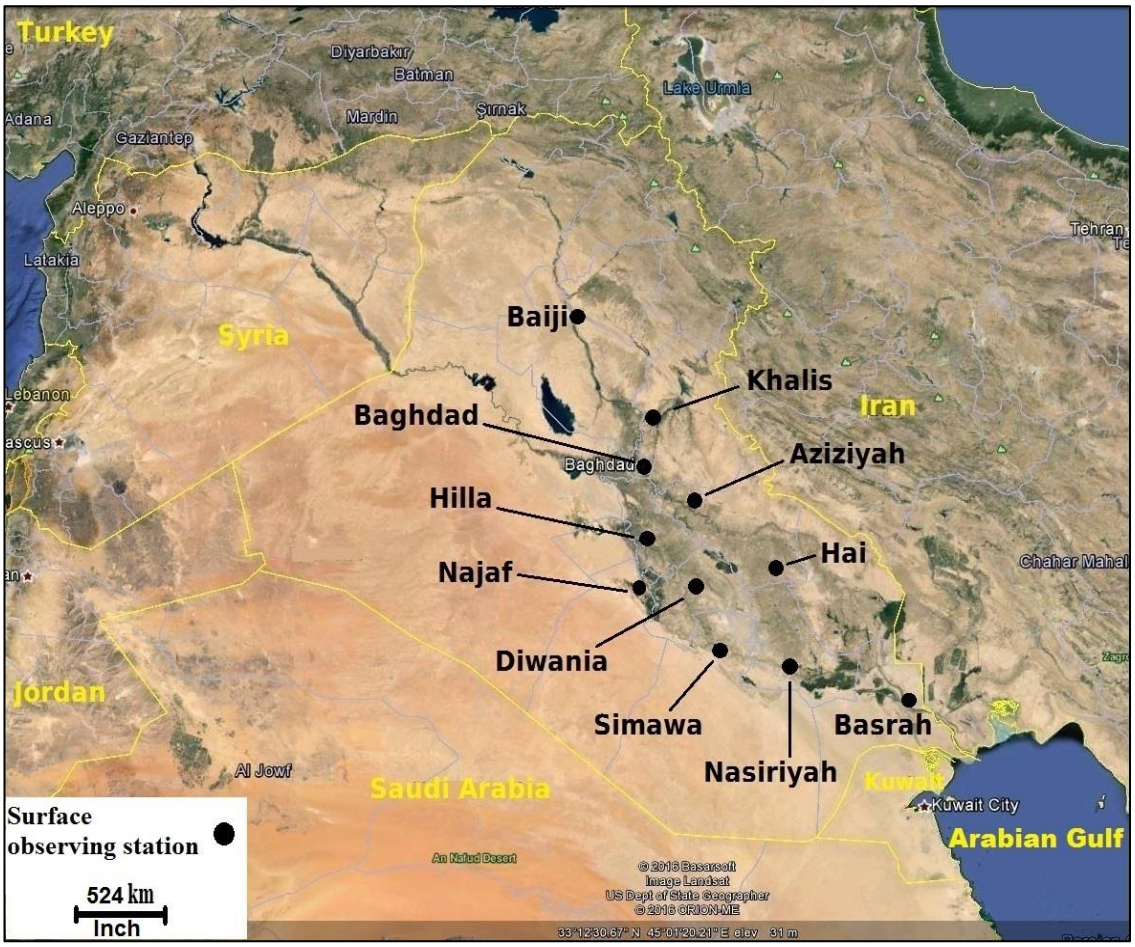

Figure 3.1: The spatial distribution of the climate stations in Iraq, source: (GoogleEarth, 2013) and the Iraqi Meteorological Organisation (IMO), 2015.

no	station	longitude	latitude	Data available from	Data available to	Total number of observations
1	Aziziyah	45.04	32.55	01/05/1994	31/12/2013	54290
2	Baiji	43.32	34.54	01/04/1985	31/12/2013	76069
3	Baghdad	44.24	33.18	01/01/1984	31/12/2013	81104
4	Basrah	47.47	30.31	01/08/1987	30/06/2013	70557
5	Diwania	44.57	31.57	01/04/1985	31/12/2013	75154
6	Hai	46.02	32.08	01/04/1985	31/12/2013	74467
7	Hilla	44.27	32.27	01/12/1987	31/12/2013	71927
8	Khalis	44.32	33.50	01/12/1990	31/12/2013	60120
9	Najaf	44.19	31.57	01/04/1985	31/12/2013	71465
10	Nasiriyah	46.14	31.01	01/04/1985	31/12/2013	74184
11	Simawa	45.16	31.16	01/04/1985	31/12/2013	66991

Table 3.1: The IMO meteorological observing stations in Iraq and the total number of observations, source: (IMO, 2015). Note: all stations are missing the data of the year 2003, this was the war year and there were no observations available.

Wind speed was measured by an anemometer placed on the roof of each observing station at 10 metres above local ground level, while dust categories (suspended dust,

rising dust and dust storms) were typically interpreted visually in all stations except Baghdad, which is equipped with a Runway Visual Range (RVR) instrument, (for more details about the instrument see: (Lefkowitz and Schlatter, 1966), (Ali Tariq, personal communication, 2016). The dust observing system is based on the World Meteorological Organisation code no: 4677 that represents reporting of present weather data at a manned station.

The visual observations were made every 3 hours during the day and were based on an observer interpreting the appearance of distant objects (land features) to estimate the visibility due to airborne dust. At night time, it is possible that visual observations of dust may be systematically different to those during the day due to changing light conditions. For this potential, it has been checked in this study that for systematic bias in the dataset by comparing the manual observations that were made at all observing stations with statistics of the measurements of the automatic station at Baghdad Airport. This comparison showed no detectable day-night observation biases and that all statistics are consistent across the data set.

The WMO observing classification of dust storms (see table 3.2) are based on thresholds of wind speed greater than 7 ms^{-1} and visibility less than 1 km, are segregated based on the subjective severity of the storm and whether it is increasing or decreasing. In this study, all the records of dust storm class (codes 30-35 in table 3.2) were summed together to represent a dust storm event at a given station at that time. Suspended dust and rising dust were not considered in this analysis; however a similar analysis was performed for suspended and rising dust and compared both the annual and the diurnal cycles and the results were consistent. But, for the purpose of this work, only the frequency distribution of dust storms will be presented in this thesis since these represent the major dust incidences and do not include much localised dust resuspension events.

3.2 The Climatology of Wind Direction and Wind Speed across Iraq

Figure 3.2 shows that north-westerly winds are the most dominant across much of Iraq. It can be seen that at the Hai, Basrah, and Simawa stations, north-westerly wind directions constitute 42%, 32%, and 28% of observations, respectively. Wind directions from the north-west are also typically stronger than those from southerly and easterly directions. The wind speed reached 10-15 ms^{-1} in Khalis, Baghdad, Hilla, Diwaniyah and Aziziyah and 15-20 ms^{-1} in the southern stations of Nasiriyah, Simawa and Basrah.

Dust condition	*Definition*	*Wind speed threshold*	*Visibility*	*Code*	*Intensity*
Dust storm	Dust storm or sandstorm within sight at the time of observation, or at the station during the preceding hour.	≥7 ms^{-1}	<1000 metre	30	Slight or moderate dust storm or sandstorm - has decreased during the preceding hour.
				31	Slight or moderate dust storm or sandstorm - no appreciable change during the preceding hour.
				32	Slight or moderate dust storm or sandstorm - has begun or has increased during the preceding hour.
				33	Severe dust storm or sandstorm - has decreased during the preceding hour.
				34	Severe dust storm or sandstorm - no appreciable change during the preceding hour.
				35	Severe dust storm or sandstorm - has begun or has increased during the preceding hour.
Suspension dust	Widespread dust in suspension in the air, not raised by wind at or near the station at the time of observation.	≤6 ms^{-1}	1000-10000 metre	06	N/A
Rising dust	Dust or sand raised by wind at or near the station at the time of observation, but not well-developed dust whirl(s) or sand whirl(s), and no dust storm or sandstorm seen.	≥7 ms^{-1}	1000-10000 metre	07	N/A

Table 3.2: The World Meteorological Organisation dust code (4677). Source: (https://www.nodc.noaa.gov/woce/woce_v3/wocedata_1/woce-uot/document/wmocode.htm, accessed on 12/03/2016) and (IMO, 2015).

More frequent westerly winds (10-15 ms^{-1}) were noted in the stations of central and northern Iraq. These are: Aziziyah 22%, Khalis 11% and Baiji 10%, while a northerly component is evident in some stations, i.e. Najaf 19%, Hilla and Diwaniyah 12% (15-20 ms^{-1}). Finally, north-easterly, easterly, south-easterly, southerly and south-westerly wind directions are relatively infrequent <7% and weak <7 ms^{-1} in all cases in the region.

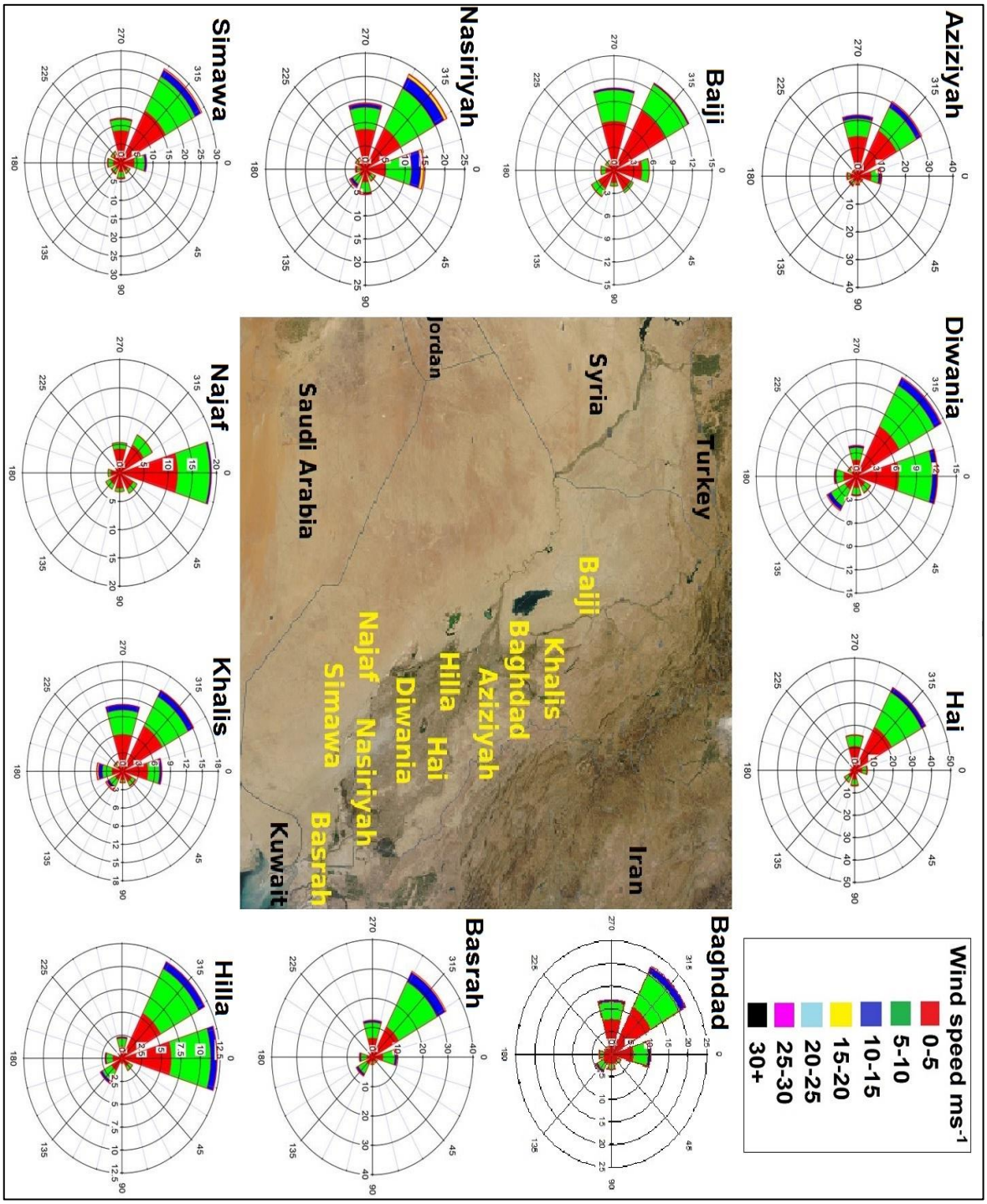

Figure 3.2: Fractional distribution of wind direction and wind speed frequency distribution in Iraq 1985-2013.

3.3 Frequency Distribution of Dust Storms and Their Relationship to Wind Direction and Wind Speed

While dust storms in Iraq can occur in any wind direction, the frequency distribution of dust storms is much higher during north-westerly, northerly and westerly wind directions. Figure 3.3 illustrates that dust storms reported at the majority of the stations are associated with a prevailing north-westerly wind in central and southern Iraq. In this analysis, each 3 hourly observation was treated as a separate dust event, given that only 17% of events last

more than >6 hours, (see sect 3.6). The statistics presented in this section will not be biased by large single dust storms lasting more than 2 successive observations. The stations with the highest frequency of dust storms occurring during periods of north-westerly wind were Basrah (65%), Aziziyah (45%) and Hai (40%).

In northern Iraq, the frequency of dust storms is greatest during westerly winds, about (65%) and (33%) of observed dust storms events at Baiji and Khalis occurred during westerly winds, respectively. Whereas in the west dust occurrence is greatest when the

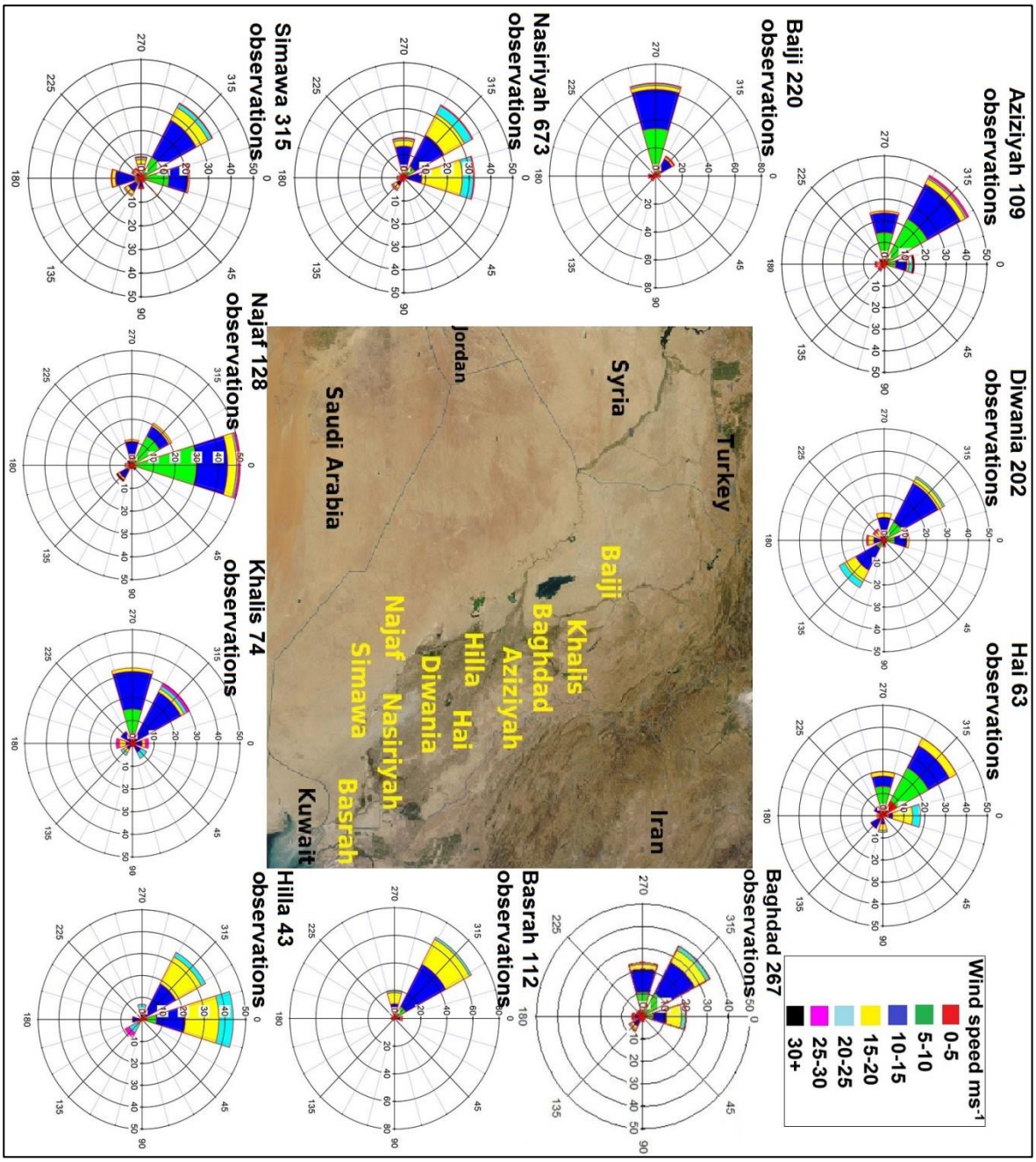

Figure 3.3: Fractional distribution of wind direction and wind speed frequency distribution only in the presence of a dust storm event in Iraq 1985-2013. This was derived by using all dust storms codes (30-35) that described in table 3.2 and section 3.1.

wind is from the north, 50% of the storms at Najaf and 45% of those at Hilla were associated with winds with a strong northerly component with speeds between 20-25 ms^{-1}.

At all stations and in all wind conditions, dust storms are more frequent in the wind speed range between 8-20 ms^{-1}. For instance, in Baiji there were 60, 34 and 60 dust storms observations (out of 220 observations) recorded at wind speeds of 9, 10 and 11 ms^{-1}, respectively.

3.4 The Seasonality of Dust Storm Events

In general, the number of dust storms in Iraq is highest in spring and summer and very low in autumn and winter. Practically, the stations can be divided into two groups: the first group is when the peak of dust storms is observed in spring and the second group represents the peak in summer. Figure 3.4 shows the number of dust storm episodes (number of dust storm (days) per month for the whole period of the study) for the stations where the peak frequency of dust storms occurred in the spring.

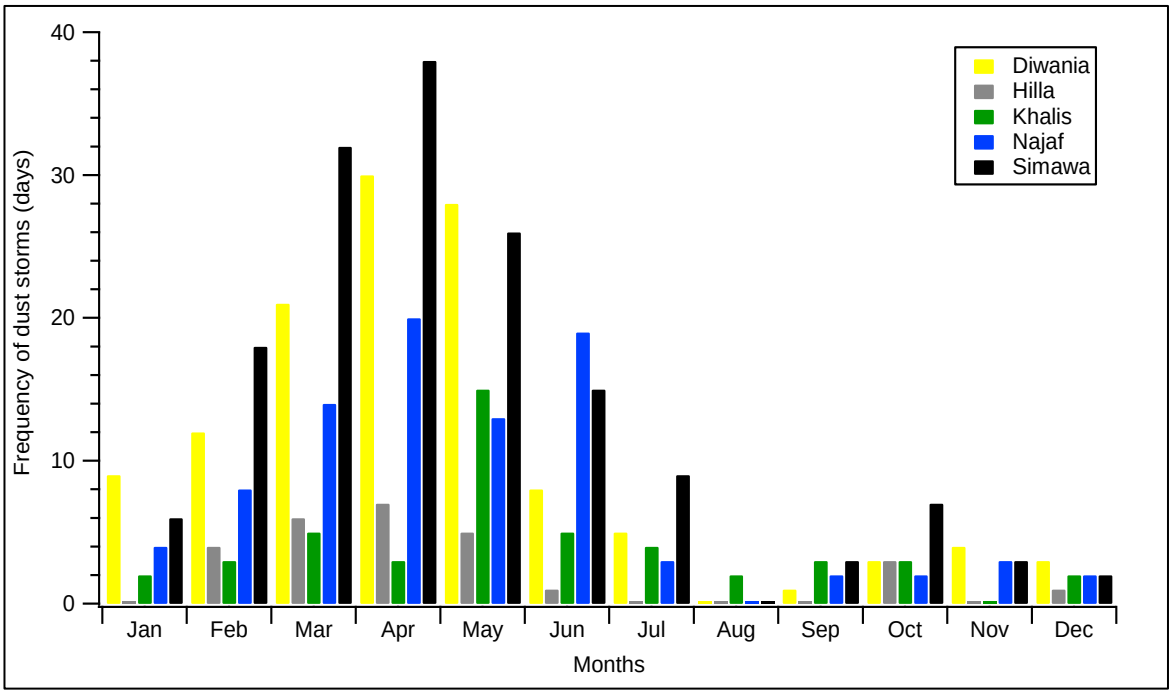

Figure 3.4: The distribution of dust storms (days) where the peak is observed in spring in Iraq 1985-2013. This was derived by using all dust storms codes (30-35) that described in table 3.2 and section 3.1. Each 3 hours observations were grouped into days, therefore each 8 observations counted as one day.

The stations recording the highest number of dust storms in spring were Simawa and Diwania in March and April (32 and 38 days respectively). While Nasiriyah and Baghdad observed as the highest number of dust storms events during the summer period with 67 (days) in June and 69 (days) in July in Nasiriyah and 39 (days) in June and 38 (days) in July in Baghdad, figure 3.5.

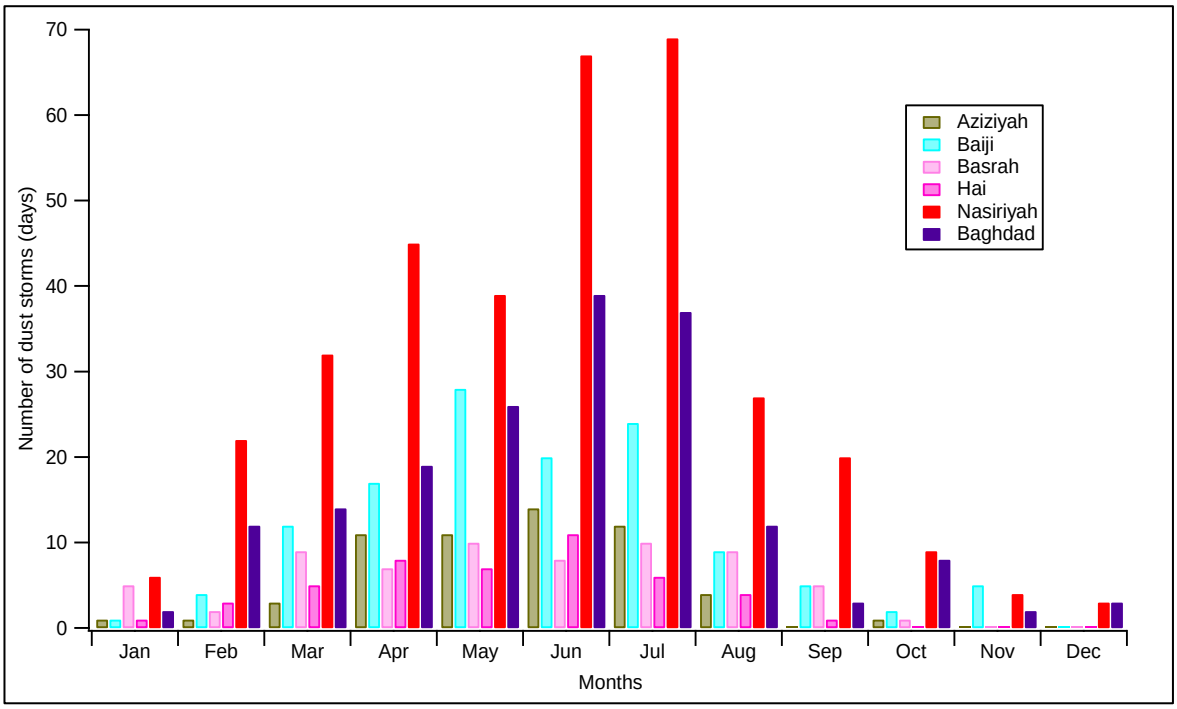

Figure 3.5: The distribution of dust storms (days) where the peak is observed in summer in Iraq 1985-2013. This was derived by using all dust storms codes (30-35) that described in table 3.2 and section 3.1. Each 3 hours observations were grouped into days, therefore each 8 observations counted as one day.

3.5 The Annual Average Number of Dust Storms

This section presents annual average numbers of dust storms over the period 1985-2013 at each of the stations. The annual average number of dust storms has been calculated in the following way:

$$\text{Annual average number of dust storms} = \left(\frac{NT}{N}\right) 8 \times 365.25$$

Where:

NT = total number of dust storms observations.

N = total number of the observations.

8 = the number of the observations/day.

365.25 = number of days/year.

There are some significant variations in the annual average number of dust storms across Iraq. The maximum annual average dust storm frequency occurred in the south of Iraq at Nasiriyah (26 days) and Simawa (14 days). Whilst, the lowest number of dust storms recorded annually were observed at stations in central Iraq at the sites of Hilla, Khalis and Hai, which recorded dust storms on 2, 3 and 4 days, respectively.

3.6 The Diurnal Distribution and the Duration of Dust Storms Frequency

There are several differences in the diurnal distribution of dust storms events between the stations (see figure 3.6). The majority of dust storm episodes generally occur in the daytime hours (peaking at around midday) and decrease in the night-time. As an overall trend, it is clear that the number of dust storms increases fairly rapidly from 6:00-9:00 to 12:00-15:00 before it sharply drops from 15:00-18:00 to the end of the day.

The highest number of dust storm events seen in Nasiriyah 203, 178 and 130 happened at 12:00-15:00, 9:00-12:00 and 15:00-18:00, respectively, while at the Baghdad station there was 80 and 65 dust storm observations which occurred between 9:00-12:00 and 12:00-15:00, respectively. In all cases, there were quite low frequencies of dust storm events in the early daytime 00:00-6:00 (e.g. 2 dust storms observations only occurred at 00:00-03:00 in Basrah) and the local midnight time (21:00-24:00) (e.g. 3 dust storms observations in Basrah).

Figure 3.7 shows the frequency distribution of the duration of observed dust storm events. Most of the dust storms are short lived (83% of events last <6 hours), with the period of greatest frequency being between 0-3 hours and the great majority lasting <6 hours at all stations. The highest numbers of dust storm events were 166 and 119 observations that lasted between 0-3 hours in Nasiriyah and Baghdad, respectively. However, some dust storms were observed to last >6 hours, this can be seen, for instance in Nasiriyah where 66, 18 and 6 dust storm observations continued for 6-9, 9-12 and 12-15 hour, respectively. However, it is found that only 17% of events last more than 6 hours in the dataset, indicating that though long range transport of dust, does occur across Iraq the majority of events are locally generated.

3.7 Discussion

In this chapter, long term, routine meteorological observations for the period (1985-2013) were analysed to understand the meteorological influences on dust storm episodes in Iraq.

It is found that the high occurrence of dust storms during the dry season when north-westerly winds were dominant (March-September) was consistent with the study of Coles (1939). However, the outcome of this analysis does not support Coles' assertion that dust storms frequently occur during periods of winds from south-easterly, southerly and south-westerly directions.

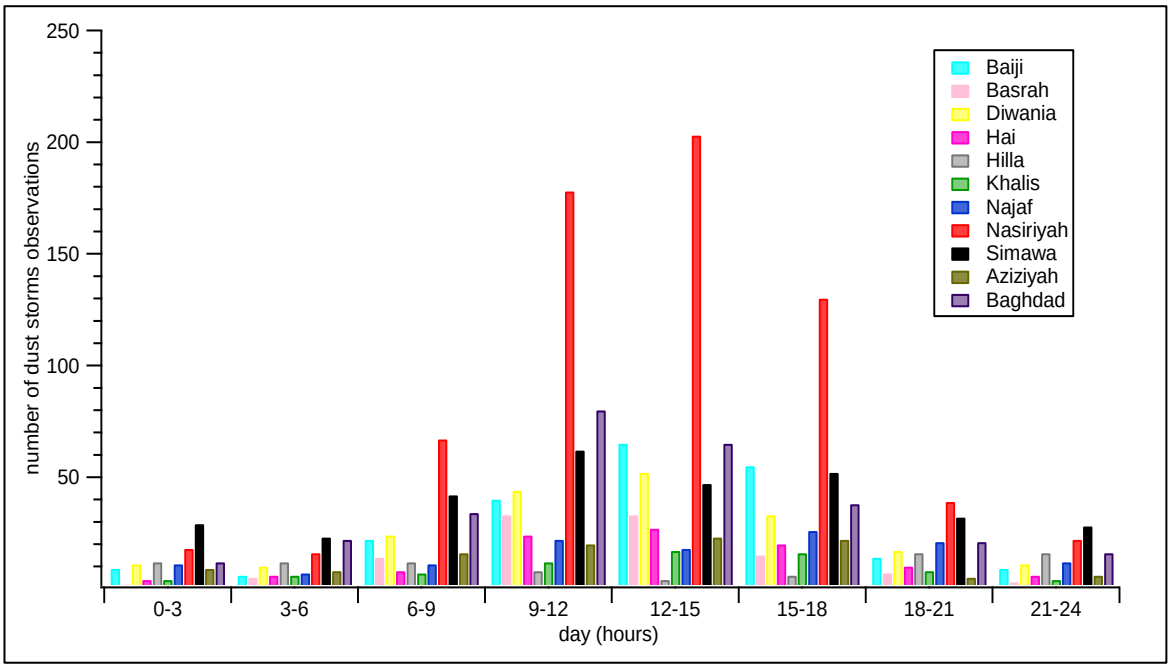

Figure 3.6: The diurnal distribution of the annual number of dust storms in Iraq (1985-2013). This was derived by using all dust storms codes (30-35) that described in table 3.2. The 3 hourly bins produced also in line with the method described in section 3.1. The local time in Iraq is GMT+3.

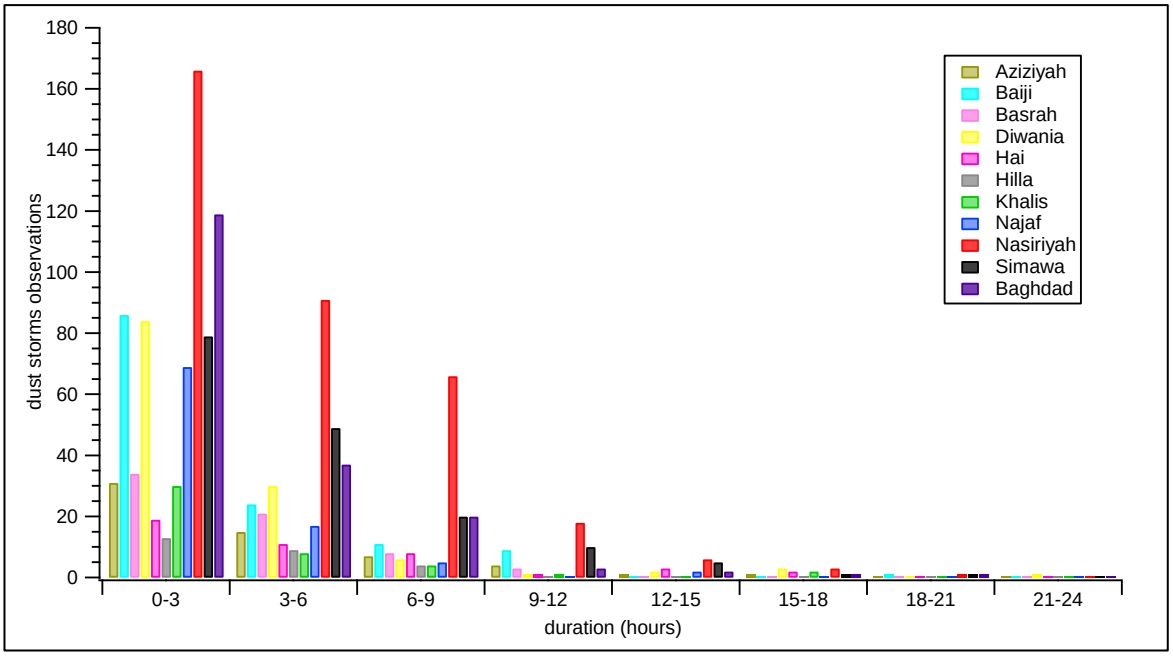

Figure 3.7: The duration (hour) of dust storms episodes in Iraq (1985-2013). This was derived by using all dust storms codes (30-35) that described in table 3.2. The 3 hourly bins produced also in line with the method described in section 3.1.

A study conducted by (Al-Najim, 1975) used a set of monthly averages of meteorology and dust storm observations for the period (1941-1970) and concluded that the desert of South West Iraq is the main source of aerosol input to dust storm events, and that the sites with the greater frequency of dust storms were Baghdad (21.5 days) and Basrah (14.7 days). Broadly, this agrees with the analysis in this chapter, but the two sites experiencing the most frequent dust events in the earlier study were not the same as in this analysis.

However, it is not possible to conclude whether this represents a shift in dust storms climatology between the study periods, or whether it is due to differences in the way observations were taken or changes in the measurements stations.

It is found that Nasiriyah and Simawa were the highest stations in the yearly average number of dust storms 26 (days) and 14 (days), respectively. These findings agrees with those of (Middleton, 1986a), who showed that Nasiriyah (33 days) recorded the highest yearly average number of dust storms.

A possible explanation of the high number of dust storms in spring (particularly in March and April in Simawa and Diwania) might be that the seasonal change in atmospheric circulation and the transition to a climatological regime dominated by the Asian high. In other words, the properties of the weather in spring are conducive to dust storm genesis, characterised by low precipitation, increasing the average of wind speed and temperature. In contrast, dust storms in summer are more frequent at some stations in comparison with spring (particularly in June and July in Nasiriyah and Baghdad). This is expected to be due to the aridity increasing in summer months leading to more frequent local dust generation.

Many studies have concluded that dust storms increase in the daytime, for example, (Middleton, 1986b) , (Orgill and Sehmel, 1976), (Orlovsky et al., 2005) and (Natsagdorj et al., 2003). They pointed out that the highest frequency of dust storms occur in the afternoon when the atmospheric boundary layer is normally deep and soon after surface heating has reached maximum intensity, creating locally unstable conditions, increasing turbulence with the surface layer and re-suspending dust particles from the ground. This process imposes a diurnal pattern onto the dust storm frequency and is consistent with dominant local and convective storm genesis, with surface heating and convectively generated winds interacting with the prevailing north-westerly, northerly and westerly flow.

This analysis showed that the diurnal variation dominates dust storm frequency in Iraq and leads to conclude that most dust storms events observed in Iraq are locally driven by convection. This is based on two observations: firstly, there is a strong association between the diurnal variability in wind speed and dust storm frequency at all stations in the region; secondly, it has been noted that dust storms in the region are typically of short duration. Dust storms across the region most frequently last for less than 3 hours and 83% of the observed dust storms last less than 6 hours. These are very likely to be formed locally, their maximum occurrence is around midday and early afternoon and they are associated with local wind speed those greater than 7 ms^{-1}. This is indicative of enhanced boundary

turbulence generated by strong surface heating and leading to local re-suspension of the dust. The more frequent events around the South of Iraq where the fine clay soil and agricultural practices play a role in breaking the soil further into finer material lead to easier re-suspension. In addition, the presence of the extensive sand dune areas near the regions surrounding the Nasiriyah and Simawa stations is likely to be the reason behind the high yearly averages of dust storms at those stations. Moreover, drying of marshlands from water in Simawa and Nasiriyah cities can be the potential of local dust uplift. The previous government (1979-2003) decided in 1991 to dry Al-Hammar marshland in Nasiryah and Simawa cities by diverting the main route of the Euphrates River for approximately 5 km to the east of its main direction in those cities. This resulted to obvious changes to the natural course of Euphrates in the Nasiryah and Simawa leading no further water supplies to Al-Hammar marshland within 2 years (1992-1994) to the extent that the marshland is entirely disappeared.

Whilst the dominant number of dust storms appears to be due to locally generated sources, a few dust storms can persist for more than 6 hours and very rarely may persist for 21-24 hours. Such long duration storms are linked to longer range transport of major dust generation events, but these only represent 17% of events in the dataset. However, long range transport of dust storms events will be discussed in chapter 4.

'Blank page'

Chapter Four: Source Identification and Transport Pathways of Large Dust Storms in Iraq

This chapter uses the same data that was presented in chapter 3 to identify large dust storm events and couples this with satellite analyses of the dust storms to identify source regions and transport pathways. Surface observations and SEVIRI satellite data are employed. The latter uses a dust product that incorporates both SEVIRI Visible and Infrared channels. The radiance data from multiple SEVIRI channels is used to create a SEVIRI dust mask and separate this from erroneously detected clouds and surface features. The ECMWF ERA-Interim global atmospheric reanalysis product will also be used to present the meteorological situation during the storms along with backward and forward trajectories from the HYSPLIT model to identify transport pathways of major dust storms events in Iraq.

4.1 Background

4.1.1 The Detection of Dust in the RGB Visible and Infrared Channels

Dust clouds in the atmosphere during the daytime absorb outgoing surface radiation and incoming solar radiation decreasing their temperature in comparison to the ground surface leading to dust detection as a cold anomaly, whilst dust clouds at night time prevent surface terrestrial radiation from escaping to space, therefore increasing the downward longwave flux leading to dust detection as a warm anomaly, (Shenk and Curran, 1974).

Dust can be detected during the day with one observation at limited temporal resolution as in MODIS, (San-Chao et al., 2006) or high temporal resolution of multiple observations during the day as in SEVIRI (Millington et al., 2012). The detection of dust can be processed through one single channel from the VIS or IR wavelengths, but the VIS channels can only be useful during the daytime due to reliance on solar radiation, therefore IR channels of single or RGB products are recommended to produce more in depth detail about dust detection, (Aminou, 2002). Each of the IR or VIS channels has specific characteristics in detecting dust and this varies depending on the time of the day when dust is being detected, as well as key object of the surface or the atmosphere, (see figure 4.1).

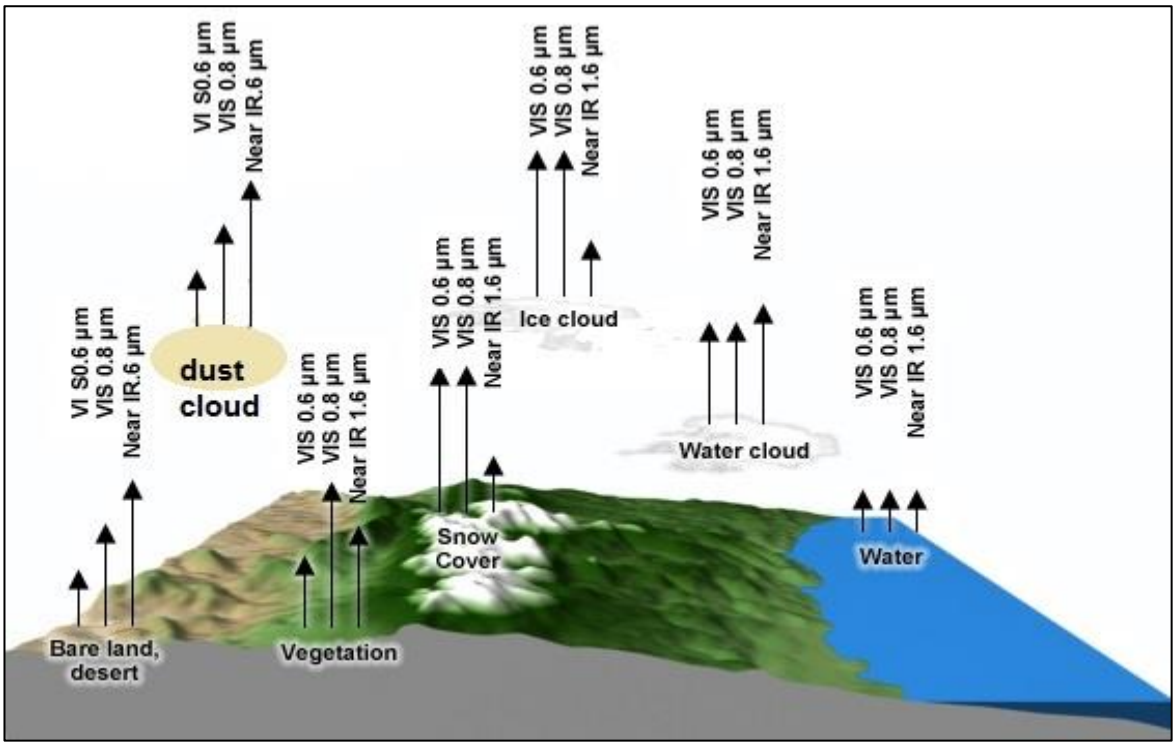

Figure 4.1: The interaction of SEVIRI VIS channels to different key surface and atmospheric objects, modified after: (https://www.meted.ucar.edu/satmet/multispectral_topics/rgb/navmenu.php?tab=1&page=3-1-6&type=text, accessed on 19/12/2017).

Dust in the RGB VIS channels (true colour images) appears as shades of light brown and light orange due to the strong signal of dust in the Near Infrared 1.6 µm visible channel (which is assigned to be red in the RGB false colour images), 0.8 µm visible channel (which is assigned to be green in the RGB false colour images) and a very limited contribution from the 0.6 µm visible channel which is assigned to be blue, (https://www.meted.ucar.edu/satmet/multispectral_topics/rgb/navmenu.php?tab=1&page=1-0-0&type=text, accessed on 14/12/2017). However, it shows that more powerful results regarding dust detection can be produced through a combination of brightness temperature (BT) and RGB products from IR channels; this is due to dust high absorption in the IR spectral wavelengths which assign dust to be shades of magenta, pink to red, (e.g. Ackerman, 1997).

It is very important to note that dust detection in the VIS and IR channels is not complete and it has its drawbacks. These are, for instance the VIS channels cannot detect dust during the night time due to the reliance of wavelengths on the solar radiation, (Wald et al., 1998). Also, VIS and IR signals can be quite affected by the presence of clouds (see sect 4.2.2) water vapour (Chaboureau et al., 2007) or high surface emissivity, (Ogawa et al., 2003). In addition, the height of dust plumes in the atmosphere, (Pierangelo et al., 2004), the thickness of the dust layer (Brindley and Russell, 2009) and its physical characteristics

(Wald et al., 1998) can also affect dust detection. However, the IR channels (such as SEVIRI IR channels) can produce more precise dust detection due to their ability to detect dust during the day and night times, (e.g. Schepanski et al., 2009).

4.1.2 Dust Detection in the SEVIRI IR Channels

Dust can be detected using one or more of the 12 VIS and IR SEVIRI channels (except 9.7 µm channel 8), table 4.1. Among those channels, it has been shown that the BTD of 12.0-10.8 µm, 10.8-8.7 µm and the BT 10.8 µm IR channels can readily distinguish dust from other atmospheric and surface key features with high temporal resolution (15 minutes), (e.g. Ackerman, 1997; Ashpole and Washington, 2012; Schepanski et al., 2007; Schepanski et al., 2009).

Channel No.	Spectral Band (µm)	Characteristics of Spectral Band (µm)			Main application/s
		λ_{cen}	λ_{min}	λ_{max}	
1	VIS0.6	0.635	0.56	0.71	Surface, clouds, wind fields
2	VIS0.8	0.81	0.74	0.88	Surface, clouds, wind fields
3	NIR1.6	1.64	1.50	1.78	Surface, cloud phase
4	IR3.9	3.90	3.48	4.36	Surface, clouds, wind fields
5	WV6.2	6.25	5.35	7.15	Water vapor, high level clouds, atmospheric instability
6	WV7.3	7.35	6.85	7.85	Water vapor, atmospheric instability
7	IR8.7	8.70	8.30	9.1	Surface, clouds, atmospheric instability
8	IR9.7	9.66	9.38	9.94	Ozone
9	IR10.8	10.80	9.80	11.80	Surface, clouds, wind fields, atmospheric instability
10	IR12.0	12.00	11.00	13.00	Surface, clouds, atmospheric instability
11	IR13.4	13.40	12.40	14.40	Cirrus cloud height, atmospheric instability
12	HRV	Broadband (about 0.4 – 1.1 µm)			Surface, clouds

Table 4.1: The band characteristics and main atmospheric applications of SEVIRI VIS and IR channels. From (Schmetz et al., 2005).

In the presence of dust during the day light, the SEVIRI IR channels interact differently with the radiant flux from the dust aerosols. For example, the SEVIRI 10.8 µm channel is considered to be the most sensitive channel for dust retrieval since dust absorbs most of the radiant energy from the surface at this wavelength compared with the 12.0 µm and 8.7 µm IR channels. This results in a low BT at 10.8 µm and higher in the 12.0 µm and 8.7 µm regions leading to a positive BTD in the difference between 12.0-10.8 µm (where dust is represented in bright shades), whilst negative BTD from the 10.8-8.7 µm pair are retrieved (where dust is represented in less bright shades), (see https://www.meted.ucar.edu/satmet/multispectral_topics/rgb/navmenu.php?tab=1&page=3

-2-4&type=text, accessed on 20/12/2017) figure 4.2. This leads to different colour shades in the SEVIRI dust scheme that was identified in section (4.2.2).

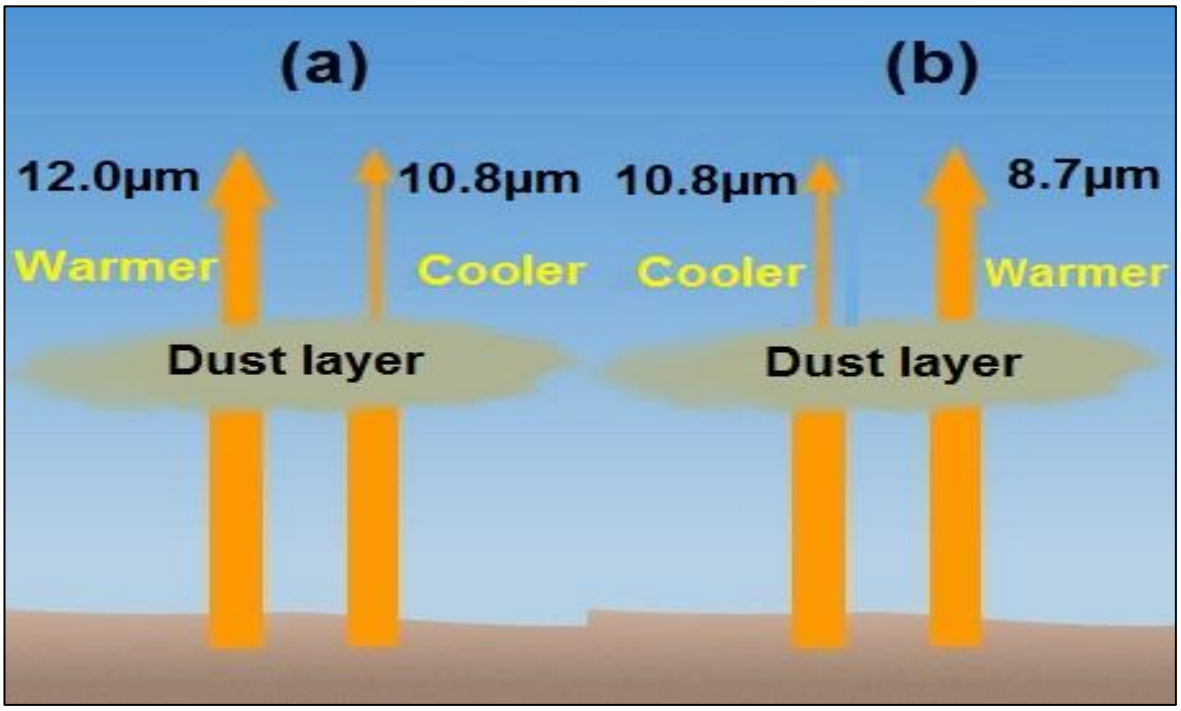

Figure 4.2: The interaction of the 8.7 µm, 10.8 µm and 12.0 µm IR channels with a dust layer in the atmosphere. The 10.8 µm channel is absorbed more upwelling energy coming from the surface in comparison with either the 12.0 µm or 8.7 µm channels, source: https://www.meted.ucar.edu/satmet/multispectral_topics/rgb/navmenu.php?tab=1&page=3-2-4&type=text accessed on 20/12/2017.

The positive BTD from the 12.0-10.8 µm will be strongly presented in bright shades of light to dark red (during high dust loading), while the negative BTD from the 10.8-8.7 µm will be presented in shades of light to dark blue, (as in figure 4.6). The case with the BT of the 10.8 µm which assigned to be blue is different, particularly during the daytime and when there is high dust loading and high surface emissivity. The BT values from the 10.8 µm channel will be saturated due to the high sensitivity of this channel to the energy of the dust layer itself, in addition to its high sensitivity to upwelling terrestrial and reflected incoming solar radiations, (Ashpole and Washington, 2012).

During night time, the temperature of dust clouds decreases to be equivalent to the temperature of the ground surface causing a limited thermal contrast in the IR channels between surface and dust aloft, (Legrand et al., 1988). This leads to lowering BT values at the IR wavelengths making dust harder to be detected at night, However, dust signals will not be much affected during the night time if dust loading is high and no clouds are present in the scene (Klüser and Schepanski, 2009).

On the back of the discussion above, the performance of the SEVIRI IR channels showed that the BTD 12.0-10.8 μm (see figure 4.6/c) has the strongest signal showing dust in shades of dark red, while the BTD 10.8-8.7 μm (figure 4.6/b) (dark blue shades) showed lower brightness differences in comparison with BTD 12.0-10.8 μm, however both components showed obvious brightness temperature differences between dust and dust free regions. There is a sufficient contribution from the BT 10.8 μm (figure 4.6/a) in this example showing dust in bright yellow shades, although strong dark red colour covers almost the whole region which reflects how this wavelength can be saturated due to the effect of high surface emissivity, particularly during the day time.

4.2 Data and Methodology

Satellite data from SEVIRI were used in this thesis for the purpose of identifying source regions and transport pathways of large (major) dust storms in Iraq between 1985 and 2013. The term "large (major)" implies high dust loading of long range transport (i.e. wide geographical extent).

4.2.1 Defining Large Dust Storms Events

In order to identify major dust storms events in the region, a Nearest Neighbour Analysis (NNA), (see: Wilkinson et al., 1983; Yakowitz, 1987) was carried out to identify which of the reported dust storms were reported by multiple stations simultaneously. The distances among surface meteorological observing stations using their coordinate information (table 3.1) were examined. This was achieved by searching in the surface observations for all the records of dust storms class codes 30-35 (table 3.2) following the same procedure as in section 3.1. The class codes 30-35 were summed together to represent a dust storm event at a given station at that time.

The NNA is used to identify when a dust storm event was flagged at a station (A) at a given time whether there is or there is not a dust storm event at the same time in the first closest neighbour (B). If there is no storm at (B) at the same time that it was detected in (A), then the search was repeated in the next two consecutive observations at station (B). If no storm was recorded at B then the same process was repeated with the second closet neighbour (C), if not then third neighbour (D) and fourth neighbour (E), respectively. However, if a dust storm event was identified at (B) at the same time as it was detected in (A), then the NNA algorithm used station (B) as the new start point to continue the search for more nearest neighbours and station (A) was not included in further analysis.

Figure 4.3 demonstrates the process of NNA analysis using an actual event from the surface observations. In the below event, the dust storm was detected in Hilla station at 00:00 UTC on 17/10/2002, the event was detected at the same time at the closest neighbour station to Hilla, which is at Najaf. It was subsequently detected at the next closest station to Najaf, which is Diwania station, then it was detected too at Simawa station (as Simawa is considered to be the first closest neighbour to Diwania station in this example) and finally the storm was detected at Nasiriyah station (which assigned to be the closest neighbour to Simawa station).

The minimum number of nearest neighbour stations that were considered in this analysis to define an event as major dust storm is four stations and above. The logic behind including 4 neighbours only is that if an event was detected in station (A), but it was not detected in the first, second, third or fourth of its neighbours, it would be geographically too far from being reasonable to include more than 4 neighbours in the same event. The reasoning is that the distances among observing stations are not huge and instead they are close to each other and all located on the valley of the Tigris and Euphrates Rivers (see figure 4.3).

4.2.1.1 SEVIRI Major Dust Storms in Iraq (1985-2013)

The identification process presented in section (4.2.1) shows that there are 26 dust storms events were observed simultaneously in the surface data between 1985-2013 in ≥4 climatological stations; therefore they were classed as large dust storms events

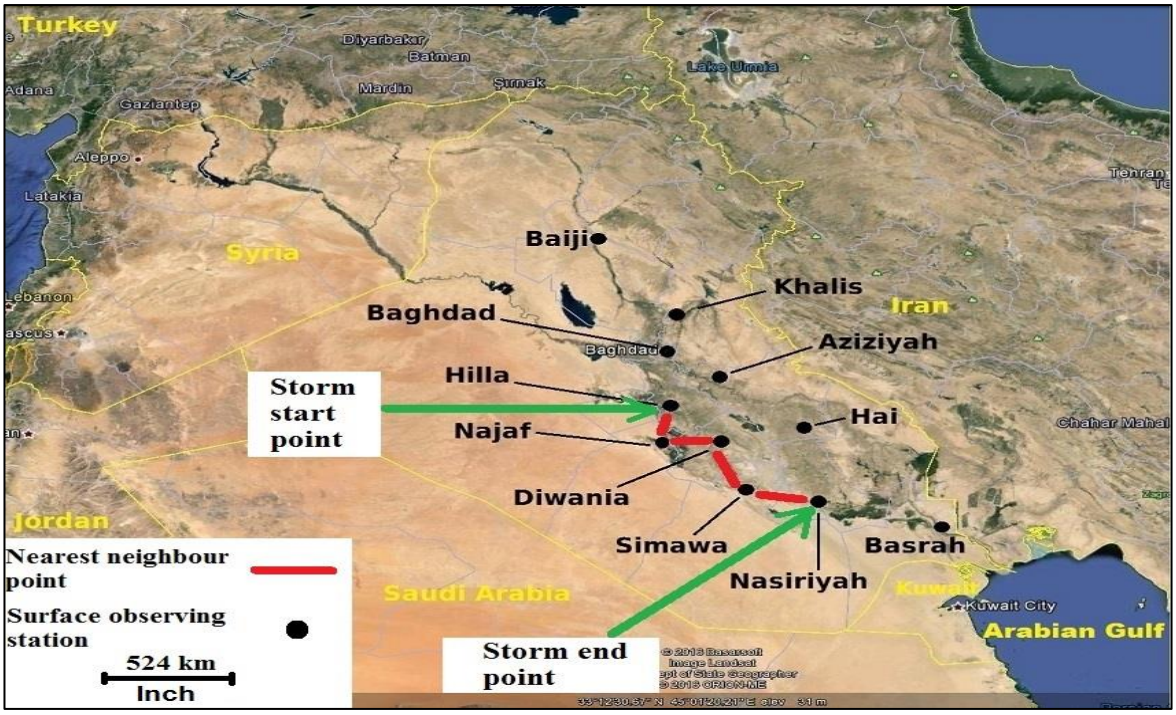

Figure 4.3: The process of the NNA analysis. This demonstrated on an actual dust storm event that was detected first at Hilla station at 00:00 UTC on 17/10/2002 and then detected at a number of neighbouring stations to Hilla, modified after (Google, 2013).

Storm no	*Start date*	*Start time*	*End date*	*End time*	*Number of stations*
1	16/04/2008	17:00	18/04/2008	06:00	5
2	07/08/2005	07:00	09/08/2005	10:00	5
3	18/06/2008	05:00	18/06/2008	23:00	5
4	07/06/2010	10:00	07/06/2010	19:00	5
5	***17/03/2012***	***04:00***	***N/A***	***N/A***	***11***
6	28/07/2009	14:00	30/07/2009	06:00	5
7	12/04/2011	08:00	13/04/2011	23:00	11
8	31/08/2015	11:00	02/09/2015	10:00	N/A
9	***31/01/2008***	***05:00***	***N/A***	***N/A***	***5***
10	07/06/2008	08:00	09/06/2008	06:00	4
11	***24/03/2009***	***04:00***	***N/A***	***N/A***	***7***
12	***17/03/2010***	***09:00***	***N/A***	***N/A***	***6***
13	24/05/2010	08:00	25/05/2010	03:00	4
14	***22/06/2010***	***13:00***	***N/A***	***N/A***	***9***
15	***08/03/2011***	***02:00***	***N/A***	***N/A***	***7***
16	02/06/2011	00:00	03/06/2011	06:00	4
17	19/04/2012	05:00	20/04/2012	07:00	4
18	***09/03/2006***	***03:00***	***N/A***	***N/A***	***6***
19	27/07/2008	00:00	28/07/2008	06:00	5
20	***22/04/2011***	***04:00***	***N/A***	***N/A***	***5***
21	***04/04/2011***	***12:00***	***N/A***	***N/A***	***5***
22	***22/05/2012***	***03:00***	***N/A***	***N/A***	***5***

Table 4.2: All dust storms that were identified by NNA as large events. There are 12 events (including event 8 from outside the surface observing data) where SEVIRI start and end times were available (columns 3 and 5), while 10 events (in bold and Italic) where SEVIRI could not see them due to high and thick clouds scene.

according to the nearest neighbour analysis. Five out of the 26 storm events occurred between May 1992 and October 2002 when there was no SEVIRI data available. Table (4.2) shows that there are 12 dust storms events when SEVIRI start and end times could be identified and when data could be retrieved from below extensive clouds, while the rest (10 events) they were very difficult to make a clear judgement regarding their source regions and spatial extent due to widespread cloud cover, (see figure 4.4) (note: all cloudy events will be demonstrated in the CD with SEVIRI images as part of the analysis in this thesis).

All the events were investigated in the same manner but due to the number of events, only one dust storm (event 1 in table 4.2) will be demonstrated in detail in section (4.3.1) and it will be compared to a second event (8 in table 4.2) which represents a more recent event from outside the surface observation period (1985-2013) (see sect 4.3.2). The remaining events are all shown in detail in the CD including the SEVIRI brightness temperature differences images, ECMWF wind-fields and HYSPLIT backward and forward trajectories.

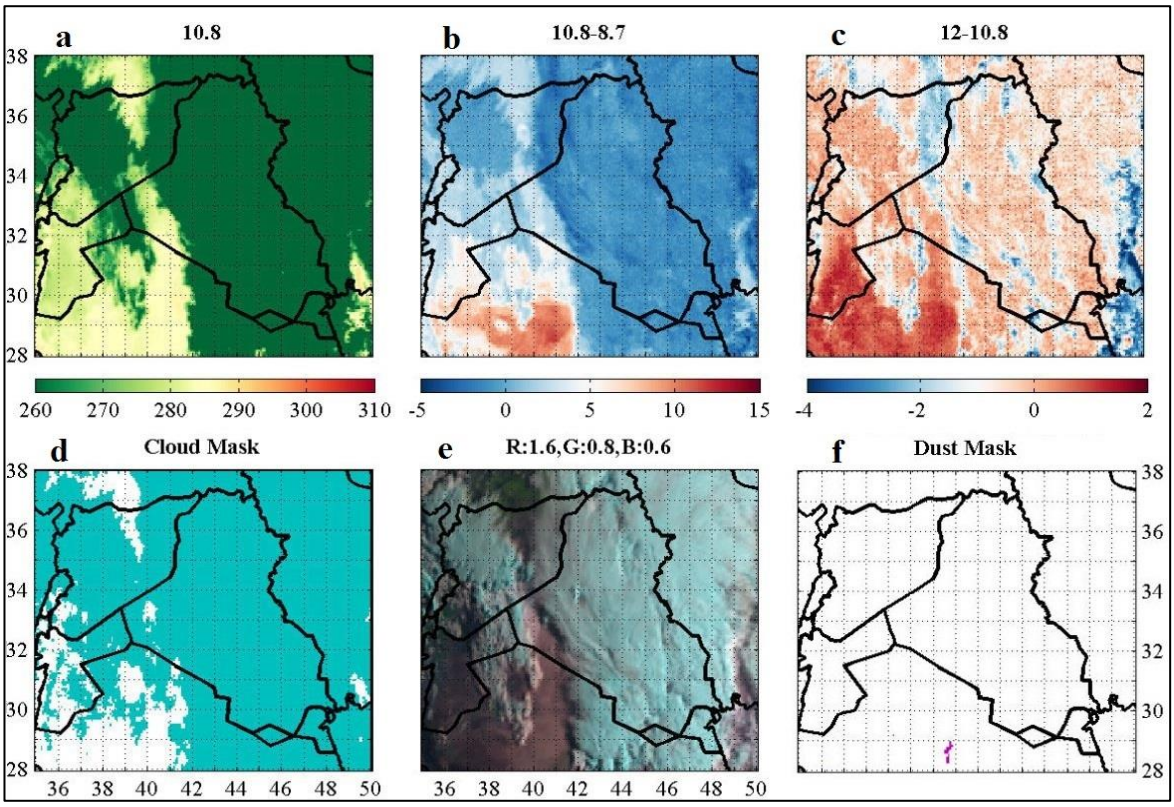

Figure 4.4: The effects of clouds on SEVIRI Fields. This retrieved at 04:00 UTC on 22/04/2011 where a strong signal of high and thick clouds in the RGB VIS (e) shown as cyan due to the strong reflectivity of high clouds in the 0.8 µm and 0.6 µm channels. The 10.8 µm (a) is highly saturated and the BTD products (b and c) show no values of dust which led to no dust in the dust mask (f). The cloud mask (d) adds extra information of the spatial extent of clouds during this dust storm (event 20 in table 4.2). There were records of (30-35) (records of dust) from the surface observations at 04:00 UTC at 5 different stations, but due to thick clouds it was not possible to capture this event in any of SEVIRI channels. Figures (a, b and c) were derived by using BT and BTD values from the SEVIRI IR channels as introduced in section (4.2.2), figure (d) was created from the cloud mask data of SEVIRI (0 degree) as introduced in section (4.2.2). While figure (e) was derived by assigning SEVIRI VIS RGB channels as introduced in section (4.2.2.2) and finally figure (f) was derived from SEVIRI brightness temperature differences values and clouds filtering process as introduced in sections (4.2.2 and 4.2.2.1).

4.2.2 SEVIRI Satellite Data

Satellite data was then used to examine each of these large dust storms once they had been identified. Satellite data from SEVERI on the Meteosat Second Generation satellite were obtained from (http://archive.eumetsat.int/). The High Rate level 1.5 rectified SEVIRI image data at 3 x 3 km spatial resolution in the nadir view was used throughout this work. The Level 1.5 image data corresponds to the geo-located and radiometrically pre-processed image data and they were transmitted at high rate in 12 spectral channels of SEVIRI, table 4.1. The SEVIRI dust index that was used in this work does not retrieve the height of the dust in the atmosphere, but was only used to identify whether dust is present or not at a given time and location.

The dust scheme used in this work was calculated from the brightness temperature difference (BTD) between the SEVIRI IR channels 7, 9 and 10 (8.7 μm, 10.8 μm and 12.0 μm, respectively) using the approach of (Ashpole and Washington, 2012). In summary dust is identified when: the brightness temperature at 10.8 μm was in the temperature range 260-210Kelvin; the BTD between 12.0 and 10.8 μm was greater than 0 Kelvin; and the BTD between 10.8 and 8.7 μm was less than 10 Kelvin. The SEVIRI dust composite scheme can be summarised as follows:

BT 10.8 μm ≥ 275K

BTD (12.0-10.8) μm ≥ 0K

BTD (10.8-8.7 μm) ≤ 10K

The dust scheme that introduced by Ashpole and Washington performed well in the Sahara in Africa in terms of identifying dust presence. They tested the results of the dust scheme by comparing dust outbreaks hot spots that identified by SEVIRI dust scheme with Aerosol Optical Depth (AOD) and Absorbing Aerosol Index (AAI) and it showed that it successfully and consistently performed well providing a direct way to build up an objective and readily reproducible method to be used in dust satellite retrievals applications. However, it is important to note that in this work the brightness temperature threshold at 10.8 μm was adjusted to ≥ 275K in contrast to the Ashpole and Washington study which used a threshold of ≥ 285K. This is because the 10.8 μm channel has high sensitivity to the radiant energy of the dust layer itself as well as the underlying surface emissivity.

For instance, during the daytime in the presence of high dust loading and high surface temperature, the 10.8 μm channel will be saturated (see figure 4.5) due to high amounts of absorbed energy. Consequently, it was difficult to capture some small dust plumes at ≥ 285K; therefore the threshold wavelength was reduced to ≥ 275K in order to decrease the effect of saturation. In the example shown in figure 4.5 the MODIS AOD shows high aerosol loading. This and other examples of where MODIS clearly identified dust were used to identify the correct threshold brightness temperature in the SEVERI 10.8 um channel, consequently leading to more precise dust judgement in the SEVIRI dust scheme, figure 4.6.

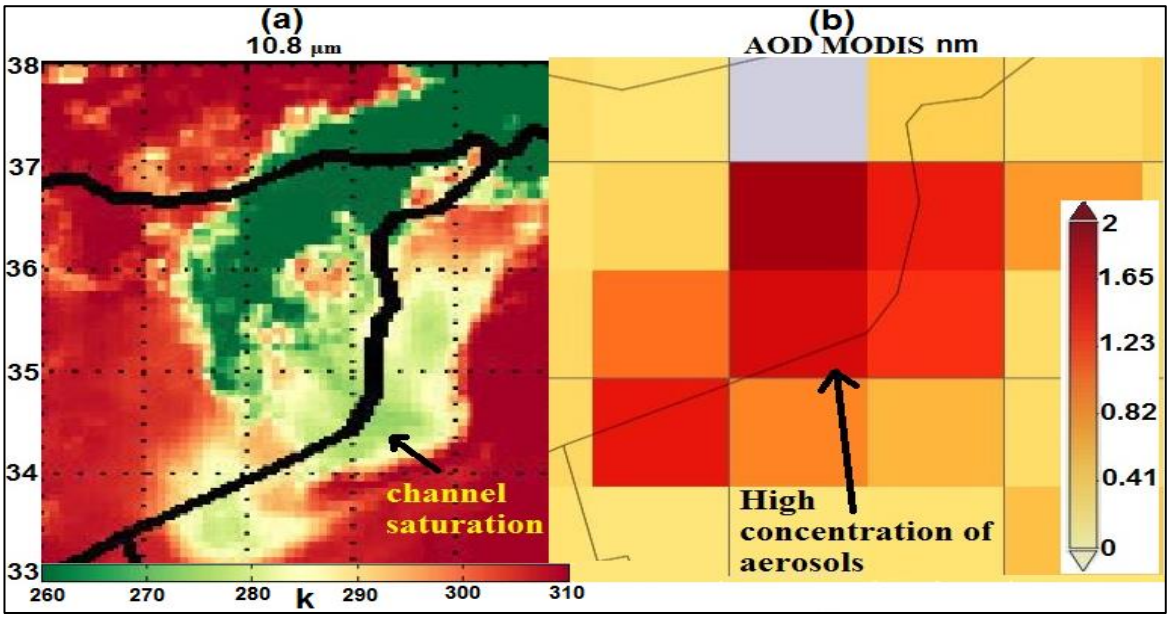

Figure 4.5: The saturation of 10.8 µm IR channel. This is an example of a dust storm event occurred on the borders of North West of Iraq and Eastern Syria (35.9033E, 28.5645N, 48.6475E, 38.0127N) on 31/08/2015. Figure (a) shows a brightness temperature of around 275K at 10.8 µm which could not be seen if its threshold was 285K. Evidence of high aerosol concentration is presented (figure b) from the MODIS Aerosol Optical Depth 550 nm (Deep Blue, Land only, daily 1 degree) [MODIS-Aqua MYD08_D3 v6] retrieval at the same location and time. Figure (a) was derived as in figure (4.4/a), while the MODIS data (b) was obtained from GIOVANNI tool: (https://giovanni.gsfc.nasa.gov/giovanni/#service=TmAvMp&starttime=2015-08-31T00:00:00Z&endtime=2015-08-31T23:59:59Z&bbox=35.9033, accessed on 21/12/2017.6475,38.0127&data=MYD08_D3_6_Deep_Blue_Aerosol_Optical_Depth_550_Land_Mean&variableFacets=dataFieldMeasurement%3AAerosol%20Optical%20Depth%3B.).

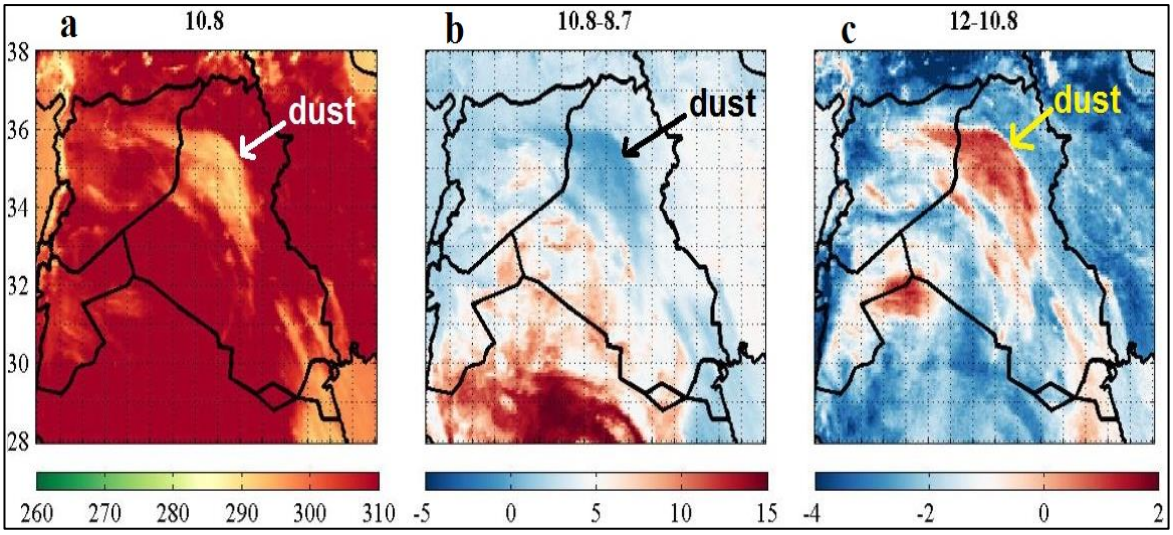

Figure 4.6: The performance of SEVIRI IR dust scheme. This was during a dust storm event that affected Iraq on 7th August 2005 at 10:00 UTC. The brightness temperature differences are presented as follows: (a) BT 10.8 µm, (b) BTD 10.8-8.7 µm, (c) BTD 12.0-10.8 µm. This figure was derived as in figure (4.4) (a, b and c respectively).

It is found (Schepanski et al., 2007) that when high surface emissivity is presented, it becomes a challenge to distinguish dust signals. This issue particularly occurs in the range of the 8.7 µm IR channel which has fairly high reflectivity towards surface features (mainly in deserts regions due to their remarkable surface characteristics), (see Li et al.,

2007). Therefore, in some cases the BTD 10.8-8.7 μm incorrectly detected surface features as dust. As a result it was necessary to process SEVIRI dust images by isolating (filtering) surface features from the scene used to identify dust. This was done by using a cloud anomaly threshold based on the BTD 10.8-8.7 being ≤-2K, following a method introduced by (Ashpole and Washington, 2012).

The method consists of producing a reference image from the SEVIRI cloud screened data BTD 10.8-8.7 μm to create the actual background surface emissivity image to be used to remove the wrongful assignment of surface features as dust in the BTD 10.8-8.7 μm. This was achieved by selecting 15 consecutive days in order to examine each pixel in the scene. The example 15 days used based on visual images to select a period of time when the scene is as possible as dust and clouds free. The 15 days (1st-15th June 2010) were selected from the land surface reflectance by MODIS on both Aqua and Terra true colour images (https://worldview.earthdata.nasa.gov/). The logic behind the 15 days assumption is that the period is sufficient to present each pixel for a minimum one time as dust and cloud free, therefore each pixel will be presented with highly reduced surface signals or clouds effects and thus produces more accurate information about dust in the region.

However, after examining each pixel in the scene, it was noticed that there was still clouds in the scene because SEVIRI clouds mask incorrectly flagged dust as clouds, (see figure 4.7). For this, The SEVIRI cloud mask data (0 degree) that was obtained from (http://oiswww.eumetsat.org/IPPS/html/MSG/PRODUCTS/CLM/, accessed on 24/10/2017) was also used in this method for the same 15 days period above. The cloud mask was created by the 12 channels of SEVIRI (apart from the ozone channel 9.7 μm), (see Just, 2000; http://www.eumetsat.int/). The cloud mask was used whether it is clear sky or not at given time and location on a pixel by pixel basis. Consequently, a reference image was provided which once created was subtracted from the values of the BTD 10.8-8.7 μm for each dust storm event separately. This will create BTD 10.8-8.7 μm reference image (see figure 4.8 (a)) that was applied on each dust storm event to better separate erroneous flagging of surface and clouds assignments from dust.

A similar analysis (see figure 4.8 (b, c and d) was performed for different periods of time (17th-21st September 2016, 18th-22nd August 2017 and 17th-21st July 2018, respectively) in order to examine for any systematic bias that may occur due selecting a representative period of time used in figure (a) and the results were consistent. But, for the purpose of this work, only the reference image (a) was applied on each dust storm event in this thesis since

it does not include any obvious localised dust points in comparison with the reference images in b, c and d.

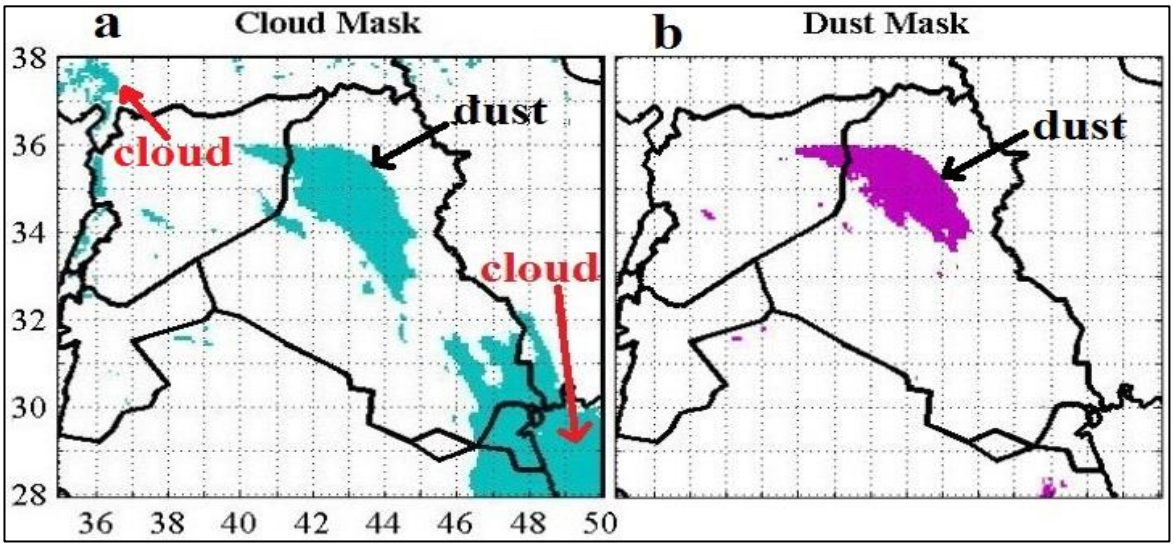

Figure 4.7: SEVIRI cloud and dust masks. This was during a dust storm event affecting Iraq on 7th August 2005 at 10:00 UTC where figure (a) shows how the SEVIRI cloud mask flagged dust as clouds. While figure (b) shows the SEVIRI dust mask with the unique magenta colour of dust after filtering the clouds and surface BTD effects using the SEVIRI cloud screened BTD 10.8-8.7 ≤ -2 that introduced by (Ashpole and Washington, 2012). Figure (a) was created as in figure (4.4/d) whilst figure (b) was derived as in figure (4.4/f) as well as by applying the cloud anomaly image reference using (BTD 10.8-8.7anom ≤ -2) that introduced in section (4.2.2).

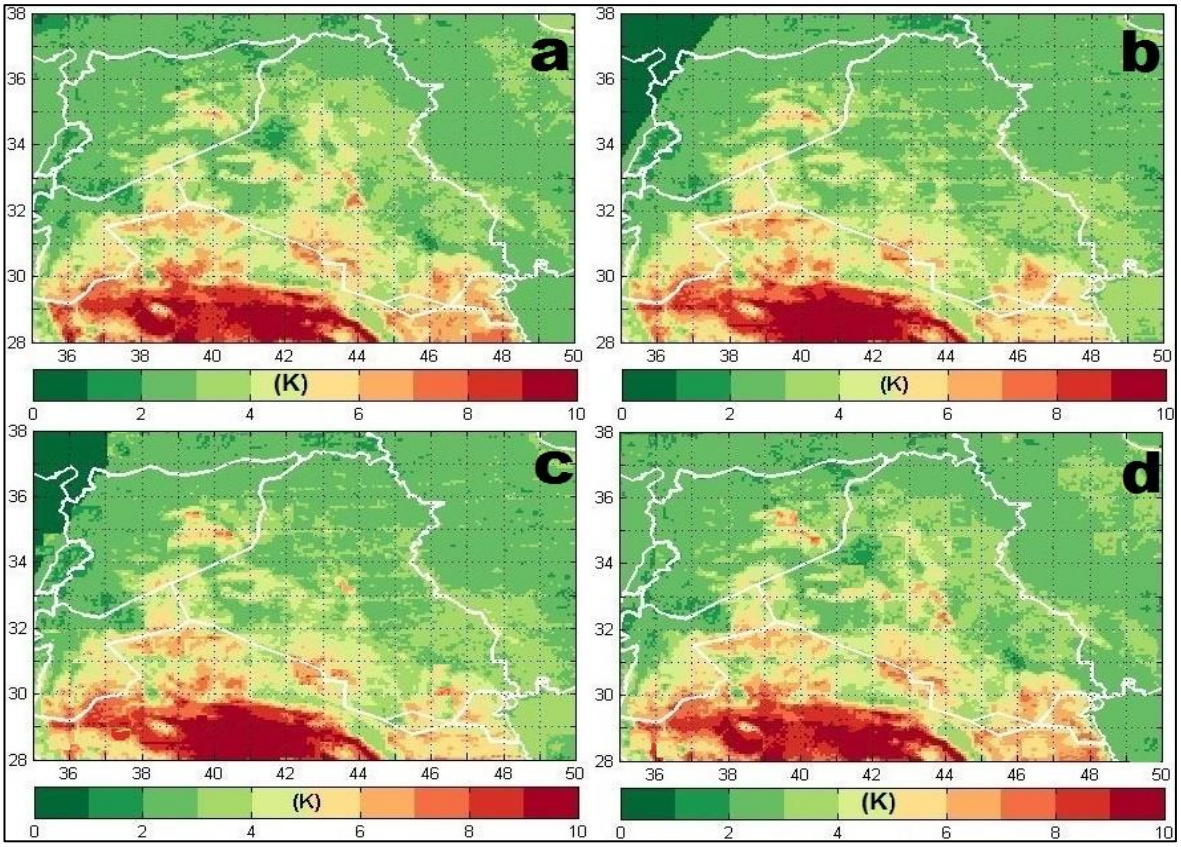

Figure 4.8: The reference images from the SEVIRI cloud screened data BTD 10.8-8.7 µm. Image (a) was created as described in section (4.2.2) for the period 1st-15th June 2010, while the reference images b, c and d were created using the same process as in (a) but for the periods 17th-21st September 2016, 18th-22nd August 2017 and 17th-21st July 2018, respectively.

4.2.2.1 SEVIRI Dust Mask

The result of filtering surface features and clouds produced a SEVIRI dust mask (see figure 4.7/b). The dust mask was then used to identify the source regions and the transport pathways of the major dust storms events in Iraq. Although SEVIRI provides high temporal resolution (every 15 minutes) it is found that hourly intervals can achieve the purpose required by this analysis and maintain the required quality since dust outbreaks have been shown to occur on timescales longer than 15 minutes. This is illustrated by a series of images with a 15 minute time interval in the bottom row in figure 4.9 as an example. Therefore, only hourly intervals will be shown in this analysis to demonstrate the case studies in sections 4.3.1 and 4.3.2 (note: all events will be fully demonstrated in the CD attached with this thesis).

4.2.2.2 SEVIRI RGB IR and VIS Products

SEVIRI RGB IR dust product was derived from combining the BT and BTDs (these are 12.0-10.8 μm which assigned to be red, 10.8-8.7 μm which assigned to be green and 10.8 μm which assigned to be blue) all together in one product. As well as dust was also detected by using the SEVIRI visible (VIS) channels (true colour images). This was done by simply assigning Near Infrared 1.6 μm (which assigned to be Red), 0.8 μm visible channel (which assigned to be Green) and 0.6 μm (which assigned to be Blue) (see section 4.1.1). Both products add an extra piece of information to observe dust. However, neither of them will be used in the process of identifying large dust storms in Iraq and instead they will only be presented in the CD.

4.2.3 Defining Start and End Points of SEVIRI Large Dust Storms

The combination of products offers the possibility of developing an algorithm to track the start and end points of a dust storm computationally. However, there were challenges to defining these points systematically and without bias. The main one was the variability in dust generation and intensity between different major events. In other words, some dust storm events were generated from multiple discrete points (as in fig 4.9) in the source region before merging together and advecting away as one dust plume. As a result, during this work the start and end points were selected visually for each of the major dust storm events that were identified by the NNA analysis. This achieved by the following steps:

1- The nearest neighbour analysis of dust occurrence at adjacent surface stations described in section (4.2.1) and summarised as in table (4.2) was used to identify large dust storms events. This process identified events when large storms occurred

and identified an exact date of occurrence for each major dust storm episode (e.g. dust storm event on 16/04/2008) based on reporting of dust at multiple surface observing stations simultaneously.

2- The date of each major dust storm was used to target satellite imagery to identify the start point and location. This was achieved by visually searching the SEVERI dusk mask information on the date of a large dust storm event. In other words, the initial source of the dust was recorded as being the first appearance of dust in the SEVERI dust mask field. The start point and location of the storm was identified as being when there is no more dust being generated in the source location and the dust plume can be clearly seen moving from the source region in the dust mask field. To ensure that the start point of each event had been established correctly, a period of 24 hours prior to the exact date of the event was also examined in the SEVERI dust mask field to ensure that there was no dust present in the earlier images.

3- The transport of the initial dust outbreak (as described in point 2 above) was tracked in order to identify the end point for each major dust storm event. This was achieved by visually tracking the transport of the dust plume in the dust mask field until:

   a- The dust plume leaves the borders of Iraq towards a neighbouring country.

   b- The dust plume cannot be seen further in the SEVERI dust mask field.

   c- The dust plume disappears in the SEVERI dust mask field or no further advection of the dust plume was observed.

4.2.4 Obtaining a Frequency Distribution of Dust Source Region during Major Storms

To examine the spatial distribution of the source regions of the major dust storms affecting Iraq, a frequency distribution of the start points of all dust storms was created. A dust mask frequency composite was created by using the start time following the method outlined in section 4.2.3 from the SEVIRI dust mask of each large dust storm event on a 1° x 1° grid. To create the dust mask frequency composite the presence of dust in every single event from the separate dusk masks in each pixel were recorded as either 1 (which means there was dust in a given pixel during a single event) or 0 (which means no dust was flagged at a given pixel in a single event). Then, the masks from the initial field of each dust event were added together to create a frequency distribution as a function of location. This gives

a sense of the most frequent locations for dust emission at the starting point of the storm for a given pixel to identify the source regions of dust (see figure 4.14).

4.2.5 Spatial Representation of the Frequency of Dust Events across Iraq during Major Storm Events

The same procedure used in section (4.2.4) for calculating the frequency distribution of the source of major storms, but instead of only adding the start points of major dust storms events, all the dust masks from the start until the end of the events are combined together. This product is used to show the regions that most frequently experience high dust loadings during major events (see section 4.5).

4.2.6 Calculating Wind-Fields Averages from ECMWF Data

Wind-fields from the ECMWF ERA-Interim reanalysis product were used in this study. The main data from the ECMWF reanalysis used in this work was the 3 hourly averages of surface wind speeds and wind direction at 10 metre altitudes at horizontal resolution of 0.5 degree. The meteorology for each case study was inspected separately but in many cases similar behaviour was observed so average statistics were also calculated. Average wind speed and wind direction maps for all events were created by using the start times of dust storms provided in section (4.2.4). Based on this the average U (zonal velocity, i.e. the component of the horizontal wind towards east) and V (meridional velocity, i.e. the component of the horizontal wind towards north) (see: http://mst.nerc.ac.uk/wind_vect_convs.html for more information) wind components from the start times were averaged across all storms to build a picture of the similarity and difference between the meteorology during the different major dust storms events (ECMWF products will be presented in sections 4.3, 4.5 and 6.3).

4.2.7 Calculating Backward and Forward Trajectories from HYSPLIT

Air mass histories for each major dust storm event were determined by calculating backward trajectories which were initiated within a grid box (1° x 1°) at 3 different altitudes; ground level, 1000 and 2000 (metre above sea level) for 120 hours (5 days) previous to an origin centred over the start point of the dust event (that were identified in section 4.2.4) using HYSPLIT (see Stein et al., 2015) model and GDAS (0.5°) meteorological fields. Then the backward trajectories for all cases are gridded into a one 2D histogram. This is then normalised to the total number of trajectory points, so that each pixel presents the % of dust laden air which passes through. Similarly, forward trajectories were initiated with hourly intervals from the start point of each large dust storm event to a

maximum 72 hours (3 days). A period of 72 hours was chosen because it was noticed that none of the major dust storms events lasted longer than 3 consecutive days (HYSPLIT products will be presented in sections 4.3, 4.5 and 6.3).

4.3 Case Studies

The section uses a case study from 16/04/2008 to illustrate the overall analysis approach taken (sects 4.2.1 and 4.2.1.1) to analyse each case study. Two case studies were analysed in this section only, while the other cases are presented using similar statistical approach and are shown in the CD and they are summarised following the same procedure of the case study presented here. The analysis was carried out in this section based on the following steps: (1) Investigation of SEVIRI retrievals starting in the hours preceding the event until the event ended; (2) Exploration of the cloud conditions in the SEVIRI IR and VIS wavelengths during the progression of the event; and (3) Exploration of air mass trajectories from HYSPLIT as well as wind-fields data from ECMWF. Finally the case study from 16/04/2008 is compared to another more recent one (31/08/2015) which represents a case study from outside the observing study period (1985-2013) but offers some comparison and contrast.

4.3.1 Case Study 16/04/2008

Although SEVIRI provides high temporal resolution (15 minutes), it was found that hourly intervals can well achieve the purpose in this section and this is what is shown throughout the discussion in here. The CD attached to this work shows the detailed information from SEVIRI for the 12 large dust storms events at hourly intervals, backward and forward trajectories and wind-fields for all those 12 events. A severe dust storm event observed in the Euphrates River basin (as in figure 2.2) in the SEVIRI dust mask on 16/04/2008 (event 1 in table 4.2) at start generation time at 09:00 UTC. By inspection of the individual SEVERI images it was observed that during the preceding hours (00:00-09:00 UTC) of the storm start generation time above, SEVIRI images identified the region was largely covered in clouds, however no dust was observed during those hours. The cloud scene was observed using the 10.8 μm channel and the RGB VIS images, figure (4.9). The principle of this synoptic condition that demonstrate the association between clouds and dust generation was typically observed as low-pressure systems generate over the East of the Mediterranean Sea moving eastward across the northern Arabian Peninsula, Iraq, Iran and Arabian Gulf, (Hamidi et al., 2013).

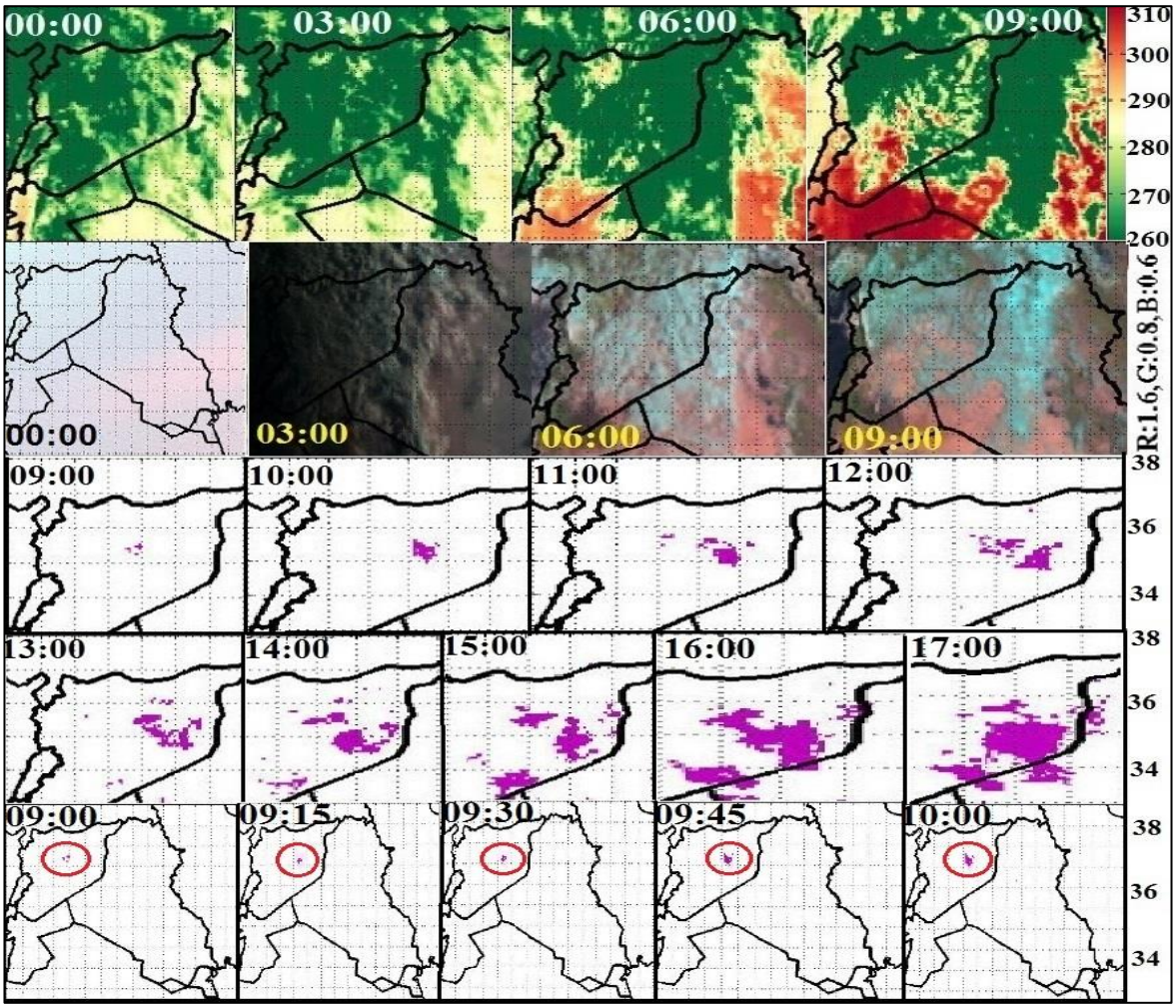

Figure 4.9: Clouds scene and SEVERI dust mask during the 16/04/2008 dust storm event. The upper row shows a strong signal of clouds in the 10.8 µm channel presented in dark green shades. The 2nd row RGB VIS at selected observations during the preceding hours (00:00-09:00 UTC) of the event. The evolution of the dust plume represented in the SEVIRI dust mask in the 3rd and 4th rows). The 5th row shows dust generation (circled in red for easier identification) for every 15 minutes between 09:00 and 10:00. The 1st row was derived as in figure (4.4/a), 2nd row was derived as in figure (4.4/e) while rows 3, 4 and 5 as in figure (4.7/b).

Then, between the period 09:00-1700 UTC cloud moves away to the east towards the north, middle and east of Iraq, but throughout this time isolated dust events are observed in the SEVIRI dust mask, none of which show signs of transport and advection from the source area. Only around 17:00 UTC does the dust appear to be transported away from the source region in the SEVIRI dust mask.

Although the scene was partially cloudy during the preceding hours, however there was no formation of dust in the Euphrates River basin until 09:00 UTC when dust was seen for the first time in the SEVIRI dust mask. The evolution time of dust generation continued for 9 hours (09:00-17:00 UTC) in the basin region and during these hours, it showed that dust plume had a very limited spatial extent before it was gradually developed from discrete points in the basin during those hours. At 17:00 UTC, there was no more generation of dust and the dust plume begun to travel clearly away from the source region in the basin

towards Iraq internal lands. Figure 4.10 shows the air mass history of backward trajectories at ground level, 1000 and 2000 (m.a.s.l) as well as wind-fields for the case study on 16/04/2008, respectively.

The trajectories presented were calculated from each pixel identified by the dust mask at a given time. The trajectories show a strong contribution of air masses from the east of the Mediterranean Sea (west of the source region of dust in the Euphrates River basin) at ground level elevation where most of the air masses were between approximately 0-600 metre with the vast majority at 0-100 metres. While some trajectories were from the north of the Red Sea where they were presented at about 1200 metre. Notably, at upper altitudes (1000 and 2000 m.a.s.l) air masses mainly originated from the Mediterranean Sea with little exception of few air parcels which travelled from West Africa at around 1600 and 2600 metres of the altitudes 1000 and 2000 metre, respectively. Overall, air mass of backward trajectories found to be consistent with wind-field climatologies (see ECMWF wind fields in figure 4.10) showing that the dominating winds advected from eastern of the Mediterranean Sea towards the source region of the Euphrates River basin in this particular dust storm event.

Figure 4.11 shows the SEVIRI dust mask observations, forward trajectories from HYSPLIT, in addition to the ECMWF wind-fields for the period during which dust advected from the source region across the region. The transport of dust plume started from 17:00 UTC and the dust cloud was well captured by the SEVIRI dust mask showing spatial extent of the dust increases gradually from 18:00 UTC on 16/04/2008 reaching its maximum spatial extent at 15:00 UTC on 17/04/2008.

An important observation can be reported regarding dust storm position from ground based observations, this was that the storm was reported for the first time at the Baiji observing station at 21:00 UTC on 16/04/2008 (00:00 on 17/04/2008 Iraqi local time) which means that the storm reached the first station of the climatological surface network in about 3 hours at approximately 8-≥10 ms^{-1}. It was reported at Baiji station that the storm reduced visibility from 56 km at 15:00 UTC to 3 km at 18:00 UTC on 16/04/ 2008 before it dropped further to 1 km at 00:00 UTC on 17/04/2008.

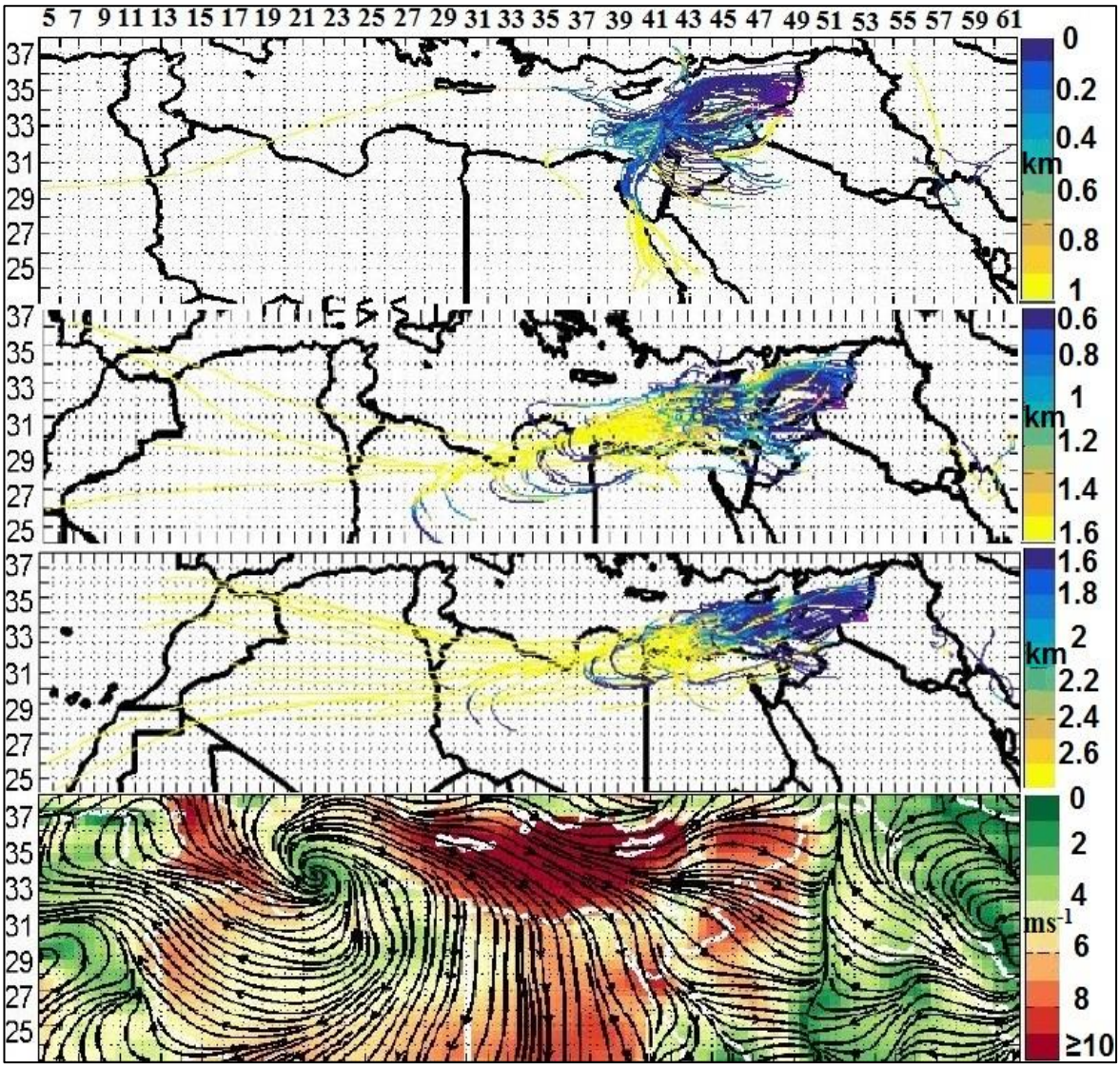

Figure 4.10: Air mass history of backward trajectories from HYSPLIT during the 16/04/2008 dust storm event. This launched at ground level (first row), 1000 metre (second row) and 2000 metre (third row) from each of the dust mask pixels between 17:00 UTC on 11/04/2008 and 17:00 UTC on 16/04/2008 as described in sections (4.2.4 and 4.2.7). The fourth row represents a linearly interpolated of wind fields 10m from the ECMWF ERA-Interim reanalysis product (as presented in section 4.2.6) where the black streamlines represent the wind direction and the colour scale represents the wind speed (ms^{-1}).

The plume transported dust from north-westerly to south-easterly direction over the valley of the Tigris and Euphrates Rivers of the Alluvial Plain in Iraq from the transport time at 17:00 UTC (16/04/2008) to the disappearance time in the south region of Iraq and the Arabia Gulf at 06:00 UTC (18/04/2008). The direction of transport appeared to be well represented by the dominant forward trajectory at the ground level. This is strongly supported by wind-field observations showing an overall north-westerly wind direction and high wind speeds particularly across the Euphrates River basin (8-≥10ms^{1}) where the storm was generated. Furthermore, the wind speed averages were consistently high (≥8 ms^{-1}) around the dust storm during its transport.

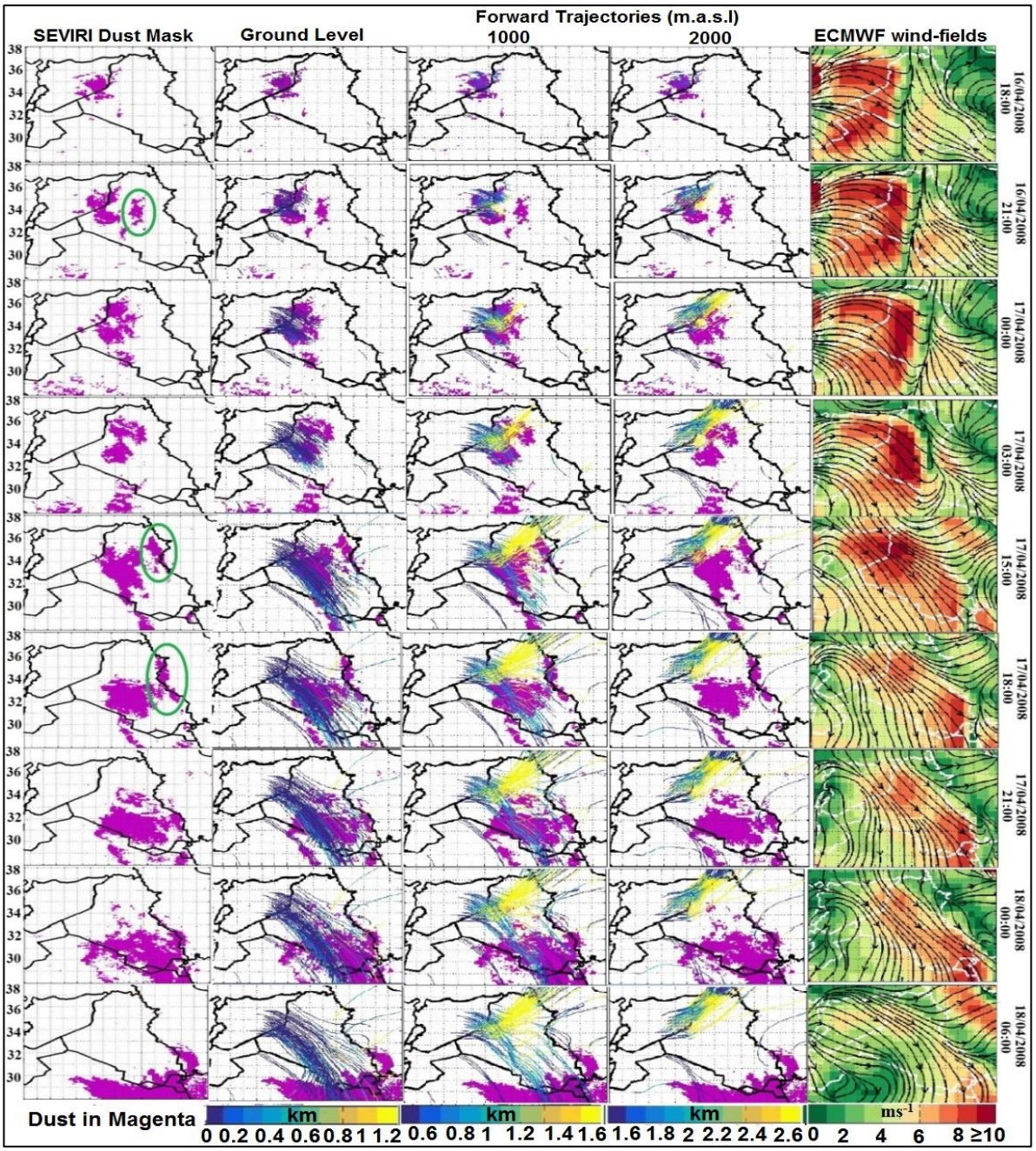

Figure 4.11: The transport of the 16/04/2008 dust storm event and associated meteorology and trajectories. This launched at 18:00 UTC on 16/04/2008 for the duration of the storm at selected observations. The SEVIRI dust mask observations are shown in the left column (derived as in figure 4.7/b), whilst air mass forward trajectories from HYSPLIT are shown in the 2nd, 3rd and 4th columns (these were calculated by using the pixel values of the dust mask from the start point (17:00 UTC on 16/04/2008) to the disappearance time (06:00 UTC on 18/04/2008) as described in sections (4.2.4 and 4.2.7)). Wind fields 10m of 3 hourly averages from the ECMWF ERA-Interim reanalysis product (as outlined in section 4.2.6) are shown in column 5 where the black streamlines represent the wind direction and the colour scale represents the wind speed (ms^{-1}).

The reverse also occurred, that is when no dust storm was present wind speed averages dropped down to around, for example (around 6-7 ms^{-1}) as in the Euphrates River basin region at (18:00, 21:00 UTC on 17/04/2008 and 00:00 UTC on 18/04/2008), respectively (see those observations in figure 4.11).

The transport of the dust plume was in a north-westerly-south easterly direction and showed very limited association with the trajectories calculated from the higher starting altitudes of 1000 and 2000 (m.a.s.l), respectively which showed advection towards Central of Iraq from around 00:00 UTC on 17/04/2008 to north-easterly direction. This is because of the convergence zone that was dominating the Central of Iraq between 18:00 UTC (16/04/2008) to 03:00 UTC (17/04/2008) (see wind-fields during those times in figure 4.11). The strong convergence zone consisting of north-westerly and south-easterly winds can be the reason that some local dust (green circles in the dust mask in figure 4.11) was observed in the Centre of Iraq at 21:00 UTC on (16/04/2008). Although this possible local dust plume merged with the main dust plume of the Euphrates River basin during the next 6 hours, part of the dust plume separated and travelled in north-westerly direction following the dominant pathways of the forward trajectories at 1000 and 2000 (m.a.s.l), respectively.

The dust storm event continued for 46 hours in total (09:00 UTC on 16/04/2008 to 06:00 UTC on 18/04/2008). This consisted of the first 9 hours of in situ dust generation (09:00-17:00 UTC on 16/04/2008) and a subsequent 37 hours of advection of a dust plume across the region (17:00 UTC on 16/04/2008 to 06:00 UTC on 18/04/2008). During this time the storm travelled from the Euphrates River basin on the Iraqi-Syrian border to the south, south east of Iraq and Arabia Gulf.

4.3.2 Case Study 31/08/2015

A more recent dust storm event occurred on 31/08/2015 (event 8 in table 4.2) which although it arose outside the period of surface observation (1985-2013) data of the Iraqi Meteorological Organisation, it nevertheless was captured by SEVIRI via the BT at 10.8 μm, the BTD 10.8-8.7 μm and the BTD 12.0-10.8 μm. The same analysis procedure was applied to this case as that above for the 16/04/2008 and other large storms shown in the CD were also analysed in the same way. The dust storm event happened between 08:00 UTC 31st August to 10:00 UTC 2nd September 2015 and is shown in figure 4.12. The initial in situ suspension of the dust lasted for only 3 hours (08:00-11:00 UTC 31/08/2015) which is unlike the other event on the 16/04/2008 shown above that carried on for 9 hours.

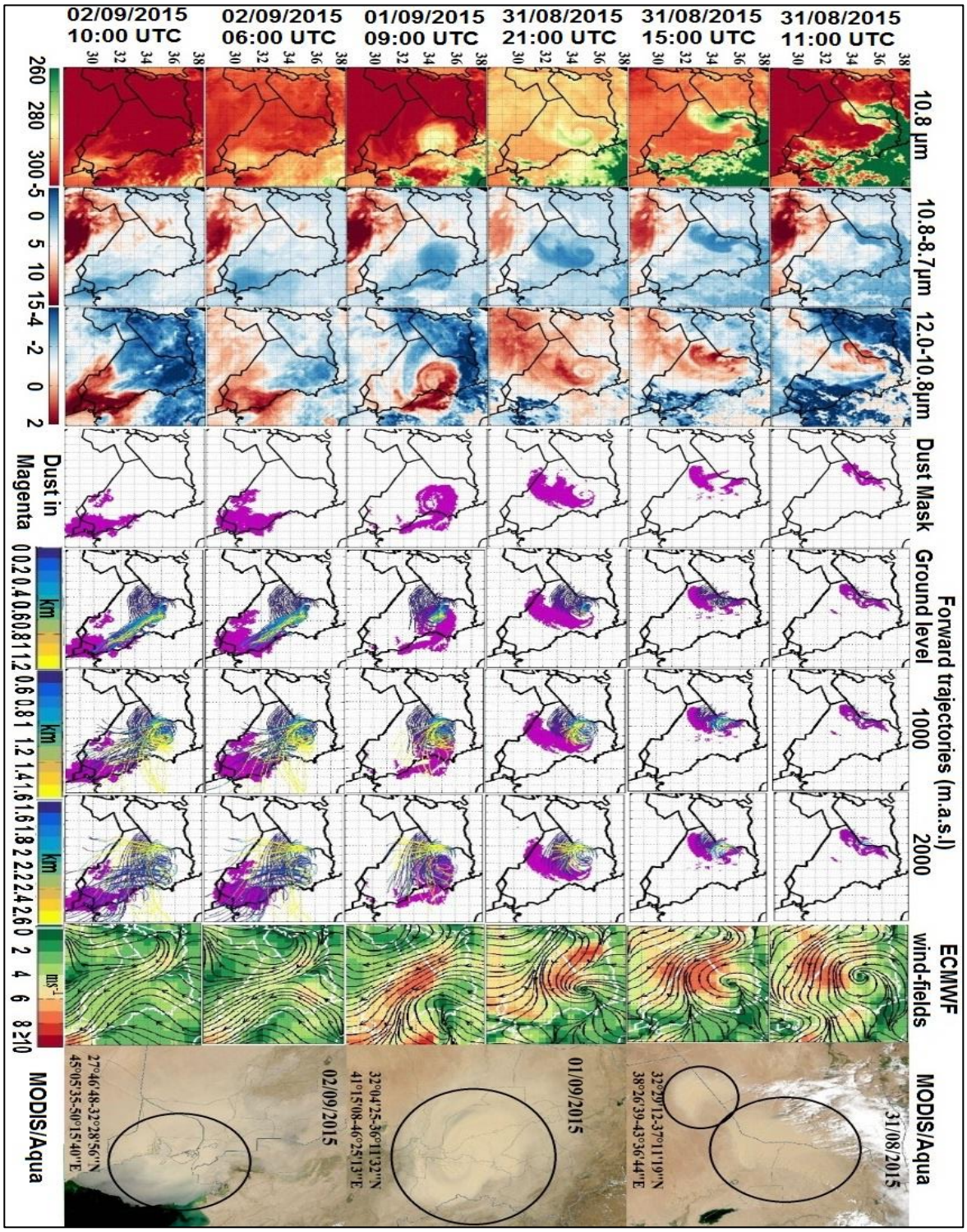

Figure 4.12: The transport of the 31/08/2015 dust storm event and associated meteorology and trajectories. The 1st, 2nd and 3rd columns show the SEVIRI BT 10.8 µm, BTD 10.8-8.7 µm and BTD 12.0-10.8 µm, respectively (derived as in figure 4.4 (a, b and c respectively). The 4th column shows the SEVIRI dust mask (created as in figure 4.7/b). Columns 5, 6 and 7 present the air mass history (%) of forward trajectories calculated as in figure (4.11 columns 2, 3 and 4) by launching the trajectories from each pixel where the dust mask was present from the start point at 11:00 UTC on 31st August to the disappearance time at 10:00 UTC on 2nd September 2015 as in sections 4.2.4 and 4.2.7. Column 8 shows wind fields from the ECMWF ERA-Interim reanalysis product as in figure (4.11/column 5) where the black streamlines present wind direction, while colours indicate wind speeds (ms^{-1}). Column 9 shows 3 true colour images from MODIS/Aqua (land surface reflectance/true colour/13:30 UTC local equatorial overpass times) that captured the storm at 3 different times. Source of MODIS images: (https://earthobservatory.nasa.gov/NaturalHazards/view.php?id=86539, on 05/01/2018).

This is an indication of the range of intensity of different generation systems (the plots showing the initial evolution of the dust is not shown in figure 4.12 and instead they are presented in case 8 in the CD). The storm was well captured in SEVIRI images in the region of the North West of Iraq and East Syria border in the Euphrates River basin. It was also clearly seen by NASA (MODIS/Aqua true colour images, see last column in figure 4.12).

A rapid cyclonic feature of an extreme low pressure system seemed to be located on the trailing edge of the Iraqi-Syrian border at 11:00 UTC (31st August) which represented a key feature in this storm. This can be clearly seen from the cyclonic low pressure shape of the wind-field observations which matches the SEVIRI dust mask and IR maps. It is interesting to notice that there were no high wind speeds along the centre of the low pressure and instead, high wind speeds were wrapped up around the centre of the low particularly between 11:00 UTC 31st August-09:00 UTC 1st September according to the wind-fields observations. As a result of this, the low pressure system forced the dust cloud to be shaped differently during the advection process. For instance, the dust cloud had a unique shape of a "hook or crescent" at 21:00 UTC 31st August and like an extreme cyclonic "pin-wheeling" shape at 09:00 UTC 1st September. On the latter observation, the dust plume seemed to be dragged further towards the East of Iraq because the low pressure system shifted to be located on the Iraqi-Iranian border, but it kept the cyclonic shape as it can be seen from SEVIRI dust mask and MODIS image on 1st September too.

The transport pathways showed that the dust plume and air mass forward trajectories were behaving similarly which was also consistent in the other case study of dust storm event on 16/04/2008 particularly at the ground level. The transport of the storm started from the Iraqi-Syrian border at 11:00 UTC (31st August) reaching southern Iraq and the Arabian Gulf at 10:00 UTC (2nd September). This consisted of 48 consecutive hours of transport travelling along the valley of Tigris and Euphrates Rivers in Iraq. The pathway of the dust cloud was quite consistent with air mass forward trajectories at all altitudes and they affected the dust plume shape in association with the cyclonic advection process. The only exception was when a small number of air samples at 1000 and 2000 (m.a.s.l) shifted towards eastern Iraq between 06:00-10:00 UTC (2ns September). However, this is probably because that the low pressure system moved eastward and no longer influenced the region during those times (as can be seen from wind-fields observations in figure 4.12 during those times). There were some reports from media regarding the dust storm event on 31st August 2015. For instance, AzerNews reported that around 140 people were

hospitalised in the provinces of Tehran and Sistan and Baluchestan due to a severe dust storm affected Iran between 1st-3rd September 2015, (https://www.azernews.az/region/87525.html, accessed on 04/01/2018).

It reported that a huge wall of dust (see figure 4.13) reached those provinces combined with a very high wind speed (19.4 ms^{-1}) causing considerable damage to electricity lines and houses in addition to tree damage. Furthermore, a civilian video was recorded (see this video https://www.youtube.com/watch?v=M0d9jMx6rJ4, accessed on 04/01/2018 from the start until (0.52) minutes was recorded in Baghdad and between (0.53-1.04) minutes in Kuwait city. The rest of the video is not related to this dust storm) in Baghdad and Kuwait cities which shows a massive wall of dust moving across houses and roads.

In the discussion above, two case studies were analysed showing high similarity between both events, particularly in terms of source region and transport pathway. The same analysis procedure was applied to the rest of the large dust storms events which will be shown in the CD. However, more statistical representation will be presented in the next 2 sections regarding the general situation of all major dust storms events from the perspectives of source region identification and transport pathways using a similar statistical approach that was used in the 2 case studies above.

Figure 4.13: Dust wall during dust storm episode on 31st September 2015. This photo was taken at night in Tehran during the event that occurred between 31st August-3rd September 2015. The original dust source of this event was the Euphrates River basin in the Iraqi-Syrian border. The storm transported to affect Iraq, Kuwait and Iran, respectively. Source: (https://www.washingtonpost.com/news/capital-weather-gang/wp/2015/09/02/dustpocalypse-huge-dust-swirl-in-iraq-iran/?utm_term=.b0c1e45e922a, accessed on 04/01/2018).

4.4 Source Region Identification of Iraq Large Dust Storms

The brightness temperature difference between the SEVIRI IR detection windows was effective in the identification of the initial detection of dust source regions. Dust plumes showed a strong positive value of the BTD at 12.0-10.8 μm and a significant negative brightness temperature difference in the 10.8-8.7 μm region as well as a high BT at 10.8 μm. Combining this together leads to sufficient information to allow identification of dust in the RGB IR channels.

The case studies in the previous section introduced that the source region of dust storms in Iraq appears strongly to be localised on the Euphrates River basin on the border of Eastern Syria and North West of Iraq (34.20.00°-36.50.00° N to 38.00.12°-41.00.20° E). This was the case as well with the other major dust storms events that was classed as large. To address the location of the main source regions of the large dust storms affecting Iraq, a spatial histogram of dust events from the source region of all major sources was compiled and as described in section (4.2.4). Figure (4.14) illustrates a histogram of dust mask information compiled from every one of the 12 large storm events identified.

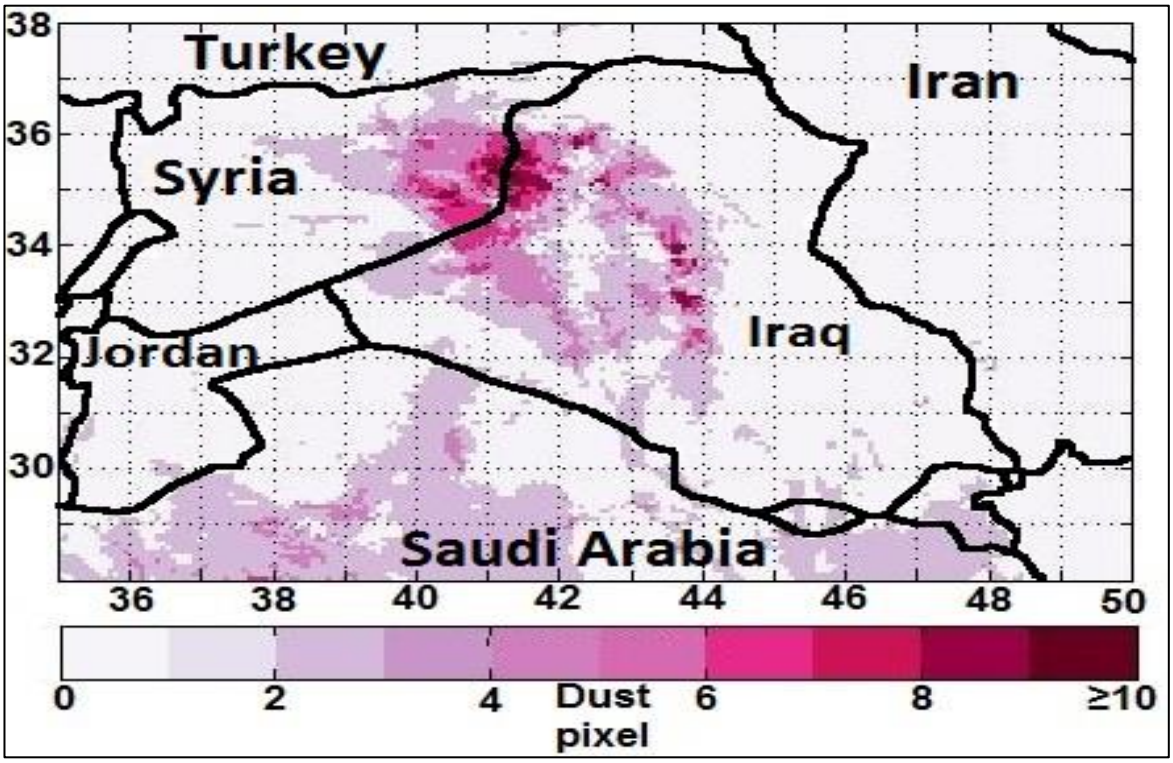

Figure 4.14: Histogram of the source region of all major dust storms events. This dust mask generated from the data during the period of dust suspension over all 12 of the large dust storm using the pixel values of the dust mask immediately prior to the dust being observed to advect away from the source region for each of the dust storm events as described in section (4.2.4).

The data were taken from the time period between the first emission detection and the period when the dust storm appeared to advect away from the region with no further dust

emitted into the region. The figure clearly shows that the dust was generated exclusively from emissions around the Euphrates River basin around the Syria-Iraq border and it is unlikely that dust can be originated from other sources (the exception of this found when some dust frequency distributed over the Central of Iraq in relation to wind convergence zone as shown in the case study on 16/04/2008).

Furthermore, figure (4.15) shows an analysis of ECMWF wind-fields data during the large dust storms generation in Iraq which indicates that highest wind speed averages (8-≥10 ms^{-1}) coincided with the spatial distribution of dust storm source regions in the Euphrates River basin in Syria and Iraq. It is important to mention that wind speed averages of the ECMWF data during dust generation period show consistency with WMO standards of wind speed threshold for dust generation (≥7 ms^{-1}) (see section 3.1) and it is also consistent with the analysis in section (3.3). While the direction of the wind-field exhibits a strong north-westerly component (this will be discussed in sect 4.5).

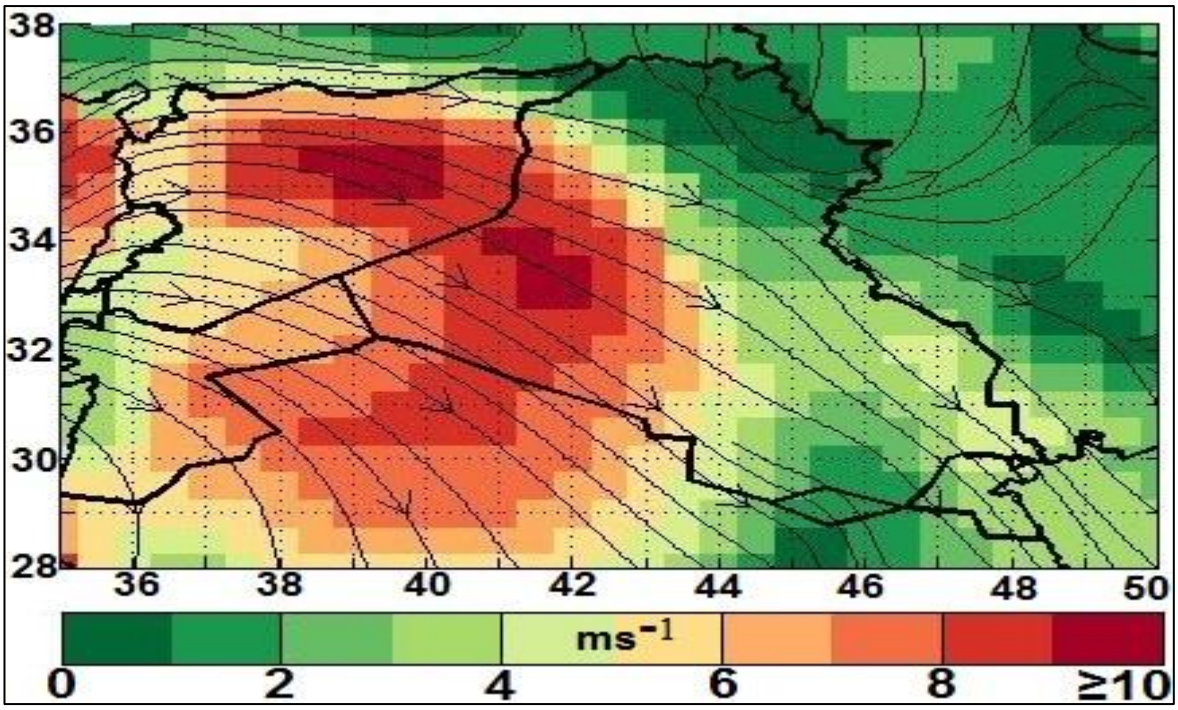

Figure 4.15: Histogram of the 10m wind-fields of the ECMWF. This compiled from 3 hourly average data of the ECMWF ERA-Interim reanalysis product taken from the period of dust storm generation across all 12 major dust storms. The black streamlines represent wind direction whilst the colours represent wind speed (ms^{-1}). This figure was derived by using the pixel values of the dust masks at the start point of each of the dust storms events prior to advection of the dust away from the source region as described in sections (4.2.4 and 4.2.6).

4.5 Transport Pathways of Iraq Major Dust Storms

Transport pathways of major dust storm events in Iraq were investigated in terms of tracking air mass source regions and pathways by using a well-known transport model, HYSPLIT. The air mass history for each large dust storm event was calculated as in

section (4.2.7). Section 6.3 will be viewing the air mass history for each major dust storm event individually).

On the one hand, the vast majority of air mass history at 0 and 1000 (m.a.s.l) elevations was from the west of the Euphrates River basin which indicates advection from the Mediterranean Sea that is consistent with the analysis in section 4.3, figure 4.16. This was found to be consistent with the wind-field climatologies as shown in figure (4.15). Notably, there was a lower contribution from air masses from the Mediterranean Sea at upper altitudes (2000 m) and air mass showed to be mainly originated from the Euphrates River basin itself as well as west of Iraq.

On the other hand, forward trajectories (bottom row in figure 4.16) indicate strong air mass flow at all altitudes towards the valley of the Tigris and Euphrates Rivers along the Alluvial Plain (where the vast majority of people are inhabited) which extends from the North West to the South East of Iraq. The strong flow apparent in the forward trajectory resulted in all large dust storms migrating along the Alluvial Plain to end up in the south and south east of Iraq. But, it is interesting to notice that only 4 out of the 12 major dust storm events ended up in the East of Iraq and West of Iran (see figure 4.17 as an example of this type of transport).

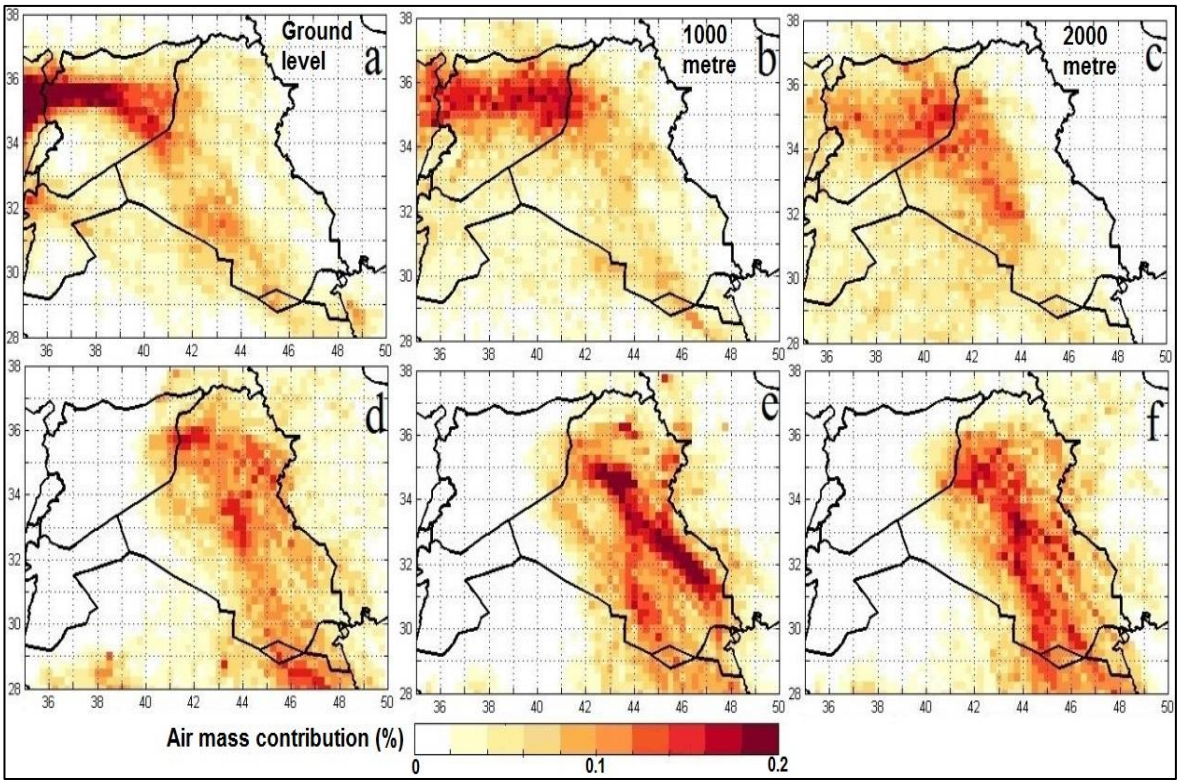

Figure 4.16: Histogram of air mass history (%) of backward and forward trajectories from HYSPLIT during all major dust storms events. Backward trajectories initiated at ground level (a), 1000 (b) and 2000 (c) metre above sea level, while forward trajectories were initiated at ground level (d), 1000 (e) and 2000 (f) metre above sea level. These were derived by using the pixels in the dust mask at the point of generation as the initiation point for each trajectory as described in sections (4.2.4 and 4.2.7).

This situation can preferentially happen when strong subsidence occurs over western Iraq that shifts air masses mostly at range of 1000 and 2000 (m.a.s.l) and partially at ground level from the Alluvial Plain towards eastern Iraq and western Iran. It can also be noted that the contribution from upper altitudes in the forward trajectories was particularly higher in the 1000 and 2000 (m.a.s.l) in comparison with the ground level altitude in those 4 events. This was also consistent with the wind-fields in those particular 4 dust storms episodes.

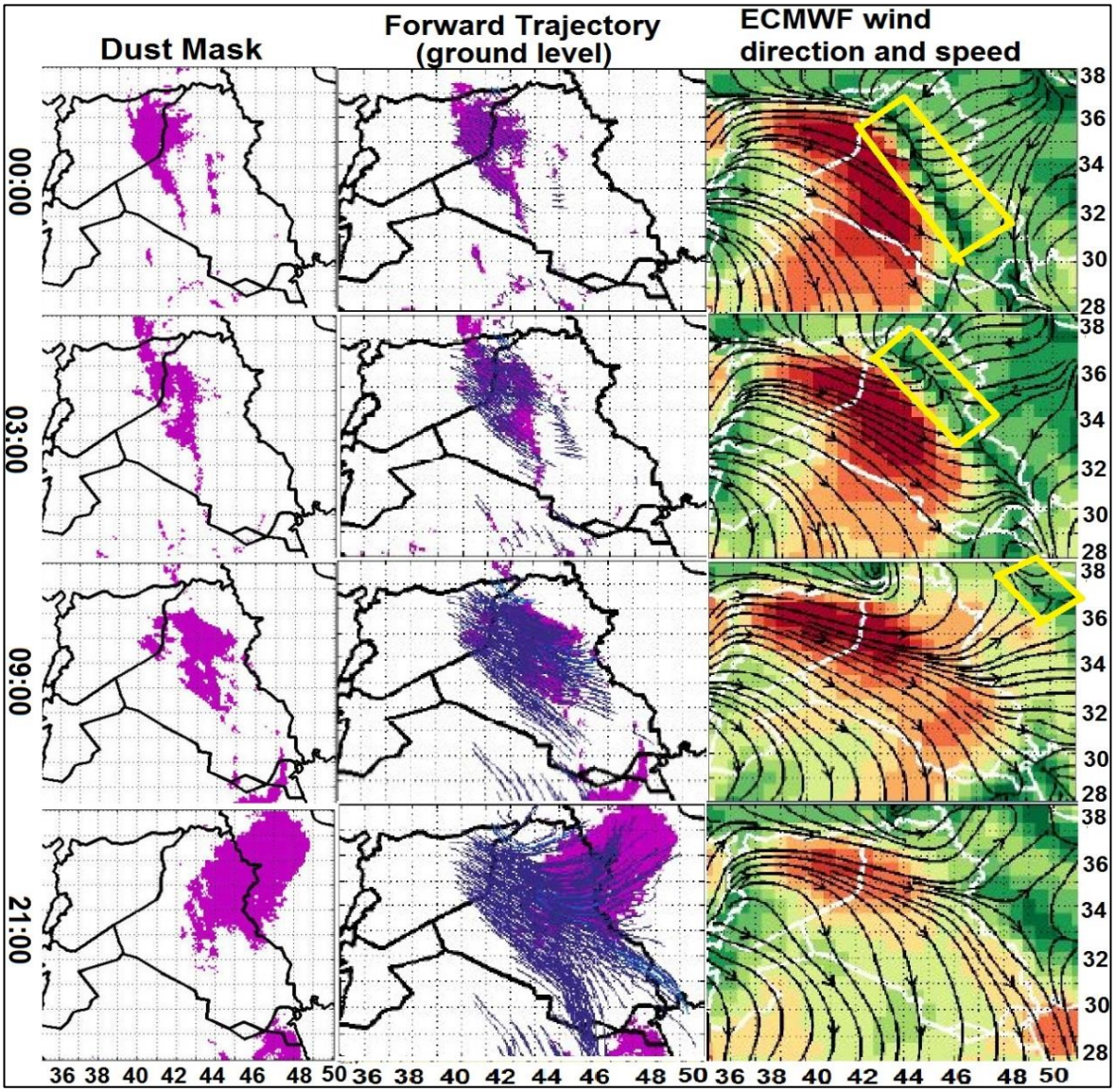

Figure 4.17: Eastern transport of Iraqi major dust storm event on 02/06/2011. This event captured by SEVIRI at 00:00. It can be clearly seen (1st column) that the dust storm was transported towards the East of Iraq and West of Iran. This seems likely to be due to a strong convergence zone (yellow box in the 3rd column) over Central Iraq between 00:00 and 09:00. The position of the convergence zone moved gradually to the West of Iran during the day of the event steering the dust plume in the same direction. This can also be seen in the air mass forward trajectories (2nd column), which show some of the air parcels at 21:00 moving in an easterly direction following the movement of the convergence zone. The 1st column was derived as described in sections (4.2.2 and 4.2.2.1), the 2nd column was generated as described in sections (4.2.4 and 4.2.7) and the 3rd column as outlined in section (4.2.6).

The backward trajectories along together with the wind-fields climatologies all point to a strong influence of the Mediterranean Sea that can establish an association on prevailing meteorological conditions during the transport of dust and that the Mediterranean Sea is the most frequent origin of air mass affecting the dust transport is consistent with (Abdi et al 2012) (see sect 2.4.1), (Ashrafi et al 2014) and Hamidi et al (2013). The latter classified dust climatologies in the Middle East as associated with low-pressure systems moving from Eastern of the Mediterranean Sea to Iraq and other regions, (see sect 2.4.2).

Likewise, the corresponding forward trajectories show strong consistency with the wind-fields climatologies, in addition to that it is also consistent with the Shamal wind advection. The Shamal advects when high pressure systems are centred above northern Africa, south of the Mediterranean and Central Europe (see sect 2.4.2) and it flows from north-westerly and northerly direction along pathways that correspond to the forward trajectory analysis presented here. When this occurs, dust travels from the source region in the Euphrates River basin to the most populated region in Iraq in the valley of the Tigris and Euphrates Rivers. The source region of dust is topographically higher than the valley of the rivers, this further constrains the flow of the Shamal wind leading to high dust concentration in the valley of the Tigris and Euphrates Rivers region (see figure 4.18).

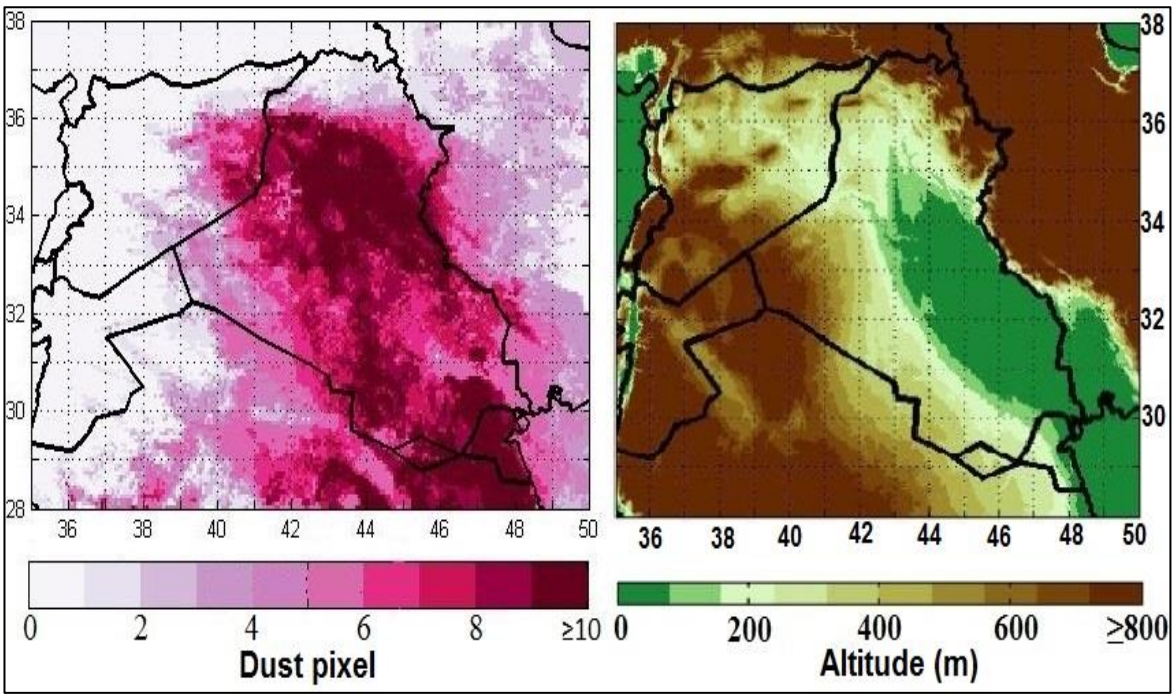

Figure 4.18: Histogram of dust concentration during the transport of all major dust storms events. The left figure was derived by counting the number of times each pixel contained a dust mask during the advection transport period of every one of the 12 large dust storms as described in sections (4.2.2.1 and 4.2.5). The topography map from (Amante and Eakins, 2009).

As the dust storm reaches the low lying region of the Tigris and Euphrates flood plain, the structure of the storm changes and splits into two, likely forced by the topography (see figure 4.18 left). An easterly arm of the storm concentrates dust on the borders of eastern Iraq and western Iran, while the more southerly arm of the dust storm advects towards southern Iraq, Kuwait and northern of Saudi Arabia affecting these neighbouring countries, (Alolayan et al., 2013; Ashrafi et al., 2014). Since the flood plain of the Tigris and Euphrates rivers is the most fertile and inhabited region of Iraq, the dust storms impact a very large number of people.

4.6 Discussion

In this chapter, large dust storms events were identified using the same routine meteorological observations for the period (1985-2013) that was presented in chapter 3 and these were coupled with SEVIRI satellite data to identify source regions and transport pathways of major dust storms events in Iraq. In addition, ECMWF ERA-Interim global atmospheric reanalysis product and backward and forward trajectories from the HYSPLIT model were also used to identify climatologies and transport pathways of major dust storms in Iraq, respectively. The combination of surface and satellite dust storm observations performed well and allowed a mask to identify dust in the SEVIRI data which was used to characterise the statistical representation of all large dust storms events which are shown to be similar from the perspectives of source region identification and transport pathways.

In terms of the identification of source regions, the SEVIRI dust mask was shown to display strong similarity across all the 12 large dust storms events. All storms were initiated with high dust frequency distribution in the Euphrates River basin on the Iraqi-Syrian border. In comparison with other studies, the Al-Najim (1975) study concluded that South West of Iraq is the main source region of dust storms. This shows no consistency with the source region of the Euphrates River basin; however it is important to mention that the data of their analysis was not based on satellite retrievals and it also does not represent similar time period compared with the period of this study. But, it is still important for comparison purposes. However, the outcome of this thesis was found to be consistent with Abdi et al (2012) and Kutuzov et al (2013) who investigated in dust storms events that affected North West of Iran and the Mount Elbrus, respectively. They showed that those dust storms were transported from the border of East Syria and North West of Iraq (see sects 2.4.1 and 2.4.6).

Moreover, (Alpert and Ganor, 2001; Prospero et al., 2002) used the Total Ozone Mapping Spectrometer to identify dust source regions over the Middle East and the globe respectively. There was a significant difference between the spatial resolution of TOMS (50 x 50 km^2) and SEVIRI IR channels (3 km) where with TOMS there are difficulties to identify small regions of dust that are located in a narrower band of spatial resolution, (Herman et al., 1997) and a similar issue can be observed with MODIS regarding the limited temporal spatial resolution, (e.g. Ginoux et al., 2012). Furthermore, the TOMS Aerosol Index (AI) flags the source region of dust storms and its pathways with the same values, where the values of AI should be the highest near the source region of dust and decreases gradually depending on how far dust travels from the source region, (Ginoux and Torres, 2003). This resulted in TOMS classifying all regions in the pathways of dust storms as dust source regions, (Ginoux et al., 2012) which leads to misidentification of the exact source region of dust.

There are several possible reasons for the source region of dust storms being localised around the Euphrates River basin in Syria and Iraq. There may well be an association with the paucity in water supplies during recent years due to the hydro-politics from Turkey and this can be illustrated using the MODIS Normalized Difference Vegetation Index (NDVI) and Enhanced Vegetation Index (EVI) data (see sect 2.4.6). In addition that in the recent years (particularly since 2003), the region of the Euphrates River basin became a war zone and the centre of political conflicts. There is some evidence (e.g. Caldwell et al., 2008; Dalldorf et al., 2008) that heavy military vehicles of different sizes and weights, which proceed over arid and unprotected soil, can destroy the top layer of the soil. This can result to altering the land use across the basin, reducing agriculture practices and leading to easier dust aerosols lifting. There was no enough evidence to link the condition of the basin over the last 2 decades to climatic changes (see Gleick, 2014).

Whether a paucity of water, the region of the Euphrates River basin being transformed into a war zone or an indicator of climate changes is the main driver remains unclear. However any of these drivers can lead to reduced agricultural practices in the region and hence reduced soil water content and a reduction in the vegetation cover in the basin. As a result this leads to breaking the soil further into finer material making it easier to be lifted in the air by wind, particularly at high wind speeds ($\geq$8 ms^{-1}) seen in the ECMWF wind-field data (as in figure 4.15).

The HYSPLIT model was used to examine the air mass history and the transport pathways of large storms in Iraq. This showed that all the 12 major dust storm events identified were strongly associated with air mass histories from the west advecting in the direction of the Euphrates River basin on the Iraqi-Syrian border, particularly at low level. This was found to be consistent with the depressions that move from the East of the Mediterranean eastwards across Lebanon, Palestine, Jordan, Israel then over the Euphrates River basin in Syria and Iraq and then towards Iran (as shown in sect 4.3.1) and thus transferring dust to and between those regions, (Hamidi et al., 2013).

It is also found that in some cases, a rapid and deep low pressure system dominates over the Euphrates River basin (as shown in sect 4.3.2) moving eastward towards Iraq and Iran. It is found that dust was generated in the basin region then advected in north-westerly wind direction over the valley of the Tigris and Euphrates Rivers in Iraq as identified in the ECMWF 10m wind-fields and forward trajectories, particularly at ground level. While rarely at (0, 1000 and 2000 m), dust advection might be directed towards East of Iraq and West of Iran. This was noted to occur when there is a convergence zone in the wind field or low pressure system was dominating over Central Iraq which shift air parcels towards easterly rather than a north-westerly direction (as shown in figure 4.17 - see also events 4, 7, 13 and 16 in the CD).

The transport of the 12 large dust storms in north-westerly direction identified crossing Iraq coincided with the corresponding forward trajectories shows strong consistency with the wind-fields climatologies from ECMWF and the prevailing Shamal wind in the region. The Shamal advects air from a north-westerly direction when high pressure systems are generated over the Mediterranean Sea and low pressure systems dominate over Iran. When the Shamal advects, it triggers dust and transports it in a south-easterly direction from the source region in the Euphrates River basin towards the most populated region in Iraq in the valley of the Tigris and Euphrates Rivers then to Kuwait, The Arabian Gulf and Iran (as in sect 4.3Al Senafi and Anis, 2015; Yu et al., 2016).

'Blank page'

Chapter Five: Economic Impacts and a Proposed Method for Producing a Warning System of Dust Storms

The objective of this chapter is to demonstrate the economic impacts of dust storm events on both global and local scales. It points to the pivotal influence of dust storms on human life and economics. This is particularly true in Iraq where dust storms activate close to densely populated regions of the country in the valley of the Euphrates and Tigris Rivers. In addition, the chapter will discuss a potential prediction system that could be developed based on results from the thesis which may provide a significant policy impact for the country. The study has identified a clear sequence of events leading to the formation and transport of large dust storms which can be used to produce a warning system in the region. This in turn would help to protect the population from the effects of dust storms.

5.1 The Economic Impacts of Dust Storms

Dust storms have a large range of economic impacts, some of these influences can be immediate (e.g. health costs, livestock mortality and costs of clearing dust particles from dams, roads, airports and irrigation channels) while others have a longer term impact (e.g. soil erosion and reducing soils fertility), (Goudie and Middleton, 2006).

There is a growing body of literature that recognises the importance of the economic impacts of dust storms. The generalisability of much published research on this issue comes from calculations of the annual money loss in a specific sector of a society. It is now globally well-established from a variety of studies on the economic effect of dust storms that there is a strong relationship between the dust storms and its economic impacts but this has been surprisingly neglected by local studies in Iraq despite the fact that a large population is potentially exposed to airborne dust and aerosol.

5.1.1 Global Trend of Economic Dust Storms Effects

Historically there is a large volume of published studies describing the role of the economic influences of dust storms. The immediate economic impacts of dust storms are well-documented in the literature. For instance, the Taiwan National Health Insurance research database reported an average of 17-20 hospital admissions which costed the health sector approximately £19400 for asthma applications during 3 days of a dust storm event, (Wang et al., 2014). A very severe dust storm occurred in the north west of China between 4th and 6th May 1993 led to a total of 85 people died and 264 were injured, massive damage of destroying 4412 houses, killing 120000 animals and burying around 2000 km of

irrigation channels. As well, the event left direct economic losses of approximately 96 million dollars, (Zhang and Wang, 1997).

It is apparent that immediate economic effects of dust storms do not only lead to economic loss on a specific sector of the society (e.g. transportation), but they could cause multiple losses by affecting other sectors and activities. This was reported, for example in the state of New South Wales in Australia due to one dust storm event happened on 23rd September 2009, (Tozer and Leys, 2013). The storm caused a total economic loss of $200 million, some of the economic losses addressed as approximately $14 million for car accidents, $20 million for flights cancelation, delays diversion, and staff over time working hours, fuel, meals vouchers and passengers' accommodations and $7 million for commercial activities which included, for instance retail purchases for food, coffee and newspapers.

Other types of immediate economic impacts of dust storms include flight cancellations, During 2002, reported sale losses of 0.6 million dollars in South Korea arose due to dust related flight cancellations, (Kang et al., 2004) while in Beijing, a total loss of $264.5 million of economic losses (manufacturing, trade and catering services, agriculture, transportation, households and construction) due to dust storms event occurred during the year 2000 alone (Ai and Polenske, 2008).

Conversely, there has been little quantitative analysis on the long-term economic effect of dust storms. This is probably due to the difficulties in calculating such impacts. For example, dust storms have been observed to be associated with wind erosion activities in the mid-1980s in the USA and in 1999 in South Australia leading to a total estimated economic loss due to soil degradation of about 466 and 40 million dollars, respectively (Huszar and Piper, 1986; Williams and Young, 1999).

5.1.2 Local Scale of Dust Storms Economic Loss

As demonstrated above, there has been no systematic study to examine the volume of the economic losses of dust storms in Iraq. However, some work has been achieved in the neighbouring countries to Iraq to estimate the immediate and long-term losses. For instance, the local government in the Sistan region of Iran recorded a total economic loss of approximately 125 million dollars during 338 days that witnessed dust storm events between the years 2000 and 2004, (Miri et al., 2009). Some of the losses (million US$) in the Sistan region were recorded as $17.2M for reduction of crop products, $25.7M of clearing accumulative sands from wells and agricultural lands and $5.4M resulting from well dryness, (Pahlavanravi et al., 2012).

Moreover, a well-detailed study was conducted in Kuwait in 2017 to calculate the economic losses of traffic accidents due to dust storm events. The study showed, for example that a total economic loss of approximately $730 and $755 thousands arose due to 11 and 14 dust storms events during the years 2011 and 2012, respectively (Al-Hemoud et al., 2017). While another study by an oil and gas company in Kuwait reported 5159 of non-productive hours used to clear accumulative sand caused by dust storms (figure 5.1) between 2015 - 2017 which led to $9.36 million economic loss, (Al-Hemoud et al., 2019).

Figure 5.1: Accumulative sand on an oil pipes in Wafra oil field, Kuwait, September 2018, from (Al-Hemoud et al., 2019).

The 2016 Global Assessment of Sand and Dust Storms (Shepherd et al., 2016) reported that there is much less action and attention of adopting some planned strategies to prevent or reduce the economic effects of dust storms, e.g. increasing the vegetation cover in the arid and semi-arid region. This is perhaps because such preventive measures need large scale international agreements and high corporative work among countries and territories.

The discussion above points out to the government in Iraq of the importance of establishing an up to date study of the economic impacts of dust storms in Iraq, as well as adopting some systematic and quantitative projects on this issue. Particularly as shown in chapter 4 that dust storms trajectories follow the track of the most populated region in the country in the Euphrates and Tigris Rivers valley.

5.1.3 An Estimation of Economic Loss from Dust Storms in Iraq

This section provides an estimate of the economic loss in Iraq based on a dust storm event that lasts for a minimum of one day. The Iraqi government usually announces a day's leave from work when a severe dust storm is about to reach the country. Such announcement does not exempt people who do not live in the track of dust storms in the Alluvial Plain (e.g. Northern provinces).

The population of Iraq is recorded as approximately 40 million people, (https://www.worldometers.info/world-population/population-by-country/, accessed on 07/02/2019) about 7.3 million are workers in different sectors of the Iraqi government, however only around 60% (4.38 million) of whom are in a full time employment positions. The typical number of working hours per day in Iraq is 6, while the minimum wage applicable to the factor assumed in this analysis is £1.3 per hour, (the information in this paragraph was obtained via a personal communication with the Central Statistical Organisation of Iraq on 3rd March 2019).

Consequently, the fraction of the Iraqi economy that can be affected due to a large dust storm event that lasts for 1 day is £34.164 million. This was simply calculated by multiplying the economic loss per day per person (£7.8) with the number of full-time employees only (4.38 million people). It is important to recognise that the government in Iraq pays wages in advance to those employees' who are in full time positions. This is regardless the number of working hours that an employee should achieve. This means that all the economic loss due to a dust storm event are already paid by the government which makes it a direct and definite financial loss and it is not from the employees' wages. However, it in turn financially affects people who are self-employed (non-governmental employees).

There are around 40% of people (2.9 million) in Iraq who are self-employed or private companies. A financial loss of approximately £22.6 million can be estimated by applying a similar analysis as above for this sector of workers. However, it is difficult to calculate the economic loss from the private and self-employed sectors due the different daily wages and working hours that those sectors execute comparing to the full-time workers of the government. Moreover, it is not necessary for some private companies or self-employed people (e.g. taxi companies and grocery shops) to stop working on a day of a dust storm event as this can purely be classed as their own decision.

In summary, the estimated calculation showed the immediate minimum economic loss in Iraq due to a dust storm lasting 1 day was £22.6M. This cost has been calculated based on the loss of paid work for the day via government employees only. It can certainly be larger if it is assumed that this reflects the wider working population (by scaling up the amount to all Iraqis of working age). As a comparison, the Gross Domestic Product of Iraq was approximately $198 billion in 2017 (https://tradingeconomics.com/iraq/gdp, accessed on 27/05/2019). Therefore, the directly attributable loss from government workers wages amounts to over 5% of the Gross Domestic Product of Iraq.

The discussion above sheds light on the importance of establishing a proposed method of a forecast tool to release warnings about dust storms for precautionary measures to people and this will be demonstrated in the next section of this chapter.

5.2 Producing a Warning System of Dust Storms for Iraq

5.2.1 The History of Dust Storms Warning Systems

Dust storms can cause devastating damage to human health, have huge human, social and economic impacts as well as have major influences on global climate change and meteorology. This drives the necessity to reduce the impact of dust storms via generating an effective forecasting tool to establish an early warning system. However, there is a critical need to monitor dust aerosols in the atmosphere which causes difficulties in terms of monitoring source regions of dust, transport pathways and deposition, (Gong and Zhang, 2008).

Monitoring dust particles has been demonstrated in a number of complementary approaches, for instance in-situ observing system of aerosols mass concentration of PM_{10} and $PM_{2.5}$, (e.g. Basart et al., 2016) visibility records and present weather data that measures at ground surface meteorological observations (e.g. Cowie et al., 2014) and ground based LIDAR and sun-photometers which involves measuring vertical sections of dust aerosols optical and microphysical properties (e.g. Amiridis et al., 2013; Liu et al., 2008; Pérez et al., 2006). In addition, satellite products are widely employed and have been widely used in combination with ground surface measurements and numerical modelling, (e.g. Cowie et al., 2015; Sodemann et al., 2015).

Satellite products can provide regular observations of large spatial coverage from local, regional to global scales which can be available to use by weather centres and other meteorological institutions in near-real-time with high resolution, (Benedetti et al. 2014).

Within this context, there are a number of dust storms forecasting systems which now operate in the regions where regular dust outbreaks occur.

Benedetti et al. 2014 provide a brief overview of dust forecasting history. (Westphal et al., 1987) was the first to attempt to use 2 numerical dust transport models in the Sahara. In the 1990s, more developed approaches into operational dust forecasting and simulations were used, such as the Dust Regional Atmospheric Model (DREAM) in 1996 which is considered the first regional model investigation dust process in the Sahara and Mediterranean regions in which the dust concentration was built into the prognostic equations of the atmospheric model driver, (Nickovic, 1996; Ničković and Dobričić, 1996). One year later, the University of Athens launched a dust forecasting model named SKIRON which provides 3 days weather forecasts in the Mediterranean region, (Kallos et al., 1997) and since then, dust weather predictions models have become more available from regional to global scales (e.g. see Barcelona model sect 2.4.5). The main objective of all models above is to combat dust storms via introducing a vital forecasting tool to the country-level authorities to take actions.

In 2005, the World Meteorological Organization conducted a survey among 40 WMO member countries to determine their interest and concern in dust storm phenomena and so launched a new program called the Dust Storm Warning Advisory and Assessment System in the year 2007, (Pérez and Baldasano, 2008). The WMO mission behind this program is to enhance the ability of countries to deliver timely and high-quality dust storms forecasts and observations to users through an international partnership of research, (Nickovic et al., 2015). Therefore, the result of such cooperation may provide a global network of research, operational communities and users with enhanced information about dust storms employing satellite products and dust modelling particularly in 3 regional nodes, these are (1) Northern Africa, Middle East and Europe, (2) Asia and Central Pacific and (3) Pan-America, (Shepherd et al., 2016; Terradellas et al., 2015).

Since then, a number of well-developed early warning systems are operating in different parts of the world from global (e.g. The UK Met Office, Japan Meteorological Agency and The National Centres for Environmental Prediction in the United States) to regional (e.g. Barcelona Supercomputing Centre in Spain, The Egyptian Meteorological Authority in Cairo and China Meteorological Administration), (Shepherd et al., 2016). In the next section, a potential early warning system which can be operated locally in Iraq from the outcome of this study will be discussed.

5.2.2 Developing This Study to Produce a Warning System of Dust Storms in Iraq

There is the potential to develop a dust storm prediction system arising from the work in this thesis that can provide a significant policy impact for Iraq. With this in mind, it is important to understand about the current forecasting tool used by the Met Office in Iraq to predict large dust storms. The central Met Office in Baghdad uses the outcomes of NASA observations to identify whether a major dust storm event is transporting towards Iraq or not (personal communication with Nasiriyah Met Office in Iraq on 26th March 2019). In other words, an access to the NASA online website is made to observe related dust storms announcements (by television, radio and the Met Office website) on a daily basis by employees from Baghdad Met Office. In this context, the work in this thesis has identified a clear sequence during the development of large dust storm events (this distinctly assists with large dust storms and not local dust events) which can be employed to produce a more reliable early warning system in Iraq than is currently in place which in turn will protect the population from the effects of major events.

A number of key findings and methods were presented in this thesis; these broadly determined the meteorological conditions, source regions and transport pathways of dust storms in Iraq. First, the analysis in this work showed that the main advantage of SEVIRI is that it can produce a reliable and free dust mask every 15 minutes and thus can determine the source of large dust storms as it generates. This is in contrast to products from polar orbiting satellites such as MODIS which provide only two overpasses per day at most at fixed times. The online access to the archive of SEVIRI, their temporal resolution and the quick availability of this product make it ideal for dust monitoring. This means that the major source region of dust storms can be monitored continuously and hence it can be seen whether the uplifted dust advects towards the major population regions or not.

Furthermore, the analysis of major dust storms in Iraq carried out in this thesis showed that the meteorological conditions during storm development were broadly consistent and they all occurred during periods when the source region was impacted by low pressure systems that had travelled eastward from the Mediterranean Sea and were highly associated with the Shamal north-westerly winds causing massive dust concentration along the valley of the Tigris and Euphrates Rivers of the Alluvial Plain. The data of SEVIRI can be complemented with backward trajectories which allow investigating the origin of the air mass present over a particular site. This can be acquired via the HYSPLIT model which developed by NOAA as presented in chapter 4.

At this stage, a possible early warning system for dust storms based on the available resources of this work could be based on the following:

1) Download the data that will be needed and that is currently available in near real time. This is mainly SEVIRI data (see sect 4.2.2) which is freely accessible, wind-fields from the ECMWF ERA-Interim reanalysis product (see sect 4.2.6) and meteorological files from HYSPLIT (see sect 4.2.7).

2) Collate and pre-process all the data required above using a specific algorithm. The algorithm (which is available on request) used in this study functioned in MATLAB (https://uk.mathworks.com/products/matlab.html, accessed on 27/05/2019), however it is important to recognise that MATLAB is not open source and requires an expensive license.

3) Monitor meteorological forecast fields to identify the potential for conditions suitable for dust storm generation. This study showed that a recipe list of dust storms drivers (i.e. high wind speed $\geq$7 ms^{-1}, north-westerly wind component at the source region and north-westerly to south-easterly during the advection process) can be established. Since information about wind fields can be obtained from an operational forecasting system in the region, i.e. local weather observing centres, this can be made operational (see sects 3.2 and 3.3).

4) Routinely monitor dust using SEVERI every 15 minutes once the generation of a dust storm in the region of interest (described as in sects 4.2.2.1, 4.2.2.2 and 4.2.3) has been identified.

5) Initiate forward trajectory modelling using HYSPLIT, driven by a meteorological forecast model, to predict the advection of dust across Iraq (see sect 4.2.7).

6) At this point, it is no use having an operational system that produces a large number of false positives since forecasts will either not employ the tool or at least will not rely on it when they construct their forecasts. For this, the false positive is a test for the recipe list mentioned above. The false positive analysis can address, for example "how often does the SEVIRI dust mask flag dust in the source region but dust does not advect towards the main population regions?". In other words, it is a false outcome when the dust flag shows dust over the source region and the trajectories predict advection through Iraq, and the wind flow is confirmed by measurements but no dust is observed (assuming there are no other removal processes such as rainfall).

7) After approximately an hour from the first identification of the storm in the source region, send a text alert to local forecasters in the local observing centres with the SEVIRI plots included for some manual analysis based on the known conditions. Updated plots could be generated every 15 minutes. It is apparent from the case studies discussed in this work that the evolution time of large dust storm generation continued for a minimum of 9 hours in the Euphrates River basin region and during these hours, it showed that dust plume had a very limited spatial extent before it was gradually developed from discrete points in the basin. At this particular point and before the storm advects away from the basin region towards Iraq internal lands, it potentially suggests that it can give a matter of time to ensure that people take appropriate mitigation measures (e.g. staying indoors). Consequently, this produces a powerful tool to issue short-term predictions and early warning notices.

The above procedure can be operationally employed in near real time whether there is a potential advection towards the populated regions of Iraq during the first 1-3 hours from the identification of dust storm or not. Consequently, a warning can be disseminated to the general public via mobile apps (these can be vital and spread information very quickly), television or radio.

In the case of a positive dust storm flag, the alert should approximately continue between 1-3 days after of the first identification time in order to identify its possible arrival over the populated regions of Iraq. The information from the analysis outlined above can be used to inform response actions. If this procedure could not be operationalised a similar trajectory tool might be embedded within a forecasting system to be used as an operational tool. This process would help to decide how a forecast tool could be introduced and it may point to a method to develop a dust storms forecasting system (from an air quality perspective).

'Blank page'

Chapter Six: Conclusion

This thesis provides insight into dust storms events in Iraq, a region that experiences a considerable amount of dust loadings into the atmosphere across a range of timescales. The key importance of this work appears from the huge dust aerosol influences on humans and global climate which points to national mitigation measures involving local agriculture and land management practices being required to reduce the impact of dust on human health close to densely populated regions of the country. The observations in this thesis show important outcomes and differences in comparison with previous studies of dust outbreaks in Iraq, particularly the region of the Euphrates River basin on the Iraqi-Syrian border that represents a significant and previously not completely explored portion of the topic and the region in particular. This thesis has employed a set of surface meteorological data that have been obtained from the Iraqi Meteorological Organisation; no single study has used this data in a similar analysis in the past and this reflects the importance of such analysis. As well as that this thesis investigated in the Iraqi dust storms events from SEVIRI satellite data point of view. This thesis can aid future studies in the field of dust storms in Iraq from the perspectives of acting as an indicator to compare further changes against, and through the possibility of developing more research methods and data analysis.

6.1 Summary of Findings:

The key drivers of determining the meteorological, source region identification and transport pathways of dust storms events in Iraq are clarified in this thesis using both ground surface and satellite observations.

This thesis presents analysis of a multi-decadal multi-site surface observation record to examine the importance of the meteorological of dust storms events in Iraq. North-westerly winds are the most dominant wind direction across much of Iraq and are often associated with periods of high wind speeds of 15-20 ms^{-1}. In the central and south west of Iraq northerly winds are much more frequent and typically associated with wind speeds of 10-15 ms^{-1}. Westerly winds (10-15 ms^{-1}) can be seen in few stations in the west and central of Iraq. At all sites, the frequency of the local wind arising from other directions is relative low and associated with low wind speeds <7 ms^{-1}.

Dust storms distribution is highly associated with wind direction and wind speed in Iraq. Dust storms are particularly frequent during periods of north-westerly wind in central and south of Iraq, westerly wind to the north of Iraq and northerly winds in the west of the

country. Most dust storms are observed during periods when the wind speeds were between the 7 ms^{-1} threshold and 20 ms^{-1} at all sites.

In general, dust storms were observed to be more frequent in the south and south west of Iraq during spring and summer (March-September) since the weather in spring is conducive to dust storm genesis, characterised by low precipitation, increasing in wind speed and high temperature averages in comparison with autumn and winter. During the summer, increased aridity leads to increased likelihood of resuspension.

The average annual number of dust storms is highest in the south of Iraq at the Nasiriyah and Simawa stations where the agricultural activity and the widespread presence of sand dunes play a role in re-suspending dust particles. The lowest number of dust storms was recorded in the centre of Iraq at the Hilla, Khalis and Hai stations, respectively.

The majority of dust storms occur in the daytime between the hours of 06:00 and15:00, and peak around midday. This is because surface heating reaches its maximum in the afternoon, increasing turbulence and re-suspending dust particles from the ground.

In all cases, dust storms in Iraq are of short duration (<6 hours), with the period of greatest frequency being between (0-3 hours), implying that they are locally produced and spatially localised being mainly associated with diurnal surface heating and enhanced convection. Although a few, much larger storms were observed which are associated with large scale advection across the region.

The formation and transport of large dust storms was analysed using a combination of surface observations and satellite data. This work found that the combination of ground surface and SEVIRI satellite data was effective in identifying the source region of dust storms and their transport pathways in Iraq. SEVERI visible and IR data was combined to produce an identification of dust in the field of view. The dust mask of SEVIRI showed strong similarity for all 12 major dust storms events which were identified in the region between 1985-2013. It showed that the 12 large dust storms were similar in nature, all being initiated high frequency in the Euphrates River basin on the Iraqi-Syrian border (34.20.00°-36.50.00° N to 38.00.12°-41.00.20° E). High wind speeds (≥8 ms^{-1}) from the ECMWF 10m wind-field reanalysis data were found to be consistently present during dust generation and advection times in the Euphrates River basin across all the 12 dust storms.

Air mass history identified using backward trajectories from the HYSPLIT model at three levels (0, 1000 and 2000 m.a.s.l) showed that all the 12 major dust storms events were strongly associated with the air masses histories from the west and in the direction of the Euphrates River basin which is an indication for the low pressure systems over the East of the Mediterranean Sea moving eastward towards Iraq, (Hamidi et al., 2013). The SEVIRI dust mask was used to show that all the 12 large dust storms advected away from the source region in the Euphrates River basin in a north-westerly direction across the valley of the Tigris and Euphrates in Iraq and ended up in south and south east of Iraq, Kuwait, The Arabian Gulf and Iran.

ECMWF 10m wind-fields and forward trajectories from the HYSPLIT model particularly at ground level (0 m.a.s.l) were used to show that these events were associated with Shamal winds. Forward trajectories at (0, 1000 and 2000 m.a.s.l) showed air had a somewhat different path across the region during large dust storms sometimes advecting air parcels towards eastern of Iraq and West of Iran; however this situation was only observed in 4 dust events at those 2 altitudes.

This work has shown that when dust storms advect air from a north-westerly direction the highest frequency of dust during its advection across Iraq was along the most populated region in Iraq in the valley of the Tigris and Euphrates Rivers. These events coincided with the advection of the Shamal wind along the valley steered by topography.

6.2 Possible Reasons to Generate Dust Events in the Euphrates River Basin

The main implication from the observations presented in this work is identifying the source region that causes the advection of large dust storms across Iraq. Notably, the satellite data showed strong evidence that all major dust storms in Iraq were generated from the same source region in the Euphrates River basin. Most importantly that when dust generates in the basin it was shown to be advected along the most densely populated region in Iraq along the valley of the Tigris and Euphrates Rivers across the Alluvial Plain.

The hydro-politics by Turkey who reduced water supplies leading to reduced soil humidity and rapid soil deterioration. This in turn has led to a decrease in agricultural practices which affected the vegetation cover, consequently leading to high dust loadings in the basin region. There has clearly been substantial change in the water supply where Turkey

has gradually decreased the monthly averages water discharge in the Euphrates and Tigris Rivers between 1948-2012 (see sect 2.4.6).

Moreover, it has been shown by NASA who has demonstrated that Turkey, the upstream user of the Euphrates River, has been controlling the headwater of the Tigris and Euphrates Rivers basin on the downstream users in Syria and Iraq. For instance, (Jongerden, 2010; Voss et al., 2013) showed that during the period 2003-2009, around 144 cubic kilometres of water was lost in the Euphrates River basin, dropping the amount of water from 145 metre (elevation) on 7th September 2006 to 120 metre on 15th September 2009 in Qadisiyah reservoir in Iraq (see figure 2.11), consequently resulted in decreasing the vegetation cover in the Euphrates River basin which clearly can be demonstrated via NDVI and EVI analysis (see figures 2.12 and 2.13). During the period above, there have not been any other extreme changes in the climatology of the Euphrates River basin that might lead to another conclusion (e.g. climate changes) behind the deterioration of the vegetation cover in the basin.

In addition, the Euphrates River basin has been and continues to be affected by wars and political conflicts over the last 2 decades and has experienced heavy military vehicle activities. Caldwell et al and Dalldorf et al (2008) showed, for example that between 1991-2003 heavy military vehicles were carried thousands of tons of weapons and tanks crawling off roads over arid and unprotected soil in the south region of Iraq. Those actions were similar to what has been carried out on the Iraqi-Syrian border, (see https://www.haaretz.com/.premium-scientists-syrian-war-was-one-of-causes-for-dust-storm-1.5406082, accessed on 24/01/2018) that can be responsible of destroying the compacted top layer of soil, reducing agriculture practices, altering the land use across the basin and leading to easier dust aerosols lifting in the air.

Although, it is difficult to conclude whether the cause of dust storms frequency in the Euphrates basin is caused by a shift in the recent changes in the land use due to wars or whether it is due to changing the water supplies from Turkey. However either can lead to reduced agricultural practices in the region and hence reduced soil water content and a reduction in the vegetation cover in the basin. This suggests the need to investigate the differences in the nature of the basin region in terms of how it has been and may witness some changes in association with the trends of land use over the last 2 decades, which may help to shape the design of future analysis and measurement studies.

6.3 Future Research Recommendations

The work presented in this thesis is an important contribution to the region of Iraq in particular and Syria too. The findings of this study have a number of important implications for future practice, however this research has thrown up many questions in need of further investigations and measurements of dust studies in Iraq to mainly assess to what extent these dust storms event are representative in the region. The importance of dust storms comes from their considerable impact on human health (Shepherd et al., 2016) and can cause severe economic losses too, (Ai and Polenske, 2008). This work has shown that major dust storms in Iraq typical form in the Euphrates River basin in the Iraqi-Syrian border and travel across the most populated region in the Tigris and Euphrates Rivers valley. There is, therefore, a definite need for further research in dust storm studies which can be addressed by focussing on the following aspects:

1- A greater focus in particular should be paid to the Euphrates River basin region as it represents the main source area of large dust storms events. An assessment of the current conditions and the nature of land use are strongly recommended to identify whether the basin region could recover due to lack of water supply and wars or not. Unless governments in Syria, Turkey and Iraq adopt a reasonable approach to tackle the rapid land deterioration and desertification in the Euphrates basin region, this issue will not be attained. Ensuring that appropriate systems, services and support should be a priority to suppress the role of the basin region being the main source area of major dust storms, consequently reducing their harmful effect on human health.

2- These outcomes could support the necessity for a systematic study of the negative effects of dust storms on human health and economic losses in Iraq. Such studies would enhance awareness and could reduce dust storms effects on people who are prone to its danger. However, continued efforts are needed from some government offices in Iraq (e.g. Ministries of Health and transportation) to ensure that more accessible up-to-date data is available as it will be a key priority for the long-term effectiveness of such investigations.

   Roadside sings can be used to notify people of speed limits during dust storms events on motorways and inner roads in cities and towns. Reducing car speed helps to decrease car accidents and therefore human lives.

3- Another important practical recommendation is to require some new ground surface observing sites as the current ones are not sufficient. All climate surface stations

that currently exist are geographically distributed around the valley of the Tigris and Euphrates Rivers in the Alluvial Plain in Iraq and further sites are highly required, particularly near the Iraqi-Syrian border since these are where the source regions are located. The work has also motivated the use of more advanced instruments at surface observing stations to observe and monitor dust uplift automatically. For instance the Runway Visual Range (RVR) instrument that is only used in Baghdad Airport climate station (as introduced in sect 3.1) could be employed more widely across the network.

4- More broadly, research is also needed to determine how much dust is deposited in different parts of Iraq. This information can be used to develop targeted interventions aimed to measure dust concentration on the valley of the Tigris and Euphrates Rivers along the Alluvial Plain region because it considers the main pathway of dust storms as well as it is the most populated region in the country. Therefore, it can be substantially powerful information from human health point of view.

'Blank page'

Bibliography

Abdi Vishkaee, F., Flamant, C., Cuesta, J., Oolman, L., Flamant, P., Khalesifard, H.R., 2012. Dust transport over Iraq and northwest Iran associated with winter Shamal: A case study. Journal of Geophysical Research: Atmospheres 117.

Ackerman, S.A., 1997. Remote sensing aerosols using satellite infrared observations. Journal of Geophysical Research: Atmospheres 102, 17069-17079.

Ackerman, S.A., Chung, H., 1992. Radiative effects of airborne dust on regional energy budgets at the top of the atmosphere. Journal of Applied Meteorology 31, 223-233.

Ai, N., 2003. Socioeconomic impact analysis of yellow-dust storms: a case study in Beijing, China.Unpublished Master Thesis, MIT.

Ai, N., Polenske, K.R., 2008. Socioeconomic impact analysis of yellow-dust storms: An approach and case study for Beijing. Economic Systems Research 20, 187-203.

Al-Ansari, N., 2013. Management of water resources in Iraq: perspectives and prognoses. Engineering 5, 667-684.

Al-Dabbas, M.A., Abbas, M.A., Al-Khafaji, R.M., 2012. Dust storms loads analyses—Iraq. Arabian Journal of Geosciences 5, 121-131.

Al-Dassea, A., 2010. The practical analysis of Iraq climate. Dar Al-Pharahidi for publication, Baghdad, Iraq.

Al-Dousari, A.M., Al-Awadhi, J., Ahmed, M., 2013. Dust fallout characteristics within global dust storm major trajectories. Arabian Journal of Geosciences 6, 3877-3884.

Al-Hemoud, A., Al-Dousari, A., Misak, R., Al-Sudairawi, M., Naseeb, A., Al-Dashti, H., Al-Dousari, N., 2019. Economic Impact and Risk Assessment of Sand and Dust Storms (SDS) on the Oil and Gas Industry in Kuwait. Sustainability 11, 200.

Al-Hemoud, A., Al-Sudairawi, M., Neelamanai, S., Naseeb, A., Behbehani, W., 2017. Socioeconomic effect of dust storms in Kuwait. Arabian Journal of Geosciences 10, 18.

Al-Malikey, 2007. The Geography of Iraq. The Ministry of Higher Education and Scientific Research in Iraq, The University of Basrah, Basrah, Iraq.

Al-Najim, F.A., 1975. Dust storms in Iraq. Bulletin College Science, College of Sciences, University of Baghdad, Baghdad, Iraq. 16, 14.

Al-Shahrabaly, Q., 2008. River discharges for Tigris and Euphrates gauging stations. Ministry of Water Resources, Baghdad.

Al-Taiar, A., Thalib, L., 2014. Short-term effect of dust storms on the risk of mortality due to respiratory, cardiovascular and all-causes in Kuwait. International journal of biometeorology 58, 69-77.

Al Senafi, F., Anis, A., 2015. Shamals and climate variability in the Northern Arabian/Persian Gulf from 1973 to 2012. International Journal of Climatology 35, 4509-4528.

Allen, C.J., Washington, R., Engelstaedter, S., 2013. Dust emission and transport mechanisms in the central Sahara: Fennec ground-based observations from Bordj Badji Mokhtar, June 2011. Journal of Geophysical Research: Atmospheres 118, 6212-6232.

Alolayan, M.A., Brown, K.W., Evans, J.S., Bouhamra, W.S., Koutrakis, P., 2013. Source apportionment of fine particles in Kuwait City. Science of the total environment 448, 14-25.

Alpert, P., Ganor, E., 2001. Sahara mineral dust measurements from TOMS: Comparison to surface observations over the Middle East for the extreme dust storm, March 14–17, 1998. Journal of Geophysical Research: Atmospheres (1984–2012) 106, 18275-18286.

Amante, C., Eakins, B.W., 2009. ETOPO1 1 Arc-Minute Global Relief Model: Procedures, Data Sources and Analisis. NOAA Technical Memorandum NESDIS NGDC-24. NAtional Geophysical Data Center, NOAA.

Aminou, D., 2002. MSG's SEVIRI instrument. ESA Bulletin(0376-4265), 15-17.

Amiridis, V., Wandinger, U., Marinou, E., Giannakaki, E., Tsekeri, A., Basart Alpuente, S., Kazadzis, S., Gkikas, A., Taylor, M., Baldasano Recio, J.M., 2013. Optimizing CALIPSO Saharan dust retrievals. Atmospheric Chemistry and Physics 13, 12089-12106.

Ashpole, I., Washington, R., 2012. An automated dust detection using SEVIRI: A multiyear climatology of summertime dustiness in the central and western Sahara. Journal of Geophysical Research: Atmospheres 117.

Ashrafi, K., Shafiepour-Motlagh, M., Aslemand, A., Ghader, S., 2014. Dust storm simulation over Iran using HYSPLIT. Journal of environmental health science and engineering 12, 9.

Balme, M., Metzger, S., Towner, M., Ringrose, T., Greeley, R., Iversen, J., 2003. Friction wind speeds in dust devils: A field study. Geophysical Research Letters 30.

Banks, J., Brindley, H., 2013. Evaluation of MSG-SEVIRI mineral dust retrieval products over North Africa and the Middle East. Remote Sensing of Environment 128, 58-73.

Bartlett, K.S., 2004. Dust storm forecasting for Al Udeid AB, Qatar: an empirical analysis. DTIC Document.

Basart, S., Vendrell, L., Baldasano, J.M., 2016. High-resolution dust modelling over complex terrains in West Asia. Aeolian Research 23, 37-50.

Benedetti, A., Baldasano, J.M., Basart, S., Benincasa, F., Boucher, O., Brooks, M.E., Chen, J.-P., Colarco, P.R., Gong, S., Huneeus, N., 2014. Operational dust prediction.

Boegh, E., Søgaard, H., Broge, N., Hasager, C., Jensen, N., Schelde, K., Thomsen, A., 2002. Airborne multispectral data for quantifying leaf area index, nitrogen concentration, and photosynthetic efficiency in agriculture. Remote Sensing of Environment 81, 179-193.

Brindley, H., Knippertz, P., Ryder, C., Ashpole, I., 2012. A critical evaluation of the ability of the Spinning Enhanced Visible and Infrared Imager (SEVIRI) thermal infrared red-green-blue rendering to identify dust events: Theoretical analysis. Journal of Geophysical Research: Atmospheres 117, D7.

Brindley, H.E., Russell, J.E., 2009. An assessment of Saharan dust loading and the corresponding cloud-free longwave direct radiative effect from geostationary satellite observations. Journal of Geophysical Research: Atmospheres 114.

Brunekreef, B., Forsberg, B., 2005. Epidemiological evidence of effects of coarse airborne particles on health. European Respiratory Journal 26, 309-318.

Bullard, J.E., 2013. Contemporary glacigenic inputs to the dust cycle. Earth Surface Processes and Landforms 38, 71-89.

Buringh, P., 1960. Soils and soil conditions in Iraq. Ministiry of Agricuture, Baghdad, Iraq.

Cakmur, R., Miller, R., Perlwitz, J., Geogdzhayev, I., Ginoux, P., Koch, D., Kohfeld, K., Tegen, I., Zender, C., 2006. Constraining the magnitude of the global dust cycle by minimizing the difference between a model and observations. Journal of Geophysical Research: Atmospheres 111.

Cakmur, R., Miller, R., Torres, O., 2004. Incorporating the effect of small-scale circulations upon dust emission in an atmospheric general circulation model. Journal of Geophysical Research: Atmospheres 109.

Caldwell, T.G., McDonald, E.V., Bacon, S.N., Stullenbarger, G., 2008. The performance and sustainability of vehicle dust courses for military testing. Journal of Terramechanics 45, 213-221.

Carkoglu, A., Eder, M., 2001. Domestic concerns and the water conflict over the Euphrates-Tigris river basin. Middle Eastern Studies 37, 41-71.

Chaboureau, J.P., Tulet, P., Mari, C., 2007. Diurnal cycle of dust and cirrus over West Africa as seen from Meteosat Second Generation satellite and a regional forecast model. Geophysical Research Letters 34.

Choobari, O.A., Zawar-Reza, P., Sturman, A., 2014. The global distribution of mineral dust and its impacts on the climate system: A review. Atmospheric Research 138, 152-165.

Chung, Y., Kim, H., Jugder, D., Natsagdorj, L., Chen, S., 2003. On sand and duststorms and associated significant dustfall observed in Chongju-Chongwon, Korea during 1997–2000. Water, Air and Soil Pollution: Focus 3, 5-19.

Claquin, T., Schulz, M., Balkanski, Y., 1999. Modeling the mineralogy of atmospheric dust sources. Journal of Geophysical Research: Atmospheres 104, 22243-22256.

Coles, F.E., 1938. Dust-Storms in Iraq. HM Stationary Office, York House, London, UK. 6, 17.

Cowie, S., Knippertz, P., Marsham, J., 2014. A climatology of dust emission events from northern Africa using long-term surface observations. Atmospheric Chemistry and Physics 14, 8579-8597.

Cowie, S.M., Knippertz, P., Marsham, J.H., 2013. Are vegetation-related roughness changes the cause of the recent decrease in dust emission from the Sahel? Geophysical Research Letters 40, 1868-1872.

Cowie, S.M., Marsham, J.H., Knippertz, P., 2015. The importance of rare, high-wind events for dust uplift in northern Africa. Geophysical Research Letters 42, 8208-8215.

Cragin, J., Herron, M., Langway Jr, C., Klouda, G., 1977. Interhemispheric comparison of changes in the composition of atmospheric precipitation during the late Cenozoic era. Polar Oceans, 617-631.

Crook, J., 2009. Climate analysis and long range forecasting of dust storms in Iraq. DTIC Document, Naval Postgraduate School Monterey CA, 2009.

Crusius, J., Schroth, A.W., Gasso, S., Moy, C.M., Levy, R.C., Gatica, M., 2011. Glacial flour dust storms in the Gulf of Alaska: Hydrologic and meteorological controls and their importance as a source of bioavailable iron. Geophysical Research Letters 38.

Cuesta, J., Marsham, J.H., Parker, D.J., Flamant, C., 2009. Dynamical mechanisms controlling the vertical redistribution of dust and the thermodynamic structure of the West Saharan atmospheric boundary layer during summer. Atmospheric Science Letters 10, 34-42.

Dalldorf, G.K., McDonald, E.V., Bacon, S.N., Nikolich, G., 2008. Testing and evaluation of a synthetic polymer for dust suppression in military applications, Geological Society of America Meeting, Houston.

Darmenov, A., Sokolik, I.N., 2005. Identifying the regional thermal-IR radiative signature of mineral dust with MODIS. Geophysical Research Letters 32.

De Villiers, M.P., 2010. Predicting the development of weather phenomena that influence aviation at Abu Dhabi International Airport. University of Pretoria.

Draxler, R.R., Gillette, D.A., Kirkpatrick, J.S., Heller, J., 2001. Estimating PM< sub> 10</sub> air concentrations from dust storms in Iraq, Kuwait and Saudi Arabia. Atmospheric Environment 35, 4315-4330.

Draxler, R.R., Hess, G., 1997. Description of the HYSPLIT4 modeling system.

Duce, R., Liss, P., Merrill, J., Atlas, E., Buat-Menard, P., Hicks, B., Miller, J., Prospero, J., Arimoto, R., Church, T., 1991. The atmospheric input of trace species to the world ocean. Global biogeochemical cycles 5, 193-259.

Fang, X., Xie, Y., Li, L., 2003. Effects of duststorms on the air pollution in Beijing. Water, Air and Soil Pollution: Focus 3, 93-101.

Feng, Q., Endo, K., Cheng, G., 2002. Dust storms in China: a case study of dust storm variation and dust characteristics. Bulletin of Engineering Geology and the Environment 61, 253-261.

Field, C.B., 2012. Managing the risks of extreme events and disasters to advance climate change adaptation: special report of the intergovernmental panel on climate change. Cambridge University Press.

Fisher, D.A., 1979. Comparison of 10 5 years of oxygen isotope and insoluble impurity profiles from the Devon Island and Camp Century ice cores. Quaternary Research 11, 299-305.

Flamant, C., Chaboureau, J.P., Parker, D., Taylor, C., Cammas, J.P., Bock, O., Timouk, F., Pelon, J., 2007. Airborne observations of the impact of a convective system on the planetary boundary layer thermodynamics and aerosol distribution in the inter-tropical discontinuity region of the West African monsoon. Quarterly Journal of the royal meteorological society 133, 1175-1189.

Fleming, Z.L., Monks, P.S., Manning, A.J., 2012. Untangling the influence of air-mass history in interpreting observed atmospheric composition. Atmospheric Research 104, 1-39.

Gillies, J., Nickling, W., McTainsh, G., 1996. Dust concentrations and particle-size characteristics of an intense dust haze event: inland delta region, Mali, West Africa. Atmospheric Environment 30, 1081-1090.

Ginoux, P., Prospero, J.M., Gill, T.E., Hsu, N.C., Zhao, M., 2012. Global-scale attribution of anthropogenic and natural dust sources and their emission rates based on MODIS Deep Blue aerosol products. Reviews of geophysics 50.

Ginoux, P., Torres, O., 2003. Empirical TOMS index for dust aerosol: Applications to model validation and source characterization. Journal of Geophysical Research: Atmospheres 108.

Gleick, P.H., 2014. Water, drought, climate change, and conflict in Syria. Weather, Climate, and Society 6, 331-340.

Goldman, J., 2003. Dust storms, sand storms and related NOAA activities in the Middle East. NOAA Magazine.

Gong, S., Zhang, X., 2008. CUACE/Dust–an integrated system of observation and modeling systems for operational dust forecasting in Asia. Atmospheric Chemistry and Physics 8, 2333-2340.

Gonzalez-Martin, C., Teigell-Perez, N., Valladares, B., Griffin, D.W., 2014. The global dispersion of pathogenic microorganisms by dust storms and its relevance to agriculture. Adv Agron 127, 1-41.

GoogleEarth, 2013. Map of Iraq. Image Landsat, US Department of State Geographer, 33 12' 30.67 N 45 01' 20.21 E., US.

Gordon, H., 1948. The natural foundations of geographic Iraq,, first ed. Bibliotheca Alexandrina, Arab printing press, Beirut, Lebanon.

Goudie, A., 1983. Dust storms in space and time. Progress in Physical Geography 7, 502-530.

Goudie, A.S., Middleton, N., 2006. Desert dust in the global system. Springer Science & Business Media.

Goudie, A.S., Middleton, N.J., 1992. The changing frequency of dust storms through time. Climatic Change 20, 197-225.

Grant, K., 1983. Vector mean winds and humidities in the lower troposphere over Arabia and environs in July. 111, 32.

Griffin, D.W., 2007. Atmospheric movement of microorganisms in clouds of desert dust and implications for human health. Clinical microbiology reviews 20, 459-477.

Griffin, D.W., Garrison, V.H., Herman, J.R., Shinn, E.A., 2001. African desert dust in the Caribbean atmosphere: microbiology and public health. Aerobiologia 17, 203-213.

Griffin, D.W., Kellogg, C.A., 2004. Dust storms and their impact on ocean and human health: dust in Earth's atmosphere. EcoHealth 1, 284-295.

Griggs, M., 1975. Measurements of atmospheric aerosol optical thickness over water using ERTS-1 data. Journal of the Air Pollution Control Association 25, 622-626.

Grousset, F.E., Ginoux, P., Bory, A., Biscaye, P.E., 2003. Case study of a Chinese dust plume reaching the French Alps. Geophysical Research Letters 30.

Guo, M., Wang, X., Liu, Y., Li, J., Wang, H., Matsuoka, N., Tani, H., 2012. The effects of sand dust storms on greenhouse gases. International Journal of Remote Sensing 33, 6838-6853.

Hamidi, M., Kavianpour, M.R., Shao, Y., 2013. Synoptic analysis of dust storms in the Middle East. Asia-Pacific Journal of Atmospheric Sciences 49, 279-286.

Hammer, C., Clausen, H., Dansgaard, W., Neftel, A., Kristinsdottir, P., Johnson, E., 1985. Continuous impurity analysis along the Dye 3 deep core. Greenland ice core: geophysics, geochemistry, and the environment 33, 90-94.

Hanson, C.M., 2007. Long-range operational military forecasts for Iraq. DTIC Document, Naval Postgraduate School Monterey CA, 2007.

Harrison, S.P., Kohfeld, K.E., Roelandt, C., Claquin, T., 2001. The role of dust in climate changes today, at the last glacial maximum and in the future. Earth-Science Reviews 54, 43-80.

Heinold, B., Knippertz, P., Marsham, J., Fiedler, S., Dixon, N., Schepanski, K., Laurent, B., Tegen, I., 2013. The role of deep convection and nocturnal low-level jets for dust emission in summertime West Africa: Estimates from convection-permitting simulations. Journal of Geophysical Research: Atmospheres 118, 4385-4400.

Herman, J., Bhartia, P., Torres, O., Hsu, C., Seftor, C., Celarier, E., 1997. Global distribution of UV-absorbing aerosols from Nimbus 7/TOMS data. Journal of Geophysical Research: Atmospheres 102, 16911-16922.

Hinman, N.W., Lindstrom, R.F., 1996. Seasonal changes in silica deposition in hot spring systems. Chemical Geology 132, 237-246.

http://oiswww.eumetsat.org/IPPS/html/MSG/PRODUCTS/CLM/, accessed on 24/10/2017.

http://www.thelivingmoon.com/45jack_files/03files/Weather_Warfare_Sand_Storms_Over_Iraq.html, accessed on 11/05/2017.

https://earthobservatory.nasa.gov/IOTD/view.php?id=80613, accessed on 24/11/2017.

https://earthobservatory.nasa.gov/NaturalHazards/view.php?id=86539, on 05/01/2018.

https://en.wikipedia.org/wiki/Mesopotamian_Marshes#Geography, accessed on 21/11/2017.

https://giovanni.gsfc.nasa.gov/giovanni/#service=TmAvMp&starttime=2015-08-31T00:00:00Z&endtime=2015-08-31T23:59:59Z&bbox=35.9033,48.6475,38.0127&data=MYD08_D3_6_Deep_Blue_Aerosol_Optical_Depth_550_Land_Mean&variableFacets=dataFieldMeasurement%3AAerosol%20Optical%20Depth%3B, accessed on 21/12/2017.

https://giovanni.gsfc.nasa.gov/giovanni/#service=TmAvMp&starttime=&endtime=&data=MOD13C2_006_CMG_0_05_Deg_Monthly_EVI&dataKeyword=evi, accessed on 05/01/2019.

https://public.wmo.int/en/our-mandate/focus-areas/environment/sand-and-dust-storm, accessed on 08/05/2017. Sand and Dust Storms.

https://tradingeconomics.com/iraq/gdp, accessed on 27/05/2019.

https://uk.mathworks.com/products/matlab.html, accessed on 27/05/2019.

https://www.azernews.az/region/87525.html, accessed on 04/01/2018.

https://www.britannica.com/place/Iraq#toc22923, accessed on 21/11/2017.

https://www.haaretz.com/.premium-scientists-syrian-war-was-one-of-causes-for-dust-storm-1.5406082, accessed on 24/01/2018.

https://www.independent.co.uk/news/world/asia/china-dust-storm-air-quality-decline-gobi-desert-mongolia-beijing-visibility-pollution-children-a7717241.html, accessed on 21/06/2017.

https://www.meted.ucar.edu/satmet/multispectral_topics/rgb/navmenu.php?tab=1&page=1-0-0&type=text, accessed on 14/12/2017.

https://www.meted.ucar.edu/satmet/multispectral_topics/rgb/navmenu.php?tab=1&page=3-1-6&type=text, accessed on 19/12/2017.

https://www.meted.ucar.edu/satmet/multispectral_topics/rgb/navmenu.php?tab=1&page=3-2-4&type=text, multispectral satellite applications: RGB products explained.

https://www.meted.ucar.edu/satmet/multispectral_topics/rgb/navmenu.php?tab=1&page=3-2-4&type=text, accessed on 20/12/2017.

https://www.ncdc.noaa.gov/data-access/model-data/model-datasets/global-data-assimilation-system-gdas, accessed on 18/10/2017.

https://www.nodc.noaa.gov/woce/woce_v3/wocedata_1/woce-uot/document/wmocode.htm, accessed on 12/03/2016. WMO Code Tables - NODC.

https://www.washingtonpost.com/news/capital-weather-gang/wp/2015/09/02/dustpocalypse-huge-dust-swirl-in-iraq-iran/?utm_term=.b0c1e45e922a, accessed on 04/01/2018.

https://www.worldometers.info/world-population/population-by-country/, accessed on 07/02/2019.

https://www.youtube.com/watch?v=M0d9jMx6rJ4, accessed on 04/01/2018.

Hudson, P.K., Young, M.A., Kleiber, P.D., Grassian, V.H., 2008. Coupled infrared extinction spectra and size distribution measurements for several non-clay components of mineral dust aerosol (quartz, calcite, and dolomite). Atmospheric Environment 42, 5991-5999.

Huszar, P.C., Piper, S.L., 1986. Estimating the off-site costs of wind erosion in New Mexico. Journal of soil and water conservation 41, 414-416.

Idso, S.B., 1976. Dust storms. Scientific American 235, 108-115.

IMO, 2015. Present Weather Data 1985-2013, Iraqi Meteorological Organisation and Seismology, Baghdad, Iraq, in: Seismology, I.M.O.a. (Ed.), Baghdad, Iraq.

Jafari, R., Malekian, M., 2015. Comparison and evaluation of dust detection algorithms using MODIS Aqua/Terra Level 1B data and MODIS/OMI dust products in the Middle East. International Journal of Remote Sensing 36, 597-617.

Jongerden, J., 2010. Dams and politics in Turkey: utilizing water, developing conflict. Middle East Policy 17, 137-143.

Jugder, D., Shinoda, M., Sugimoto, N., Matsui, I., Nishikawa, M., Park, S.-U., Chun, Y.-S., Park, M.-S., 2011. Spatial and temporal variations of dust concentrations in the Gobi Desert of Mongolia. Global and Planetary Change 78, 14-22.

Just, D., 2000. SEVIRI instrument Level 1.5 data, First MSG RAO Workshop, pp. Vol. 452, p. 429.

Kaimal, J.C., Finnigan, J.J., 1994. Atmospheric boundary layer flows: their structure and measurement. Oxford university press.

Kallos, G., Nickovic, S., Papadopoulos, A., Jovic, D., Kakaliagou, O., Misirlis, N., Boukas, L., Mimikou, N., Sakellaridis, G., Papageorgiou, J., 1997. The regional weather forecasting system SKIRON: An overview, Proceedings of the symposium on regional weather prediction on parallel computer environments, p. 17.

Kang, K.K., Chu, J.M., Jeong, H.S., Han, W.J., Yu, N.M., 2004. A Study on the Analysis of Damages of Northeast Asian Dust and Sand Storm and of the Regional Cooperation Strategies. Korea Environment Institute 2, 112-118.

Kaufman, Y., Koren, I., Remer, L., Tanré, D., Ginoux, P., Fan, S., 2005. Dust transport and deposition observed from the Terra-Moderate Resolution Imaging Spectroradiometer (MODIS) spacecraft over the Atlantic Ocean. Journal of Geophysical Research: Atmospheres 110.

Kellogg, C.A., Griffin, D.W., Garrison, V.H., Peak, K.K., Royall, N., Smith, R.R., Shinn, E.A., 2004. Characterization of aerosolized bacteria and fungi from desert dust events in Mali, West Africa. Aerobiologia 20, 99-110.

Klüser, L., Schepanski, K., 2009. Remote sensing of mineral dust over land with MSG infrared channels: A new Bitemporal Mineral Dust Index. Remote Sensing of Environment 113, 1853-1867.

Knippertz, P., Deutscher, C., Kandler, K., Müller, T., Schulz, O., Schütz, L., 2007. Dust mobilization due to density currents in the Atlas region: Observations from the Saharan Mineral Dust Experiment 2006 field campaign. Journal of Geophysical Research: Atmospheres 112.

Knippertz, P., Stuut, J.-B.W., 2014. Introduction, Mineral Dust. Springer, pp. 1-14.

Krug, H.F., Wick, P., 2011. Nanotoxicology: an interdisciplinary challenge. Angewandte Chemie International Edition 50, 1260-1278.

Kutiel, H., Furman, H., 2003. Dust storms in the Middle East: Sources of origin and their temporal characteristics. Indoor and Built Environment 12, 419-426.

Kutuzov, S., Shahgedanova, M., Mikhalenko, V., Ginot, P., Lavrentiev, I., Kemp, S., 2013. High-resolution provenance of desert dust deposited on Mt. Elbrus, Caucasus in 2009-2012 using snow pit and firn core records. The Cryosphere 7, 1481.

Laurent, B., Marticorena, B., Bergametti, G., Léon, J., Mahowald, N., 2008. Modeling mineral dust emissions from the Sahara desert using new surface properties and soil database. Journal of Geophysical Research: Atmospheres 113.

Lazaridis, M., 2011. First principles of meteorology, First Principles of Meteorology and Air Pollution. Springer, pp. 67-118.

Lefkowitz, M., Schlatter, E.E., 1966. An Analysis of Runway Visual Range. ESSA Report No. RD-66-100, Washington,D.C.

Legrand, M., Desbois, M., Vovor, K., 1988. Satellite detection of Saharan dust: Optimized imaging during nighttime. Journal of Climate 1, 256-264.

Li, J., Zhang, P., Schmit, T., Schmetz, J., Menzel, W., 2007. Quantitative monitoring of a Saharan dust event with SEVIRI on Meteosat-8. International Journal of Remote Sensing 28, 2181-2186.

Li, X., Zhang, H., 2012. Seasonal variations in dust concentration and dust emission observed over Horqin Sandy Land area in China from December 2010 to November 2011. Atmospheric Environment 61, 56-65.

Li, X., Zhang, H., 2014. Soil moisture effects on sand saltation and dust emission observed over the Horqin Sandy Land area in China. Journal of Meteorological Research 28, 444-452.

Liu, D., Wang, Z., Liu, Z., Winker, D., Trepte, C., 2008. A height resolved global view of dust aerosols from the first year CALIPSO lidar measurements. Journal of Geophysical Research: Atmospheres (1984–2012) 113.

Liu, X., Huneeus, N., Schulz, M., Balkanski, Y., Griesfeller, J., Prospero, J., Kinne, S., Bauer, S., Boucher, O., Chin, M., 2011. Global dust model intercomparison in AeroCom phase I. Atmospheric Chemistry and Physics 11, 7781.

Mabbutt, J., 1986. Desertification indicators. Climatic Change 9, 113-122.

Mahowald, N., Albani, S., Kok, J.F., Engelstaeder, S., Scanza, R., Ward, D.S., Flanner, M.G., 2014. The size distribution of desert dust aerosols and its impact on the Earth system. Aeolian Research 15, 53-71.

Mahowald, N., Kohfeld, K., Hansson, M., Balkanski, Y., Harrison, S.P., Prentice, I.C., Schulz, M., Rodhe, H., 1999. Dust sources and deposition during the last glacial maximum and current climate: A comparison of model results with paleodata from ice cores and marine sediments. Journal of Geophysical Research: Atmospheres 104, 15895-15916.

Mahowald, N.M., Muhs, D.R., Levis, S., Rasch, P.J., Yoshioka, M., Zender, C.S., Luo, C., 2006. Change in atmospheric mineral aerosols in response to climate: Last glacial period, preindustrial, modern, and doubled carbon dioxide climates. Journal of Geophysical Research: Atmospheres 111.

Marsham, J.H., Hobby, M., Allen, C., Banks, J., Bart, M., Brooks, B., Cavazos-Guerra, C., Engelstaedter, S., Gascoyne, M., Lima, A., 2013. Meteorology and dust in the central Sahara: Observations from Fennec supersite-1 during the June 2011 Intensive Observation Period. Journal of Geophysical Research: Atmospheres 118, 4069-4089.

Marsham, J.H., Parker, D.J., Grams, C.M., Taylor, C.M., Haywood, J.M., 2008. Uplift of Saharan dust south of the intertropical discontinuity. Journal of Geophysical Research: Atmospheres 113.

Martínez, M.A., Ruiz, J., Cuevas, E., 2009. Use of SEVIRI images and derived products in a WMO Sand and Dust Storm Warning System, IOP Conference Series: Earth and Environmental Science. IOP Publishing, p. 012004.

McPeters, R.D., Bhartia, P., Krueger, A.J., Herman, J.R., Wellemeyer, C.G., Seftor, C.J., Jaross, G., Torres, O., Moy, L., Labow, G., 1998. Earth probe total ozone mapping spectrometer (TOMS): data products user's guide.

Merrifield, A., Schindeler, S., Jalaludin, B., Smith, W., 2013. Health effects of the September 2009 dust storm in Sydney, Australia: did emergency department visits and hospital admissions increase? Environmental Health 12, 32.

Middleton, N., 1986a. Dust storms in the Middle East. Journal of Arid Environments 10: 83-96.

Middleton, N.J., 1986b. The geography of dust storms. Unpublished PhD Thesis, University of Oxford, UK.

Miller, S., 2003. A consolidated technique for enhancing desert dust storms with MODIS. Geophysical Research Letters 30.

Miller, S.D., Kuciauskas, A.P., Liu, M., Ji, Q., Reid, J.S., Breed, D.W., Walker, A.L., Mandoos, A.A., 2008. Haboob dust storms of the southern Arabian Peninsula. Journal of Geophysical Research: Atmospheres (1984–2012) 113.

Millington, S., Saunders, R., Francis, P., Webster, H., 2012. Simulated volcanic ash imagery: A method to compare NAME ash concentration forecasts with SEVIRI imagery for the Eyjafjallajökull eruption in 2010. Journal of Geophysical Research: Atmospheres 117.

Miri, A., Ahmadi, H., Ekhtesasi, M.R., Panjehkeh, N., Ghanbari, A., 2009. Environmental and socio-economic impacts of dust storms in Sistan Region, Iran. International Journal of Environmental Studies 66, 343-355.

Moridnejad, A., Karimi, N., Ariya, P.A., 2015. A new inventory for middle east dust source points. Environmental monitoring and assessment 187, 582.

Muhaimeed, A., Saloom, A., Saliem, K., Alani, K., Muklef, W., &, 2014. Classification and distribution of Iraqi soils. International Journal of Agriculture Innovations and Research 2, 997-1002.

Natsagdorj, L., Jugder, D., Chung, Y., 2003. Analysis of dust storms observed in Mongolia during 1937–1999. Atmospheric Environment 37, 1401-1411.

Nickovic, S., 1996. Modeling of dust process for the Saharan and Mediterranean area, The Impact of Desert Dust Across the Mediterranean. Springer, pp. 15-23.

Nickovic, S., Cuevas Agulló, E., Baldasano, J.M., Terradellas, E., Nakazawa, T., Baklanov, A., 2015. Sand and Dust Storm Warning Advisory and Assessment System (SDS-WAS) Science and Implementation Plan: 2015-2020.

Ničković, S., Dobričić, S., 1996. A model for long-range transport of desert dust. Monthly Weather Review 124, 2537-2544.

Ogawa, K., Schmugge, T., Jacob, F., French, A., 2003. Estimation of land surface window (8–12 µm) emissivity from multi-spectral thermal infrared remote sensing—A case study in a part of Sahara Desert. Geophysical Research Letters 30.

Orgill, M., Sehmel, G., 1976. Frequency and diurnal variation of dust storms in the contiguous USA. Atmospheric Environment (1967) 10, 813-825.

Orlovsky, L., Orlovsky, N., Durdyev, A., 2005. Dust storms in Turkmenistan. Journal of Arid Environments 60, 83-97.

Pahlavanravi, A., Miri, A., Ahmadi, H., Ekhtesasi, M., 2012. The impacts of different kinds of dust storms in hot and dry climate, a case study in sistan region. Desert 17, 15-25.

Park, S.-U., Park, M.-S., Chun, Y., 2010. Asian dust events observed by a 20-m monitoring tower in Mongolia during 2009. Atmospheric Environment 44, 4964-4972.

Parsons, A.J., Abrahams, A.D., 1994. Geomorphology of desert environments. Springer.

Patz, J., Corvalan, C., Hortwitz, P., Campbell-Lendrum, D., Watts, N., Maiero, M., Olson, S., Hales, J., Miller, C., Campbell, K., 2012. Our planet, our health, our future. Human health and the Rio conventions: biological diversity, climate change and desertification. World Health Organization: Geneva, Switzerland.

Pease, P.P., Tchakerian, V.P., Tindale, N.W., 1998. Aerosols over the Arabian Sea: geochemistry and source areas for aeolian desert dust. Journal of Arid Environments 39, 477-496.

Pérez, C., Baldasano, J., 2008. WMO/GEO Expert Meeting On An International Sand And Dust Storm Warning System, IOP Conference Series: Earth and Environmental Science. IOP Publishing, p. 011001.

Pérez, C., Nickovic, S., Baldasano, J., Sicard, M., Rocadenbosch, F., Cachorro, V., 2006. A long Saharan dust event over the western Mediterranean: Lidar, Sun photometer observations, and regional dust modeling. Journal of Geophysical Research: Atmospheres 111.

Petit, J.-R., Briat, M., Royer, A., 1981. Ice age aerosol content from East Antarctic ice core samples and past wind strength. Nature 293, 391.

Pewe, T.L., 1981. Desert dust: An overview. Desert dust: Origin, characteristics, and effect on man 186, 1-10.

Pierangelo, C., Chédin, A., Heilliette, S., Jacquinet-Husson, N., Armante, R., 2004. Dust altitude and infrared optical depth from AIRS. Atmospheric Chemistry and Physics 4, 1813-1822.

Plumlee, G., Ziegler, T., Lamothe, P., Meeker, G., Sutley, S., 2003. The Toxicological Geochemistry of Dusts, Soils, and Other Earth Materials: Insights From In Vitro Physiologically-based Geochemical Leach Tests, AGU Fall Meeting Abstracts.

Plumlee, G.S., Morman, S.A., Meeker, G., Hoefen, T.M., Hageman, P.L., Wolf, R.E., BE, S.L., 2013. The environmental and medical geochemistry of potentially hazardous materials produced by disasters. Treatise on geochemistry 11, 257-304.

Prospero, J.M., Bullard, J.E., Hodgkins, R., 2012. High-latitude dust over the North Atlantic: inputs from Icelandic proglacial dust storms. Science 335, 1078-1082.

Prospero, J.M., Ginoux, P., Torres, O., Nicholson, S.E., Gill, T.E., 2002. Environmental characterization of global sources of atmospheric soil dust identified with the Nimbus 7 Total Ozone Mapping Spectrometer (TOMS) absorbing aerosol product. Reviews of geophysics 40.

Rao, P.G., Hatwar, H., Al-Sulaiti, M.H., Al-Mulla, A.H., 2003. Summer shamals over the Arabian Gulf. Weather 58, 471-478.

Remer, L.A., Kaufman, Y., Tanré, D., Mattoo, S., Chu, D., Martins, J.V., Li, R.-R., Ichoku, C., Levy, R., Kleidman, R., 2005. The MODIS aerosol algorithm, products, and validation. Journal of the Atmospheric Sciences 62, 947-973.

Rezazadeh, M., Irannejad, P., Shao, Y., 2013. Climatology of the Middle East dust events. Aeolian Research 10, 103-109.

Roberts, A., Knippertz, P., 2012. Haboobs: convectively generated dust storms in West Africa. Weather 67, 311-316.

Rutherford, S., Clark, E., McTainsh, G., Simpson, R., Mitchell, C., 1999. Characteristics of rural dust events shown to impact on asthma severity in Brisbane, Australia. International journal of biometeorology 42, 217-225.

Safar, M.I., 1980. Frequency of dust in day-time summer in Kuwait. Directorate General of Civil Aviation, Meteorological Department, Climatological Section.

San-Chao, L., Qinhuo, L., Maofang, G., Liangfu, C., 2006. Detection of dust storms by using daytime and nighttime multi-spectral MODIS images, Geoscience and Remote Sensing Symposium, 2006. IGARSS 2006. IEEE International Conference on. Ieee, pp. 294-296.

Schepanski, K., Tegen, I., Laurent, B., Heinold, B., Macke, A., 2007. A new Saharan dust source activation frequency map derived from MSG-SEVIRI IR-channels. Geophysical Research Letters 34.

Schepanski, K., Tegen, I., Macke, A., 2012. Comparison of satellite based observations of Saharan dust source areas. Remote Sensing of Environment 123, 90-97.

Schepanski, K., Tegen, I., Todd, M., Heinold, B., Bönisch, G., Laurent, B., Macke, A., 2009. Meteorological processes forcing Saharan dust emission inferred from MSG-SEVIRI observations of subdaily dust source activation and numerical models. Journal of Geophysical Research: Atmospheres 114.

Schmetz, J., Govaerts, Y., König, M., Lutz, H.-J., Ratier, A., Tjemkes, S., 2005. A short introduction to METEOSAT Second Generation (MSG). CIRA, Colorado State Univ., Fort Collins.

Schmetz, J., Pili, P., Tjemkes, S., Just, D., Kerkmann, J., Rota, S., Ratier, A., 2002. An introduction to Meteosat second generation (MSG). Bulletin of the American Meteorological Society 83, 977-992.

Schmid, J., 2000. The SEVIRI instrument, Proceedings of the 2000 EUMETSAT meteorological satellite data user's conference, Bologna, Italy.

Semenov, O., 2012. Dust storms and sandstorms and aerosol long-distance transport, Aralkum-a Man-Made Desert. Springer, pp. 73-82.

Shamout, M.N., Lahn, G., 2015. The Euphrates in crisis: channels of cooperation for a threatened river. Research Paper. April.

Shao, Y., 2001. A model for mineral dust emission. Journal of Geophysical Research: Atmospheres 106, 20239-20254.

Shao, Y., 2008. Physics and modelling of wind erosion. Science & Business Media, Springer.

Shao, Y., Wyrwoll, K.-H., Chappell, A., Huang, J., Lin, Z., McTainsh, G.H., Mikami, M., Tanaka, T.Y., Wang, X., Yoon, S., 2011. Dust cycle: An emerging core theme in Earth system science. Aeolian Research 2, 181-204.

Shenk, W.E., Curran, R.J., 1974. The detection of dust storms over land and water with satellite visible and infrared measurements. Monthly Weather Review 102, 830-837.

Shepherd, G., Terradellas, E., Baklanov, A., Kang, U., Sprigg, W., Nickovic, S., Boloorani, A.D., Al-Dousari, A., Basart, S., Benedetti, A., Sealy, A., Tong, D., Zhang, X., Shumake-Guillemot, J., Kebin, Z., Knippertz, P., Mohammed, A.A.A., Al-Dabbas, M., Cheng, L., Otani, S., Wang, F., Zhang, C., Boom Ryoo, S., Cha, J., 2016. Global assessment of sand and dust storms.

Sims, D.A., Rahman, A.F., Cordova, V.D., El-Masri, B.Z., Baldocchi, D.D., Bolstad, P.V., Flanagan, L.B., Goldstein, A.H., Hollinger, D.Y., Misson, L., 2008. A new model of gross primary productivity for North American ecosystems based solely on the enhanced vegetation index and land surface temperature from MODIS. Remote Sensing of Environment 112, 1633-1646.

Slingo, A., Ackerman, T.P., Allan, R., Kassianov, E.I., McFarlane, S.A., Robinson, G., Barnard, J.C., Miller, M., Harries, J., Russell, J., 2006. Observations of the impact of a major Saharan dust storm on the atmospheric radiation balance. Geophysical Research Letters 33.

Smalley, I., 1966. Formation of quartz sand. Nature 211, 476.

Sodemann, H., Lai, T., Marenco, F., Ryder, C.L., Flamant, C., Knippertz, P., Rosenberg, P., Bart, M., Mcquaid, J.B., 2015. Lagrangian dust model simulations for a case of moist convective dust emission and transport in the western Sahara region during Fennec/LADUNEX. Journal of Geophysical Research: Atmospheres 120, 6117-6144.

Sow, M., Alfaro, S., Rajot, J.L., Marticoréna, B., 2009. Size resolved dust emission fluxes measured in Niger during 3 dust storms of the AMMA experiment. Atmospheric Chemistry and Physics 9, 3881-3891.

Squires, V.R., 2007. Physics, Mechanics and Processes of Dust and Sandstorms.

Stefanski, R., Sivakumar, M., 2009. Impacts of sand and dust storms on agriculture and potential agricultural applications of a SDSWS, IOP Conference Series: Earth and Environmental Science. IOP Publishing, p. 012016.

Stein, A., Draxler, R.R., Rolph, G.D., Stunder, B.J., Cohen, M., Ngan, F., 2015. NOAA's HYSPLIT atmospheric transport and dispersion modeling system. Bulletin of the American Meteorological Society 96, 2059-2077.

Tegen, I., 2003. Modeling the mineral dust aerosol cycle in the climate system. Quaternary Science Reviews 22, 1821-1834.

Tegen, I., Fung, I., 1994. Modeling of mineral dust in the atmosphere: Sources, transport, and optical thickness. Journal of Geophysical Research: Atmospheres (1984–2012) 99, 22897-22914.

Tegen, I., Lacis, A.A., 1996. Modeling of particle size distribution and its influence on the radiative properties of mineral dust aerosol. Journal of Geophysical Research 101, 19237-19219,19244.

Tegen, I., Werner, M., Harrison, S.P., Kohfeld, K.E., 2004. Relative importance of climate and land use in determining present and future global soil dust emission. Geophysical Research Letters 31.

Terradellas, E., Nickovic, S., Zhang, X.Y., 2015. Airborne dust: a hazard to human health, environment and society. Boletín-Organización Meteorológica Mundial 64, 44-48.

Thompson, L.G., Mosley-Thompson, E., 1981. Microparticle concentration variations linked with climatic change: evidence from polar ice cores. Science 212, 812-815.

Tozer, P., Leys, J., 2013. Dust storms–what do they really cost? The Rangeland Journal 35, 131-142.

Tsoar, H., Pye, K., 1987. Dust transport and the question of desert loess formation. Sedimentology 34, 139-153.

Varoujan K, S., Nadhir, A.-A., Sven, K., 2013. Sand and dust storm events in Iraq. Natural Science 2013.

Vickery, K.J., Eckardt, F.D., Bryant, R.G., 2013. A sub-basin scale dust plume source frequency inventory for southern Africa, 2005–2008. Geophysical Research Letters 40, 5274-5279.

Voss, K.A., Famiglietti, J.S., Lo, M., Linage, C., Rodell, M., Swenson, S.C., 2013. Groundwater depletion in the Middle East from GRACE with implications for transboundary water management in the Tigris-Euphrates-Western Iran region. Water resources research 49, 904-914.

Wagner, F., Bortoli, D., Pereira, S., Costa, M.J., Maria Silva, A., Weinzierl, B., Esselborn, M., Petzold, A., Rasp, K., Heinold, B., 2009. Properties of dust aerosol particles transported to Portugal from the Sahara desert. Tellus B: Chemical and Physical Meteorology 61, 297-306.

Wald, A., Kaufman, Y., Tanré, D., Gao, B.C., 1998. Daytime and nighttime detection of mineral dust over desert using infrared spectral contrast. Journal of Geophysical Research: Atmospheres 103, 32307-32313.

Wang, C.-H., Chen, C.-S., Lin, C.-L., 2014. The threat of Asian dust storms on asthma patients: A population-based study in Taiwan. Global public health 9, 1040-1052.

Wang, Z.-T., 2016. A theoretical note on aerodynamic lifting in dust devils. Icarus 265, 79-83.

Westphal, D.L., Toon, O.B., Carlson, T.N., 1987. A two-dimensional numerical investigation of the dynamics and microphysics of Saharan dust storms. Journal of Geophysical Research: Atmospheres 92, 3027-3049.

WHO, 2013. Review of evidence on health aspects of air pollution–REVIHAAP Project.

Wilderson, W.D., 1991. Dust and sand forecasting in Iraq and adjoining countries. Tech. Note AWS/TN-91/001, 63 pp., Air Weather Serv., Scott AFB, Ill.

Wilkinson, G., Eckert, S., Hancock, T., Mayo, O., 1983. Nearest neighbour (NN) analysis of field experiments. Journal of the Royal Statistical Society. Series B (Methodological), 151-211.

Williams, P., Young, M., 1999. Costing Dust: How much does wind erosion cost the people of South Australia. Policy and Economic Research Unit, CSIRO Land and Water: Canberra.

World Health Organization, 2006. Air quality guidelines: global update 2005: particulate matter, ozone, nitrogen dioxide, and sulfur dioxide. World Health Organization.

Yakowitz, S., 1987. NEAREST-NEIGHBOUR METHODS FOR TIME SERIES ANALYSIS. Journal of time series analysis 8, 235-247.

Yang, C.-Y., 2006. Effects of Asian dust storm events on daily clinical visits for conjunctivitis in Taipei, Taiwan. Journal of Toxicology and Environmental Health, Part A 69, 1673-1680.

Youlin, Y., Squires, V., Qi, L., 2002. Global alarm: dust and sandstorms from the world's drylands. United Nations Convention to Combat Desertification (UNCCD).

Yu, Y., Notaro, M., Kalashnikova, O.V., Garay, M.J., 2016. Climatology of summer Shamal wind in the Middle East. Journal of Geophysical Research: Atmospheres 121, 289-305.

Zhang, J., Christopher, S.A., 2003. Longwave radiative forcing of Saharan dust aerosols estimated from MODIS, MISR, and CERES observations on Terra. Geophysical Research Letters 30.

Zhang, K., Wang, X., 1997. Investigation report and some thinking on strong sand storm in Northwest China. Journal of Beijing Forestry University 19.

Zhao, T., Gong, S., Zhang, X., McKendry, I., 2003. Modeled size-segregated wet and dry deposition budgets of soil dust aerosol during ACE-Asia 2001: Implications for trans-Pacific transport. Journal of Geophysical Research: Atmospheres 108.

Zhou, M., Chen, Z., Huang, R., Wang, Q., Arimoto, R., Parungo, F., Lenschow, D., Okada, K., Wu, P., 1994. Effects of two dust storms on solar radiation in the Beijing-Tianjin area. Geophysical Research Letters 21, 2697-2700.